ISOLATION, PURIFICATION AND CHARACTERIZATION OF POLYSACCHARIDE AND THEIR USE IN THE SYNTHESIS OF METAL NANOPARTICLES AND STUDY OF BIOLOGICAL ACTIVITIES

A THESIS

SUBMITTED FOR THE DEGREE OF
DOCTOR OF PHILOSOPHY
(IN SCIENCE)

TO

VIDYASAGAR UNIVERSITY

BY

SAIKAT MAITY

DEPARTMENT OF CHEMISTRY AND CHEMICAL TECHNOLOGY
VIDYASAGAR UNIVERSITY
MIDNAPORE-721102
WEST BENGAL, INDIA

2016

“Dedicated to
my beloved parents”

VIDYASAGAR UNIVERSITY

DEPARTMENT OF CHEMISTRY AND CHEMICAL TECHNOLOGY

Midnapore-721 102, West Bengal. INDIA

Phone: (03222) 276558, Extn. 437, Fax: (91) 03222 275329

CERTIFICATE FROM THE SUPERVISORS

This is to certify that the thesis entitled "**Isolation, purification and characterization of polysaccharide and their use in the synthesis of metal nanoparticles and study of biological activities**" submitted by **SAIKAT MAITY** who got his name registered on 19.01.2012 for the award of Ph. D. (Science) degree of Vidyasagar University is absolutely based upon his own work under the joint supervision of **Prof. Syed Sirajul Islam** and **Dr. Sumita Roy** of the Department of Chemistry and Chemical Technology, Vidyasagar University, Midnapore-721102 and neither this thesis nor any part of it has been submitted for any degree/diploma or any academic award anywhere before.

Signatures of the supervisors with date and official seal

(Prof. Syed Sirajul Islam)
Research Supervisor

(Dr. Sumita Roy)
Joint Research Supervisor

DECLARATION

I hereby declare that the research work embodied in this thesis has been carried out by me in the Department of Chemistry & Chemical Technology, Vidyasagar University, Midnapore, West Bengal, under the supervision of ***Professor Syed Sirajul Islam*** *and* ***Dr. Sumita Roy****, Department of Chemistry & Chemical Technology, Vidyasagar University, Midnapore, West Bengal. I also affirm that this work is original and has not been submitted for any other degree or diploma to this or any other University or Institution.*

Date: **(SAIKAT MAITY)**

ACKNOWLEDGEMENTS

I am delighted to render my heartfelt gratitude and indebtedness to my teacher and supervisor **Professor Syed Sirajul Islam**, Department of Chemistry & Chemical Technology, Vidyasagar University for his constant encouragement, inspiration, stimulating discussions, constructive ideas, encouraging behavior and invaluable guidance throughout the course of this investigation.

I express my warm regards and sincere thanks to my supervisor **Dr. Sumita Roy**, Department of Chemistry & Chemical Technology, Vidyasagar University for his invaluable guidance, constant support and generous help during the progress of the work.

I express my warm regards and sincere thanks to all faculty members of our department, Prof. Braja Gopal Bag, Prof. Ajay Misra, Dr. Sudipta Dalai, Dr. Sumita Roy, Dr. Subal Chandra Manna and Dr. Maidul Hussain for motivating me during my research work. I am thankful to all the staff members of this department for their co-operation and support.

I record my special thanks to all my senior and junior research scholars of our laboratory: Soumitrada, Dilipda, Indranilda, Kaushikda, Sunilda, Krishnenduda, Debsankarda, Sadhanda, Subhasda, Arnabda, Bivasda, Pradipda, Sukeshda, Soumitrada (chhoto), Kankanda, Ramsankarda, Chanchalda, Sanjoyda, Biswajitda, Sanjoy, Kousik, Eshita, Praloy, Ipsita, Surajit, Ashis, Prasenjit, Manabendra, Dilip for their co-operation and friendship.

I am extremely thankful to Mr. Barun Majumder, Bose Institute, Kolkata-700 054, West Bengal, India for preparing the NMR spectra.

It's my great pleasure to express my sincere thanks to Dr. T. K. Maiti, Department of Biotechnology, I.I.T., Kharagpur-721 302, West Bengal, India, Dr. Samir Ranjan Sikdar of Division of Plant Biology, Bose Institute, Kolkata-700 054, West Bengal, India for their co-operation and helpful suggestion.

I greatly acknowledge the Council of Scientific and Industrial Research **(CSIR)**, Government of India for providing financial assistance.

I express my profound regards to my parents (Shri Buddhadev Maity & Smt. Kalyani Maity), sister (Sanjukta), brother (Saibal) and my wife (Sangeeta) and other family members for their inspiration and encouragement during the whole course of my work.

I am also grateful to the Hon'ble Vice-Chancellor (**Prof. Ranjan Chakraborty**) and the Registrar (**Dr. Jayanta Kishore Nandi**) of my beloved institute Vidyasagar University for providing me this platform to accomplish my work.

(Saikat Maity)

PREFACE

The present work embodied in the present thesis entitled "**Isolation, purification and characterization of polysaccharide and their use in the synthesis of metal nanoparticles and study of biological activities.**" was initiated on January, 2010.

This investigation was carried out in the Department of Chemistry and Chemical Technology, Vidyasagar University, Midnapore-721102, West Bengal, India during the period **2010-2016** under the supervision of **Professor Syed Sirajul Islam** and **Dr. Sumita Roy**, Department of Chemistry and Chemical Technology, Vidyasagar University, Midnapore-721102, West Bengal, India.

The present thesis has been presented into five chapters.

Chapter-I

Part-A describes the general introduction of carbohydrates, polysaccharides, and mushroom polysaccharides and also their biological activities

Part-B represents the introduction of nanoparticles, polysaccharide stabilized nanoparticles and their catalytic activities.

Chapter-II

Part-A deals with the methodologies that included isolation, purification, determination of the structure of polysaccharides, and biological studies.

Part-B deals with the methodologies for synthesis of polysaccharide stabilized gold nanoparticles and their catalytic activity.

Chapter-III deals structural characterization and immunological activities of the polysaccharide isolated from hot aqueous extract of the fruit bodies of somatic hybrid mushroom (*pfle 1q*) obtained through intergeneric protoplast fusion between *Pleurotus florida* and *Lentinula edodes*.

This work has been published in ***Bioactive Carbohydrates and Dietary Fiber***, 2013, *1*, 72-80.

Chapter-IV contains structural characterization and study of immunomodulating properties of another polysaccharide isolated from hot aqueous extract of the fruit bodies of hybrid mushroom (*pfle 1p*), obtained through intergeneric protoplast fusion between *Pleurotus florida* and *Lentinula edodes*.

This work has been published in ***Carbohydrate Research***, 2013, *374*, 89-95.

Chapter-V deals with the green synthesis of gold nanoparticles using aqueous solution of a hetero polysaccharide, extracted from the gum of *Cochlospermum religiosum* (katira gum) and its effectiveness as a heterogeneous catalyst in the conversion of 4-nitrophenol to 4-amino phenol.

This work was published in ***Physica E***, 2012, *45*, 130-134.

The papers have been appended to the end of the thesis.

ABBREVIATIONS

0D	0-Dimensional
1D	1-Dimensional
2D	2-Dimensional
3D	3-Dimensional
4-NP	4-nitrophenol
4-AP	4-aminophenol
λ_{max}	Absorption maximum
µg	Microgram
µL	Microliter
µM	Micromolar
A.blazei	Agaricus blazei
Ac_2O	Acetic anhydride
AIDS	Acquired immune deficiency syndrome
Au NPs	Gold Nanoparticles
Au	Gold
BRM	Biological response modifier
BSTFA	Bis (trimethylsilyl) trifluroacetamide
CF_3COOH	Trifluoro acetic acid
$CH_3CHOHCOOH$	Lactic acid
$CHCl_3$	Chloroform
CH_3COOH	Acetic acid
CH_3OH	Methanol
$C_6H_{12}O_5$	Rhamnose
Cm	Centimeter
Con A	Concanavalin A
CO_2	Carbondioxide
Da	Dalton
DEPT	Distortion less enhancemrnt by polarization transfer
DMEM	Dulbecco's modified Eagle's medium
D_6-DMSO	Deuterated dimethyl sulfoxide
D_2O	Deuterium oxide
DQF-COSY	Double-quantum filtered correlation spectroscopy
EtOH	Ethyl alcohol
fcc	face centered cubic
FT-IR	Fourier transform infrared spectroscopy

g	Gram
Gal	Galactose
Gal*p*A	Galacturonic acid
GC	Gas Chromatography
Glc	Glucose
GLC	Gas-liquid chromatography
GLC-MS	Gas-liquid chromatography-Mass spectrometry
GPC	Gel permeation chromatography
h	Hour(s)
HA	Hyaluronic acid
$HAuCl_4$	Chloroauric acid
HBSS	Hank's balanced salt solution
HCHO	Formaldehyde
HCl	Hydrochloric acid
HCOOH	Formic acid
HDP	Host defense potentiator
HMBC	Heteronuclear multiple bond correlation
HSQC	Heteronuclear single quantum coherence
HR-TEM	High-resolution transmission electron microscopy
H_2SO_4	Sulphuric acid
Hz	Hertz
IL-1	Interlukine 1
IL-2	Interlukine 2
IR	Infrared spectroscopy
J	Coupling constant
Kv	Kilovolt
KBr	Potassium bromide
LED	Light emitting diode
LPS	Lipopolysaccharide
M	Molar
Man	Mannose
Me	Methyl
mg	Milligram
MHz	Mega hertz
min	Minute(s)
mL	Milliliter
mM	Millimolar
ms	Millisecond

MTT	[3-(4,5-dimethylthiazol-2-yl)-2,5-diphenyltetrazolium bromide]
MW	Molecular Weight
m/z	Mass to charge ratio
$NaBH_4$	Sodium borohydride
NaOH	Sodium hydroxide
Ni	Nickel
NK	Natural killer cell
nm	Nanometer
NMR	Nuclear magnetic resonance
NO	Nitric oxide
NOE	Nuclear overhauser effect
NOESY	Nuclear overhauser enhancement spectroscopy
NPs	Nanoparticles
p	Pyranose
P_2O_5	Phosphorus pentoxide
PBS	Phosphate buffered saline
pfle 1p	Hybrid mushroom of *Pleurotus florida* and *Lentinula edodes* of starin *1p*
pfle 1q	Hybrid mushroom of *Pleurotus florida* and *Lentinula edodes* of starin *1q*
PMAA	Partially methylated alditol acetate
ppm	Parts per million
PS	Pure Polysaccharide
PS-I	Pure Polysaccharide of fraction I
RBC	Red blood cell
Rha	Rhamnose
RPMI	Roswell Park Memorial Institute
ROE	Rotating-frame Overhauser Enhancement
ROESY	Rotating-frame Overhauser Enhancement spectroscopy
rpm	Rotation per minute
SAED	Selected area electron diffraction
SEC	Size exclusion chromatography
SERS	Surface Enhanced Raman Spectroscopy
SPI	Splenocyte proliferation index
SPR	Surface Plasmon Resonance
T	Thousand
TFA	Trifluoroacetic acid
TMS	Tetramethyl silane

TOCSY	Total correlation spectroscopy
TPI	Thymocyte proliferation index
UV	Ultra violet
vis	Visible
v/v	Volume by volume ratio
w/v	Weight by volume ratio
XRD	X-ray Diffraction

CONTENTS

Abstract

The present thesis entitled "**Isolation, purification and characterization of polysaccharide and their use in the synthesis of metal nanoparticles and study of biological activities**" is divided into five chapters.

CHAPTER-I: This chapter is subdivided into two parts.

PART A: This part of chapter-I describes the introduction of carbohydrates, polysaccharides, especially mushroom polysaccharides on which the present investigation was carried out and some of their important biological activities. Carbohydrates are essential constituents of all living organisms and have a variety of vital functions. According to Robyt "Carbohydrates are polyhydroxy aldehydes or ketones or compounds that can be derived from them by oxidation, reduction or replacement of different functional groups." These are generally classified into four classes: monosaccharides, disaccharides, oligosaccharides, and polysaccharides. The great bulk of the carbohydrates in nature are present as polysaccharides, which are very large and complex molecules. Almost all living organism like fungi, plant etc. produces polysaccharides which are made up of chains of monosaccharides (the sugars) and linked together by glycosidic bonds. According to their structural features, polysaccharides can be classified as- (1) homopolysaccharides which are composed of one type of monosaccharides e.g. starch, cellulose, dextran etc. and (2) heteropolysaccharides which are composed of different monosaccharide units e.g. mannogalactan, xyloglucan, glucomannan etc.

Since the last few decades, polysaccharides from mushroom have drawn the attention of chemist and immunobiologists due to their immunomodulatory and antitumor properties. The main active components of the mushroom polysaccharides were proved to be the glucans, specifically β-D-glucans which are important for their outstanding ability to enhance and stimulate the immune systems and are thus regarded as typical biological response modifiers (BRMs). They possess antitumor effect through host defence mechanism against tumor without side effect. Except for β-D-glucans several polysaccharides having different composition and structure also showed biological effects. Currently, several mushroom polysaccharides isolated from *Lentinus edodes*, *Schizophyllum commune*, *Agaricus blazei*, *Grifola Frondosa*, and *Ganoderma lucidum* are widely used clinically as anti-tumor agents and many of them have been commercialized throughout the world. The biological activities of polysaccharides depend on the

molecular structure, molecular weight, size, branching frequency, structural modification, conformation, and solubility. It is therefore important to determine the exact structure and biological activity of the polysaccharides isolated from mushrooms.

PART B: This part deals with the discussion about synthesis of metal nanoparticles, especially gold nanoparticles via green route and various applications of nanoparticles in different fields. Utilization of nontoxic chemicals, environmentally benign solvents and renewable materials are some of the key issues for green synthesis strategy of metal nanoparticles. In recent years, biomolecules such as polysaccharides from plant and mushrooms are used in the synthesis of gold nanomaterials. In this route, biomolecules serve both as reducing and stabilizing agent. Microorganisms are also used for the synthesis of gold nanoparticles. Among the various applications of metal nanoparticles, the role of metal nanoparticles in the field of catalysis opens a new horizon. Metal nanoparticles in particular gold nanoparticles serve as an effective catalyst in the reduction of various pollutants like 4-NP, the most common organic pollutant in industrial and agricultural waste water. Green synthesis of metal nanoparticles and role of metal nanoparticles in the field of catalysis have been illustrated in this part.

CHAPTER-II: This chapter is also subdivided into two parts.

PART A: The methodologies that have been adopted during the whole course of the research tenure to determine the structure of polysaccharides and immunomodulating studies have been discussed in this part. The immunomodulating properties of the polysaccharides depend on the size of molecule, branching rate and form. So, it is very important to determine the exact structure of the polysaccharides. Purification of the polysaccharides should be done carefully as slight contamination of foreign sugar leads to wrong interpretation of the structure. The polysaccharide was purified using chromatographic technique like gel permeation chromatography. The accurate structures of the polysaccharides were determined using two types of methods:

(1) Chemical methods that include acid hydrolysis, methylation, and periodate oxidation studies.
(2) Spectroscopic method comprising of 1D (^{1}H, ^{13}C, and DEPT-135) and 2D NMR (DQF-COSY, TOCSY, NOESY, ROESY, HSQC, and HMBC).

The immunomodulating properties of different polysaccharides were examined by NO production by macrophages using Griess reagent. The activation of splenocyte and thymocyte tests were carried out in mouse cell culture medium with polysaccharide by the MTT [3-(4,5-dimethylthiazol-2-yl)-2,5-diphenyltetrazolium bromide] method.

PART B: In this part the detailed procedure of the synthesis of the gold nanoparticles (Au NPs) and the various techniques used in the characterization of the Au NPs have been discussed. The Au NPs were synthesized using gum polysaccharide of *Cochlospermum religiosum* (Katira gum) which acts as both reducing and stabilizing agent. The synthesized Au NPs were characterized using UV-vis, HR-TEM, XRD, and FT-IR techniques. The reduction of 4-NP to 4-AP by $NaBH_4$ in aqueous phase was studied as a model reaction to prove the catalytic activity of synthesized Au NPs.

CHAPTER-III: This chapter covers the isolation, purification, structural characterization and immunomodulating properties of a polysaccharide (PS) isolated from the edible hybrid mushroom *pfle 1q*, obtained through intergeneric protoplast fusion between *Pleurotus florida* and *Lentinula edodes*. Aqueous extract of fruit bodies of the hybrid mushroom strain, *pfle 1q* yielded single polysaccharide fraction, named as PS.

Structural analysis of PS

The PS showed a specific rotation of $[\infty]_D^{30.9}$ + 50.08 (*c* 0.09, water). The apparent average molecular weight of the PS fraction was estimated as 1.55×10^5 Da. The GLC analysis of the alditol acetates of the hydrolyzed product of PS confirmed the presence of mannose and galactose in a molar ratio of nearly 1:2. The absolute configuration of the monosaccharides was determined as D. The GLC-MS analysis of partially methylated alditol acetates revealed the presence of 1,5-di-*O*-acetyl-2,3,4,6-tetra-*O*-methyl-D-mannitol, 1,5,6-tri-*O*-acetyl-2,3,4-tri-*O*-methyl-D-galactitol, 1,2,5,6-tetra-*O*-acetyl-3,4-di-*O*-methyl-D-galactitol in a molar ratio of nearly 1:1:1. Thus, PS was assumed to consist of terminal D-mannopyranosyl, (1→6)-linked D-galactopyranosyl, and (1→2,6)-linked D-galactopyranosyl moieties respectively. These linkages were further confirmed by periodate oxidation experiment. The GLC-MS analysis of the alditol acetates of periodate oxidized, reduced, methylated PS showed total disappearance of sugar residues. These results indicated that all the sugar residues were consumed during oxidation. Thus, the mode of linkages present in the PS was confirmed.

The ^{1}H NMR spectrum of PS showed the presence of three signals in the anomeric region at δ 5.14, 5.00 and 4.81 in a ratio of nearly 1:1:1. They were designated **A**, **B**, and **C** according to their decreasing proton chemical shifts. Three signals in the anomeric region of ^{13}C spectrum at δ 101.6, 98.3, and 97.8 correlated to the residues **C**, **A**, and **B** respectively from HSQC spectrum. The rest of the ^{1}H and ^{13}C signals were assigned from DQF-COSY, TOCSY, and HSQC experiments. The proton coupling constants were measured from DQF-COSY experiment.

On the basis of proton and carbon chemical shifts, proton-proton coupling constants, and C-1, H-1 coupling constants, all the sugar residues were assigned as follows:

Residue **A:** (1→2,6)-linked α-D-galactopyranosyl residue.

Residue **B:** (1→6)-linked α-D-galactopyranosyl residue

Residue **C:** terminal β-D-mannopyranosyl residue

The different linkages that connected these three residues were determined from ROESY as well as NOESY spectrum. In ROESY spectrum, the inter-residual connectivities were observed between **A**H-1/**B**H-6a and **B**H-6b, **B**H-1/**A**H-6a and **A**H-6b, and **C**H-1/**A**H-2 along with other intra-residual contacts. Thus, from ROESY spectrum the following linkages were established.

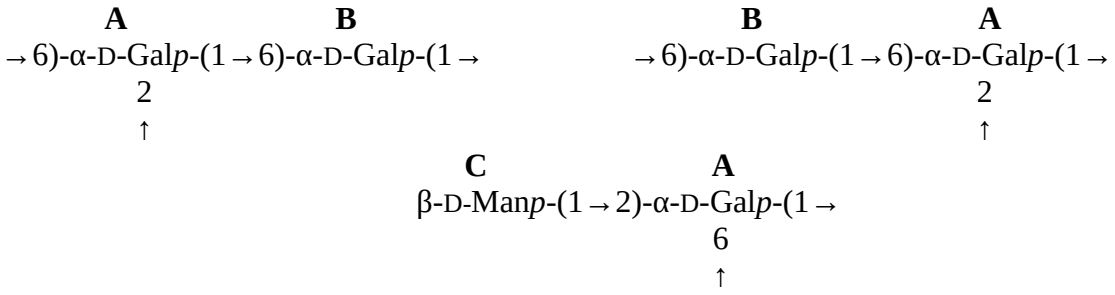

These connectivities were further confirmed from HMBC experiment. In HMBC spectrum the inter-residual cross-peaks were observed between **A**H-1/**B**C-6, **A**C-1/**B**H-6a and **B**H-6b, **B**H-1/**A**C-6, **B**C-1/**A**H-6a and **A**H-6b, **C**H-1/**A**C-2, and **C**C-1/**A**H-2. Thus, the HMBC and ROESY connectivities clearly supported the presence of the following repeating unit in the PS:

A **B**

→6)-α-D-Gal*p*-(1→6)-α-D-Gal*p*-(1→

2

↑

1

β-D-Man*p*

C

Immunomodulating properties of PS

Mushroom polysaccharides function as immunostimulator by activating the macrophages. Macrophages are white blood cells which play key roles in immune system defense. They usually engulf and destroy bacteria and viruses. Hence, macrophage activation induced by the PS was tested *in vitro*. On treatment with different concentrations of this PS it was observed that 25% to 34% of NO production increased up to 25 µg/mL. This was further increased by 87% to 114% at 50 and 100 µg/mL respectively, but decreased at 200 µg/mL. Hence, an enhanced production of NO i,e. the effective dose of this PS was observed at 100 µg/mL with optimum production of 12.8 µM NO per 5×10^5 macrophages.

Proliferation of splenocyte and thymocyte is an indicator of immunostimulation. The splenocyte and thymocyte activation tests were carried out in mouse cell culture medium with the PS by the MTT [3-(4,5-dimethylthiazol-2-yl)-2,5-diphenyltetrazolium bromide] method. The splenocyte and thymocyte proliferation indices as compared to PBS control if closer to 100 or below indicate low stimulatory effect on immune system. Both the splenocyte and thymocyte proliferation indices were found maximum at 50 µg/mL, above and below which it decreases. Hence, it can be concluded that 50 µg/mL is the optimum concentration of the PS for splenocyte and thymocyte proliferation.

CHAPTER-IV: This chapter describes the isolation, purification, and structural characterization and immunomodulating properties of a polysaccharide (PS-I) isolated from the edible hybrid mushroom *pfle 1p* obtained through intergeneric protoplast fusion between *Pleurotus florida* and *Lentinula edodes*. Aqueous extract of fruit bodies of the hybrid mushroom strain, *pfle 1p* yielded two polysaccharide fractions named as PS-I and PS-II.

Structural analysis of PS-I

The PS-I showed specific rotation $[\alpha]_D^{29.2}$ +32.6 (*c* 0.886, water). The average molecular weight of PS-I was estimated as ~2.1×10^5 Da from a calibration curve prepared with

standard dextrans. GLC analysis of alditol acetates of hydrolyzed product of PS-I confirmed the presence of glucose, galactose, and mannose almost in a ratio of 4:2:1. The absolute configuration of the sugar residues were determined as D. The GLC-MS analysis of partially methylated alditol acetates of PS-I revealed the presence of seven peaks in a molar ratio of nearly 1:1:1:1:1:1:1. The peaks were assigned as

1,5-di-*O*-acetyl-2,3,4,6-tetra-*O*-methyl-D-glucitol
1,5-di-*O*-acetyl-2,3,4,6-tetra-*O*-methyl-D-mannitol
1,5,6-tri-*O*-acetyl-2,3,4-tri-*O*-methyl-D-galactitol
1,5,6-tri-*O*-acetyl-2,3,4-tri-*O*-methyl-D-glucitol
1,3,5-tri-*O*-acetyl-2,4,6-tri-*O*-methyl-D-glucitol
1,3,4,5-tetra-*O*-acetyl-2,6-di-*O*-methyl-D-glucitol
1,2,5,6-tetra-*O*-acetyl-3,4-di-*O*-methyl-D-galactitol

Thus, PS-I was assumed to be consist of terminal D-glucopyranosyl, and D-mannopyranosyl, (1→6)-linked D-galactopyranosyl, (1→6)-linked D-glucopyranosyl, (1→3)-linked D-glucopyranosyl, (1→3,4)-linked D-glucopyranosyl, and (1→2,6)-linked D-galactopyranosyl moieties, respectively. These linkages were further confirmed by periodate oxidation experiment. The GLC-MS analysis of the alditol acetates of periodate oxidized, reduced and methylated PS-I showed the presence of 1,3,4,5-tetra-*O*-acetyl-2,6-di-*O*-methyl-D-glucitol and 1,3,5-tri-*O*-acetyl-2,4,6-tri-*O*-methyl-D-glucitol in a molar ratio of nearly 1:1. These results clearly indicated that the all other moieties except (1→3,4)-linked D-glucopyranosyl and (1→3)-linked D-glucopyranosyl were consumed during oxidation. Thus, the mode of linkages present in the PS-I were confirmed.

The ^{1}H NMR spectrum showed seven peaks in the anomeric region. The peaks were observed at δ 5.35, 5.12, 4.98, 4.78, 4.75, 4.51, and 4.49 in a ratio of nearly 1:1:1:1:1:1:1. They were designated as **A**, **B**, **C**, **D**, **E**, **F**, and **G** according to their decreasing proton chemical shifts. Seven peaks in the anomeric region of ^{13}C spectrum at δ 97.8, 98.2, 99.7 101.7, 102.4, 102.5, and 102.8 correlated to the residues **C**, **B**, **A**, **D**, **E**, **F**, and **G**, respectively from the HSQC spectrum. All the ^{1}H and ^{13}C signals were assigned using DQF-COSY, TOCSY, and HSQC experiments. The proton coupling constants were measured from DQF-COSY experiment.

On the basis of proton and carbon chemical shifts, proton-proton coupling constants, and C-1, H-1 coupling constants, all the sugar residues were assigned as follows:

Residue **A:** (1→6)-linked α-D-glucopyranosyl residue

Residue **B:** (1→2,6)-linked α-D-galactopyranosyl residue

Residue **C:** (1→6)-linked α-D-galactopyranosyl residue

Residue **D:** terminal β-D-mannopyranosyl residue

Residue **E:** (1→3)-linked β-D-glucopyranosyl residue

Residue **F:** (1→3,4)-linked β-D-glucopyranosyl residue

Residue **G:** terminal β-D-glucopyranosyl residue

The different linkages that connected these seven residues were determined from NOESY as well as ROESY spectrum. In NOESY spectrum, the inter-residual connectivities were observed between **A**H-1/**B**H-6a; **A**H-1/**B**H-6b; **B**H-1/**C**H-6a; **B**H-1/**C**H-6b; **C**H-1/**E**H-3; **D**H-1/**B**H-2; **E**H-1/**F**H-3; **F**H-1/**A**H-6a; **F**H-1/**A**H-6b; **G**H-1/**F**H-4 along with other intra-residual contacts. Finally, these connectivities were confirmed from HMBC spectrum. In this spectrum the inter-residual cross-peaks were observed between **A**H-1/**B**C-6; **A**C-1/**B**H-6a and **B**H-6b; **B**H-1/**C**C-6; **B**C-1/**C**H-6a and **C**H-6b; **C**H-1/**E**C-3; **C**C-1/**E**H-3; **D**H-1/**B**C-2; **D**C-1/**B**H-2; **E**H-1/**F**C-3; **E**C-1/**F**H-3; **F**H-1/**A**C-6; **F**C-1/**A**H-6a and **A**H-6b; **G**H-1/**F**C-4; and **G**C-1/**F**H-4. Thus, the probable structural motif present in PS-I was established as:

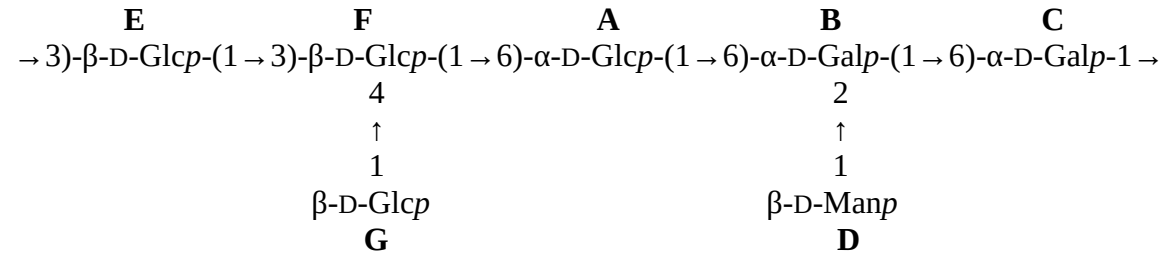

Immunomodulating properties of PS-I

To test immunomodulatory effects of PS-I, murine macrophages were incubated with PS-I in a humidified atmosphere of 5% CO_2 at 37 °C for 48 h and the production of nitric oxide (NO) was measured using Griess reagent (1:1 of 0.1% in 1-napthylethylenediamine in 5% phosphoric acid and 1% sulfanilamide in 5% phosphoric acid). On treatment with different concentrations of the PS-I, it was observed that NO production increased with increase in concentration up to 50 µg/mL with optimum production of 19.27 µM NO per 5×10^5

macrophages at 50 µg/mL which subsequently decreased with increase in concentration. Hence, the effective dose of the PS-I for macrophage activation was 50 µg/mL. Splenocyte is the cells present in the spleen that include T cells, B cells, dendritic cells, etc. that stimulate the immune response in living organism whereas thymocyte is the hematopoietic cells present in thymus and the primary function of which is the generation of T cells. Proliferation of splenocyte and thymocyte is an indicator of immunostimulation. Splenocyte and thymocyte proliferation in the presence of PS-I was used to evaluate cell stimulatory effects on the immune cell activation. Both the splenocyte and thymocyte proliferation indices were found maximum at 50 µg/mL, above and below which it decreases. Hence, it can be concluded that 50 µg/mL is the optimum concentration of the PS-I for splenocyte and thymocyte proliferation.

CHAPTER-V: A green synthesis of gold nanoparticles (Au NPs) using aqueous solution of a hetero polysaccharide, extracted from the gum of *Cochlospermum religiosum* (katira gum), has been demonstrated in this chapter. Here, the hetero polysaccharide plays the role of both reducing and stabilizing agent.

Synthesis and characterization of Au NPs

For the synthesis of Au NPs, 2 mL aqueous solution of chloroauric acid ($HAuCl_4$) with a concentration of 10^{-3} M was added to 6 mL 0.2 % (w/v) aqueous polysaccharide solution. The mixture was then heated at 70 °C for 6 h with continuous stirring on a magnetic stirrer and UV-vis spectra of the reaction mixture were recorded at different time interval till the completion of the reaction. A pale pink color was appeared after 10 min of the reaction and the color was gradually intensified as the reaction was continued with heating. A typical plasmon resonance band at 544 nm appeared after 1 h indicating formation of Au NPs. The intensity of the absorption band gradually increased and the maximum intensity of absorption was attained after 6 h of the reaction. This gradual increase in the absorption band is attributed to the fact that Au NPs concentration increases in the media as the reduction reaction proceeds. After 6 h, no significant change in intensity at 528 nm was observed which indicated almost complete reduction of Au^{+3}. The shifting of surface plasmon absorption maxima from 544 nm to a fixed value 528 nm at 6 h may be due to decrease in particles size.

The shape, morphology, and size distribution of the Au NPs were analyzed using high resolution transmission electron microscopy (HR-TEM). HR-TEM image showed that the

particles are mostly spherical with a few having rod and decahedral morphology. The average size of the particles is 6.9 nm as revealed from particle size distribution histogram. The SAED pattern showing rings ascribed to (111), (200), (220), (311), and (331) planes exhibited the face centered cubic (fcc) crystalline structure of gold. The crystalline nature of Au NPs was further confirmed by X-ray diffraction (XRD) analysis. A typical XRD pattern exhibited peaks at 38.22º, 44.40º, 64.51º, and 77.49º that can be indexed to the (111), (200), (220), and (311) facets, respectively of fcc gold. In order to investigate the interaction of Au NPs with the polysaccharide, FT-IR experiment of both the polysaccharide and Au NPs-polysaccharide bioconjugates were carried out. In the FT-IR spectrum of polysaccharide, two partially overlapped peaks at 1071 and 1043 cm^{-1} were assigned to C-OH stretching along with a broad stretching peak at 3428 cm^{-1} for hydroxyl group and a weak band at 2935 cm^{-1} for aliphatic C-H stretching. In the FT-IR spectrum of Au NPs-polysaccharide bioconjugates two overlapped peak at 1071 and 1043 cm^{-1} merged to give a single peak at 1044 cm^{-1}, which is possibly due to the interaction of Au^{+3} with the oxygen of hydroxyl group (C-OH) from polysaccharide. The peaks for hydroxyl group (3400 cm^{-1}), aliphatic C-H (2924 cm^{-1}) and C-OH (1044 cm^{-1}) are also appeared in the spectrum of Au NPs-polysaccharide bioconjugates which are the characteristic peaks of polysaccharides. So, it can be believed that there is some interaction between the Au NPs and polysaccharide with the help of which the Au NPs attain stability.

Catalytic activity of Au NPs-polysaccharide bioconjugates

To investigate the catalytic activity of Au NPs-polysaccharide bioconjugates, the reduction of 4-nitrophenol (4-NP) to 4-aminophenol (4-AP) by $NaBH_4$ in aqueous phase was chosen as a model reaction. The absorption peak of 4-NP was red shifted from 317 to 400 nm immediately after the addition of $NaBH_4$ solution, which also associated with a color change of 4-NP solution from yellow to yellow green due to formation of 4-aminophenolate ion in alkaline condition. The absorption peak at 400 nm remained unaltered for a long duration in absence of Au NPs-polysaccharide bioconjugates. In contrast, with the addition of Au NPs-polysaccharide bioconjugates, the absorption peak height at 400 nm successively decreased with a concomitant appearance of two new absorption peaks around 230 and 300 nm with time, which was because of the generation of 4-AP. The blank experiment by adding only the hetero polysaccharide into the aqueous solution of 4-NP and $NaBH_4$ mixture, did not change the color or absorption peak of 4-nitrophenolate ions for more than 24 h, which clearly demonstrated that the reduction of 4-

NP by $NaBH_4$ is solely activated by Au NPs-polysaccharide bioconjugates. The formation of 4-AP in the catalytic reaction was further confirmed by the ^1H NMR study in D_6-DMSO. As the initial concentration of $NaBH_4$ largely greater than the initial concentration of 4-NP, it can be assumed that concentration of $NaBH_4$ remains constant with time during the reaction. Hence, the reaction rate is independent on the concentration of $NaBH_4$. So pseudo-first-order rate kinetics with respect to 4-NP concentration was used to evaluate the rate of the reaction and reaction rate constant is determined to be 2.67×10^{-2} min^{-1}.

Chapter – I: PART-A

Introduction to carbohydrate and polysaccharide

1.A.1. Carbohydrates

Carbohydrates are the most abundant group of organic compounds found in nature. They originate as the product of photosynthesis and play crucial role to sustain life on the Earth. They serve as major source (sugars) and storage of energy (starch, fructan, and glycogen). They also serve as structural components such as cellulose in plants and chitin in some animals. They play the role of information transfer agent as a part of nucleic acids.

Carbohydrates are generally defined as organic compounds made up of carbon, hydrogen, and oxygen with the formula $C_x(H_2O)_y$. The name carbohydrates (i.e. hydrates of carbon) are so called because they contain hydrogen and oxygen in the same proportion as in water. Although a large number of carbohydrates fit with this general formula but certain compounds such as formaldehyde (HCHO), acetic acid (CH_3COOH), and lactic acid ($CH_3CHOHCOOH$), which have got the same empirical formula, are not regarded as carbohydrates. On the other hand some compounds like rhamnose ($C_6H_{12}O_5$) and uronic acids do not conform to the formula, although they are regarded as carbohydrates. According to Robyt [1] the more comprehensive definition of carbohydrate is "Carbohydrates are polyhydroxy aldehydes or ketones, or compounds that can be derived from them by oxidation, reduction or replacement of different functional groups".

❖ Classification of carbohydrates

Carbohydrates are generally classified as monosaccharides, disaccharides, oligosaccharides, and polysaccharides.

- **Monosaccharides** are the most fundamental units of carbohydrates consisting of polyhydroxy aldehydes or polyhydroxy ketones. They cannot be further hydrolyzed into smaller carbohydrate unit. They are usually colorless, water soluble, and crystalline solids. The most abundant monosaccharide in nature is the D-glucose. A few other examples of monosaccharide are mannose, galactose, fructose, ribose, arabinose etc.

- **Disaccharides** are produced when two monosaccharides undergo a condensation reaction involving the elimination of one molecule of water along with the formation of a glycosidic bond. Based on the monosaccharide composition, disaccharides are of two categories namely homogeneous and heterogeneous disaccharide. They can also be divided as reducing and non-reducing types depending upon whether they possess a free hydroxyl group on anomeric carbon or not. Lactose and sucrose are the most important

naturally occurring disaccharides. Lactose, made up of galactose and glucose and sucrose made up of glucose and fructose, are two important disaccharides present in the milk and sugar cane, respectively.

Oligosaccharides are joined together with three to nine monosaccharide units by glycosidic linkages and on hydrolysis it generates 3 to 9 monosaccharide units. Depending on the number of monosaccharide units, they are called trisaccharides, tetrasaccharides, pentasaccharides etc. Raffinose, maltotriose (trisaccharide) and stachyose (tetrasaccharide) are the example of oligosaccharides. Maltotriose is composed of three glucose units whereas raffinose is formed by glucose, galactose, and fructose units.

Polysaccharides are those compounds in which more than 9 monosaccharide units are joined together by glycosidic bonds.

1.A.2. Polysaccharides

Polysaccharides are considered as the first biopolymers formed on Earth [2]. They are polymeric carbohydrate molecules composed of 10 to several thousand monosaccharide units joined together by glycosidic linkages and on hydrolysis give the constituent monosaccharides or oligosaccharides. They range in structure from linear to highly branched.

❖ Classification of polysaccharides

♣ On the basis of function

- **Storage polysaccharides**- The polysaccharides which serve as energy storage in plants and animals are called storage polysaccharides. E.g. starch, glycogen, inulin etc.
- **Structural polysaccharides**- The polysaccharides which have structural roles in plant cell wall or exoskeleton of insects are called structural polysaccharides. E.g. cellulose, chitin, arabinoxylans etc.

♣ On the basis of composition

- **Homopolysaccharides**- Polysaccharides which consist of only one kind of monosaccharide units are called homopolysaccharides. E.g. starch, glycogen, cellulose, chitin, inulin etc.
- **Heteropolysaccharides**- Polysaccharides which consist of different types of monosaccharide units are called heteropolysaccharides. E.g. arabinoxylan, pectin, glucomannan, xyloglucan, galactomannan etc.

♣ On the basis of charge

- **Neutral -** cellulose, starch, amylose, guar gum etc.
- **Anionic** - alginates, xanthan, gellan, gum arabic etc.
- **Cationic** – chitosan

♣ On the basis of structure

- **Linear -** cellulose, aliginates, amylose etc.
- **Branched** – amylopectin, gum arabic, arabinoxylan etc.

❖ Structure and function of some common Polysaccharides

• Starch

Pure starch is white, tasteless, and odorless powder that is insoluble in cold water. Most of the green plants produce starch as an energy store. Potato, rice, wheat, sorghum, and maize (corn) are the major sources of starch in human diet. It generally consists of two types of molecules, 20-25% amylose and 75-80% amylopectin [3]. Both of them consist of polymers of α-D-glucose units. Amylose is a linear glucose polymer with α-(1→4) glycosidic linkages [Figure 1], whereas amylopectin is a branched glucan composed of (1→4)-α-D-Glc*p* and (1→4,6)-α-D-Glc*p* residues [Figure 2].

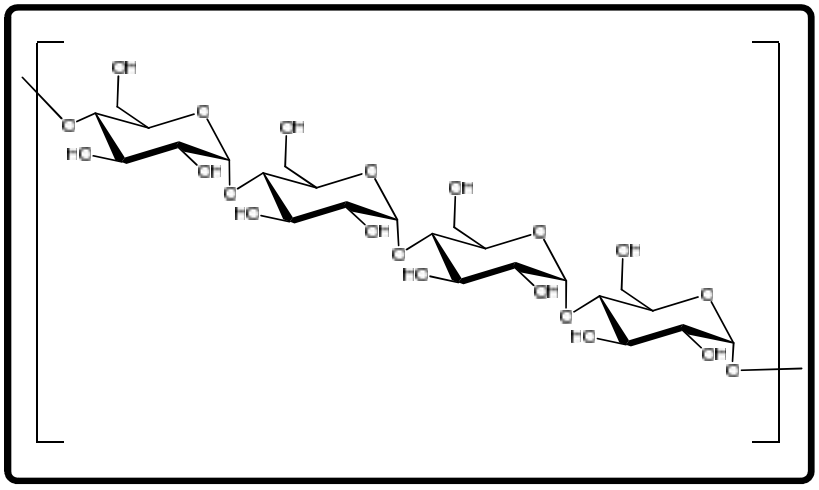

Figure 1. α-Amylose, the linear component of starch.

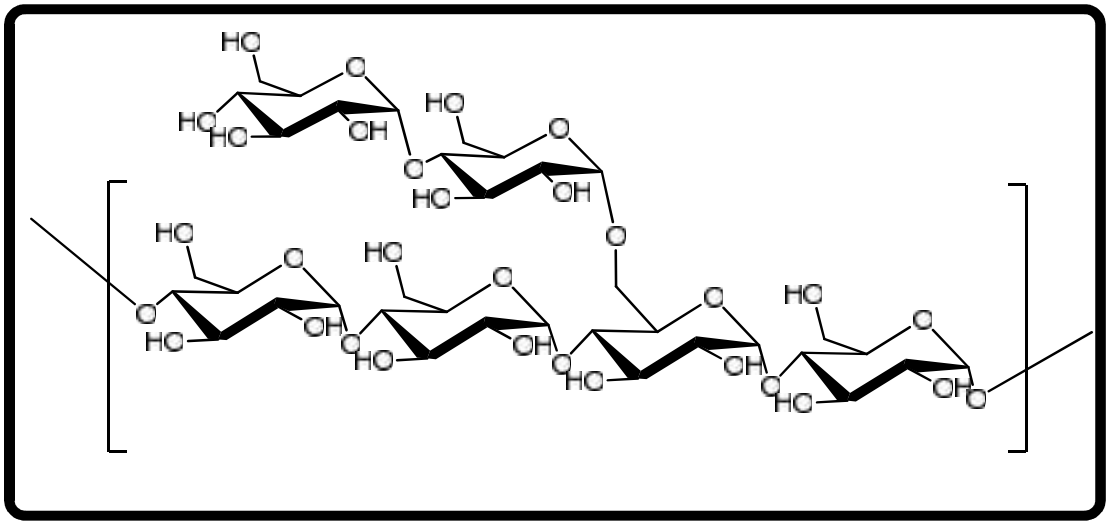

Figure 2. Amylopectin, (1→4)-α-, (1→6)-α-D-glucose polymer.

- **Glycogen**

Glycogen is the storage form of glucose in animals which is analogous to the starch in plants. It is a homopolysaccharide having same structure as amylopectin with more extensive branching. Animals use it for the short-term storage of food energy. It is stored mainly in liver and muscles of animals, and is called as 'animal starch'.

- **Cellulose**

Cellulose is the most abundant organic polymer on Earth [4]. It is the main constituent of the cell wall in all green plants [5]. It is an odorless, biodegradable fibrous polymer which is insoluble in water and most organic solvents. Cellulose [Figure 3] is high molecular weight polymer of (1→4)-β-linked-D-glucopyranosides [6,7]. In contrast to starch, β-D-glucose is oriented with $-CH_2OH$ groups alternating above and below the plane of the cellulose molecule thus producing long linear chain. The digestive enzyme of most animals including human beings cannot attack its β-(1→4)-linkages although these can digest starch, composed of glucose having α-(1→4)-linkage. Some animals, such as cows, horses, sheep and goats can digest cellulose due to presence of bacteria in their digestive tracts.

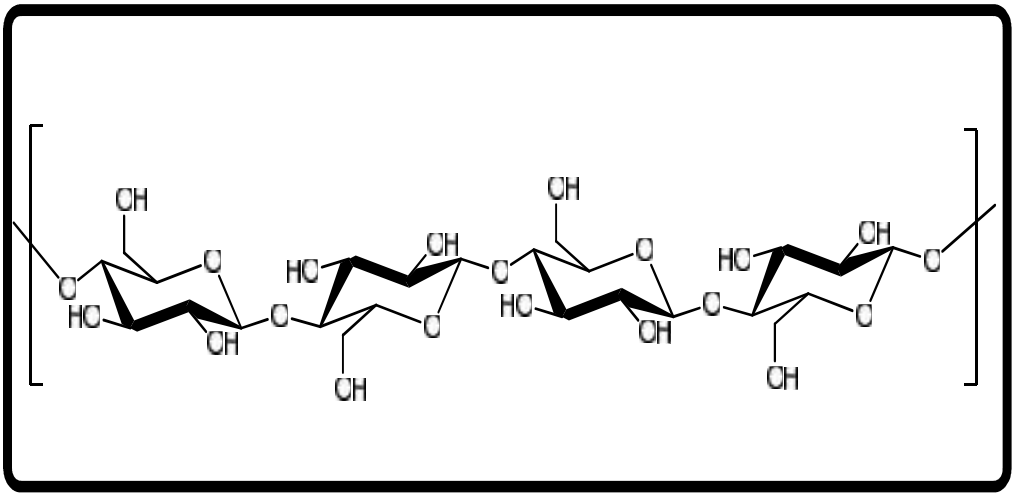

Figure 3. Cellulose, β-(1→4) linked glucose polymer.

- **Pectin**

Pectin is a complex set of heterogeneous polysaccharides containing galacturonic acid or its ester in the backbone [Figure 4]. They are present in most primary cell walls of terrestrial plants as cementing materials. These are an important part of human diet but do not play a significant role to nutrition. Apples, quinces, plums, gooseberries, guavas, oranges and other citrus fruits are rich source of pectin whereas soft fruits like cherries, grapes, and strawberries contain little amount of pectin. It is mainly used as gelling agent, thickening agent for the production of jams and jellies. It is also used in fillings, medicines, sweets, as a stabilizer in fruit juices and milk drinks, and as a source of dietary fibre [8].

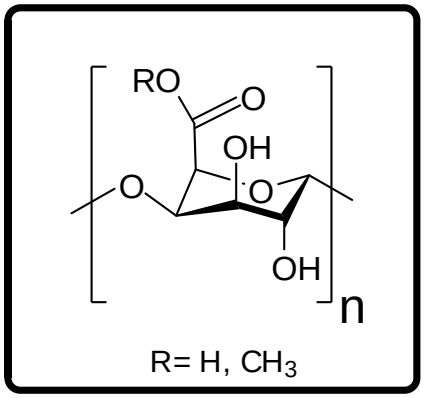

Figure 4. Pectins contain α-(1→4) linked galacturonic acid or its ester in the backbone.

- **Chitin**

Chitin is a long-chain polymer of β-(1→4)-linked N-acetylglucosamine [Figure 5], a derivative of glucose. It is the main constituent of exoskeletons of arthropods (e.g. crabs, lobsters, and shrimps) and insects, the cell walls of fungi, the radulas of molluscs and the beaks of cephalopods including octopuses. It is used as ion-exchange resins in water purification system and also as fertilizer. Surgical thread can be made from chitin because of its strength and flexibility. It accelerates healing of wounds in human [9].

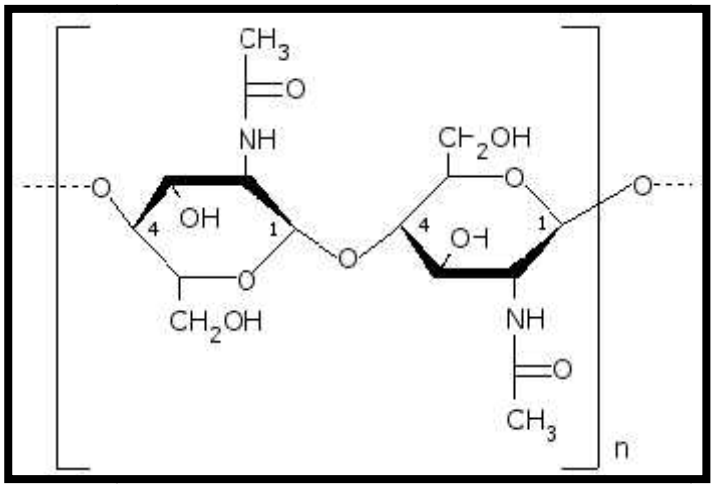

Figure 5. Chitin, a β-(1→4)-linked N-acetylglucosamine polymer.

- **Hyaluronic acid**

It is a linear polymer of disaccharides of D-glucuronic acid and N-acetyl-D-glucosamine linked via alternating β-(1→4) and β-(1→3) glycosidic bonds [Figure 6]. Hyaluronic acid is found in the skin, vitreous humour of the eye, as a coating around

the ovum and in certain bacteria. It acts as a cementing substance in connective tissue. It is also present in the synovial fluid of joints, where its viscosity makes it a good lubricant.

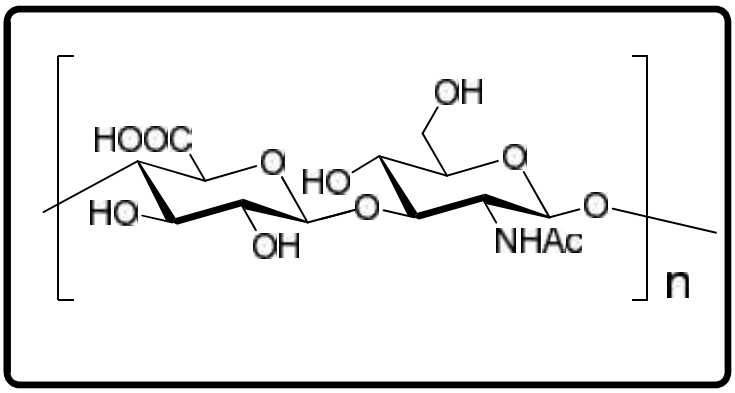

Figure 6. Hyaluronic acid, consisting of disaccharide repeating unit of glucuronic acid and N-acetyl glucosamine.

1.A.3. Mushrooms

❖ Description

Mushrooms have been valued by human kind as an edible and medical resource. According to Chang and Miles 'Mushroom' is "a macro fungus with a distinctive fruiting body which can be either hypogenous or epigeous, large enough to be seen with the naked eye and to be picked by hand" [10]. The fruiting body of mushroom is umbrella like with various shapes, size and color. They are found in soil, on decomposing leaves and in mulch and compost. A mushroom and its various parts have been shown in Figure 7.

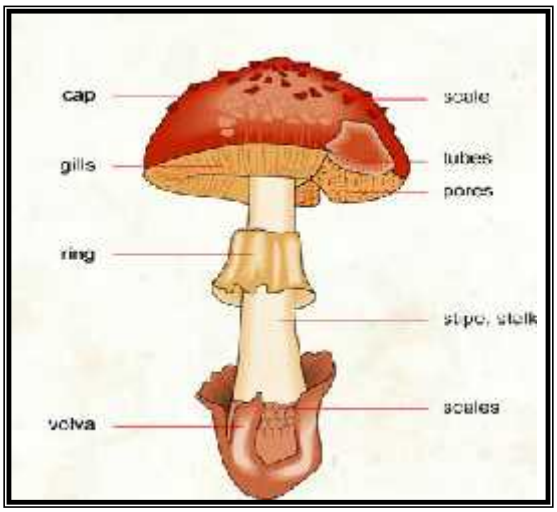

Figure 7. A true mushroom.

About 1, 40,000 mushrooms are reported to exist on Earth; 10 % of these mushrooms have been identified today, about 50 % of which are considered to possess varying degrees of edibility and more than 2000 mushrooms are safely edible and about 700 species are known for possessing significant pharmacological properties [11,12].

❖ Chemical composition

Mushrooms contain ~ 90% water by weight. The remaining portion (10%) consists of 10-40% protein, 2-8% fat, 3-32% fibre, 3-28% carbohydrate, and 8-10% ash with potassium, calcium, phosphorus, magnesium, iron, zinc, and copper [13]. Various kind of vitamins mainly niacin, thiamine, riboflavin, biotin, and vitamin C are found in mushrooms. They also contain a wide variety of bioactive molecules including terpenoids, steroids, phenols, nucleotides, glycoproteins, and polysaccharides.

❖ Nutritive value

Mushrooms have long been considered as a source of powerful nutrients. Mushrooms are low-calorie food usually eaten cooked or raw and as garnish to a meal. Mushrooms are being extensively used in many countries for food and fodder [14-16]. They are rich in high quality protein, minerals, and vitamins but low in fat content. Due to their high content of protein, mushrooms are considered as “poor man’s protein” [17]. Studies on a number of species of mushrooms have shown that the protein part of some mushrooms is equal to muscle protein in nutritive value. Chemical analyses have shown that the composition of amino and fatty acids, vitamins, minerals etc., in the main commercial mushrooms is comparable to meats and higher than fruits and vegetables.

❖ Medicinal properties

Mushrooms have been used in folk medicine throughout the world since ancient times and considered to be one of the most useful antitumor agents for clinical uses [11]. Currently mushroom derived substances having antitumor and immunomodulating properties are used as dietary supplements or drugs [18]. Different parts of the mushroom are being used for the treatment of blood sugar, high blood pressure, as well as for the beauty treatment [11].

❖ Hybrid mushroom

The present investigation was carried out with the polysaccharides isolated from hybrid mushrooms. Quality traits within the gene pool of any particular edible mushroom species are limited. Development of new hybrid strains are therefore needed in order to introduce important qualitative and quantitative traits like high bio-effeciency, high temperature tolerance, enhanced shelf life and shorter cropping periods within a gene pool. Production of hybrid mushroom strains through para-sexual mating is well known. Protoplast fusion proved to be a feasible method for inter-specific and inter-generic hybridization for strain improvement among edible mushrooms [19]. There are number of reports on production of hybrid mushroom through inter-generic protoplast fusion. Several hybrid fruit bodies e.g. PC H8, PC H11, PC H17, and PC H18 were prepared through protoplast fusion between two edible strains *Pleurotus florida* and *Calocybe indica* [20]. Protoplast fusion of *Pleurotus florida* and *Volvariella volvacea* produced two new fruit bodies *PfloVv1aFB* and *PfloVv5FB* [21]. Twelve inter-generic somatic hybrids named as *pfls* were produced through PEG-mediated protoplast fusion between *Pleurotus florida* and *Lentinus squarrosulus* using double selection method [22].

1.A.3.1. MUSHROOM POLYSACCHARIDES

Polysaccharides are the most potent mushroom derived substances with antitumor and immunomodulating properties [23-27]. Mushrooms are potential source of different polysaccharides like chitin, hemicelluloses, glucans, and heteroglycans. Mushroom polysaccharides are present mostly as glucans with different types of glycosidic linkages, such as (1→6)-β-D-glucan, (1→3)-, (1→6)-β-D-glucans, (1→3)-α-D-glucans, and some are true heteroglycans. In some mushroom species, active polysaccharides bound with proteins or peptides are known as polysaccharide-protein or polysaccharide-peptide complex [28].

❖ Structures and biological activities of mushroom polysaccharides

A wide range of biologically active polysaccharides of different chemical structures from mushrooms have been investigated. Study on medicinal properties of mushroom polysaccharides included antitumor, immunomodulating, antioxidative, antiflammatory, antiviral, antithrombotic, antimicrobial, cytotoxic, and antidiabetic effects [29-37]. The

most important molecule isolated from mushrooms is β-D-glucans. β-D-glucans are composed of D-glucose monomers, joined together by β-glycosidic linkages. The structures of the several biologically active linear and branched β-glucan have been reported. There are series of report on β-glucans regarding to their antitumor and anticancer activities [38,39]. It appears that the most active forms of β-glucans contain (1→3), (1→6) linkages. β-D-(1→3,1→6)-linked glucans have the ability of enhancing and stimulating the immune system of humans and thus called biological response modifiers (BRMs) [40]. Glucans having α- or both α- and β- linkages are also isolated in different mushrooms [41-44]. (1→3)-α-D-glucan derivatives also show important medicinal properties [45,46]. Linear low molecular weight (1→4)-α-D-glucan is also used as an immunomudulator and anticancer agent [47,48]. Besides glucans, polysaccharides having other chemical structures, such as hetero glycans [49], β-glucan-protein [50], α-manno-β-glucan [47], heteroglycan-protein complexes [51] also exhibit antitumor activity.

The activity of mushroom polysaccharide depends greatly on the molecular structure, molecular weight, size, branching frequency, structural modification, conformation and solubility [52]. It is true that structural features such as β-(1→3) linkages in the main chain of the glucan and additional β-(1→6) branch points are needed for antitumor action. β-glucan containing mainly (1→6) linkages have less activity [52]. High molecular weight glucans appears to be more effective than those of low molecular weight [53,54]. The immune functions of mushroom polysaccharides apparently depend on their conformation complexity. It has been suggested that higher degree of structural complexity is associated with more potent immunomodulatory and anti-cancer effects. Polysaccharides that form triple-helical conformation have clinical applications for the treatment of cancers like human breast cancer (MCF-7), human promyeloctytic leukemia (HL-60) and human liver cancer (HpG2) [35]. Solubility in water is one of the more important characteristics of mushroom polysaccharides. In mushrooms, β-glucans are present either in their water soluble or insoluble form. The biological activity of water soluble form, however, has been shown to be much greater in humans and animals and to more pronounced effect on their immune systems [52]. It has been found that structural modifications sometime improve the medicinal properties and water solubility of mushroom polysaccharides. The procedures used for modification of mushroom polysaccharides are Smith degradation, formolysis, and carboxymethylation. A water insoluble, alkali soluble linear (1→3)-α-D-

glucan obtained from *Amanita muscaria* and *Agrocybe aegerita* had little antitumor effect, while carboxymethylated products showed potent antitumor activity [46,55].

❖ Some important immunomodulating and antitumor mushroom polysaccharides

- **Lentinan**, produced from Shiitake mushroom, *Lentinus edodes*, is a (1→3)-, (1→6)-β-D-glucan. It was first isolated and studied by Chihara et al. who demonstrated that its antitumor effects were greater than other mushroom polysaccharides [56]. It stimulates the production of white blood cells in the human cell line U937 [57]. Clinical studies of cancer patients treated with lentinan showed a higher survival rate, higher quality of life and lower re-occurrence of cancer [58-60].

- **Schizophyllan** is the polysaccharide derived from the mushroom *Schizophyllum commune*. The polysaccharide schizophyllan shows antitumor activity against both the solid and ascite forms of Sarcoma 180, as well as against the solid form of Sarcoma 37, Erlich Sarcoma, Yoshida Sarcoma and Lewis lung carcinoma [61]. Early clinical studies with schizophyllan in combination with conventional chemotherapy (tegafur or mitomycin C and 5-fluorouracil) in a study of 367 patients with gastric cancer showed significant increase in median survival [62]. In a randomized controlled study of schizophyllan in combination with radiotherapy, showed that it significantly prolonged the overall survival of stage II cervical cancer patients [63,64].

- **Krestin,** a unique protein bound polysaccharide (PSK), was developed from turkey tail mushroom *Trametes versicolor*. It contains 75% glucan and 25% protein [65]. PSK has remarkable immunostimulating activity and exhibits a marked effect against different types of tumors. With regard to its antitumor properties, it acts directly on tumor cells, as well as indirectly in the host to boost cellular immunity [66,67]. It has shown antitumor activity in animals with adenosarcoma, sarcoma, melanoma, carcinoma, plasmacytoma, fibrosarcoma, mastocytoma, mammary, colon and lung cancer [68].

- **Agarican**, the polysaccharide isolated from *Agaricus blazei* was shown to be a stimulant of immune system, promoting body's natural defense mechanisms to fight a variety of infectious agents and conditions, including cancer. The immunostimulating

activity and antitumor action of *Agaricus blazei* extracts were investigated against Sarcoma 180 and fibrosarcoma tumor-bearing mice [69,70]. Seven polysaccharide fractions obtained from *A. blazei* fruit bodies were demonstrated to have antitumor activity [71]. A new antitumor polysaccharide, (1→2)-, (1→3)-β-D-glucomannan [72] active against Sarcoma 180 was recently separated from liquid cultured mycelium of *Agaricus blazei*.

Studies have shown that (1→3)-, (1→6)-β-D-glucan (**Grifron-D**) derived from another mushroom *Grifola frondosa* (also known as Maitake) have strong antitumor activity [73]. It has been shown to have a cytotoxic effect on human prostate cancer cells (PC9) in vitro, possibly acting through oxidative stress and causing 95% cell death by an apoptosis [74].

❖ Mechanism of antitumor and immunomodulating action of mushroom polysaccharides

Mushroom polysaccharides exert their antitumor action by stimulating the immune response of the host organism. These substances are regarded as biological response modifiers, BRMs [40] as they modify the host's biological response by stimulation of the immune system and causing no harm to the body. Mushrooms polysaccharides do not attack cancer cell directly, but they exhibit antitumor properties by stimulating macrophages such as natural killer cells (NK-cell), T-cell, B-cell and macrophage-dependent immune systems [52]. β-Glucans can stimulate macrophages [75], neutrophils [38], and NK cells [76] and thereby destroy the sensitive tumor cells. It can promote T cell-specific responses [77] through triggering the secretion of IFN-g, IL-6, IL-8, and IL-12 from macrophages, neutrophils, and NK cells [78]. A possible pathway of the biological action of β-D-Glucan has been represented in Figure 8.

Lentinan appears to act as a host defence potentiator (HDP) which is able to restore or boost the responsiveness of host cells to lymphocytokynes, hormones and other biologically active substances by stimulating maturation, differentiation or proliferation of cells involved in host defence mechanism [79]. HDP is functionally different from BRM. Lentinan is able to increase host resistance against various kinds of infectious disease including AIDS and also restore the suppressed activity of helper T-cells in the tumor-bearing host to their normal state, leading to complete restoration of humoral immune

responses [27]. The biological action of Lentinan has been demonstrated by Chihara [80] and represented in Figure 9.

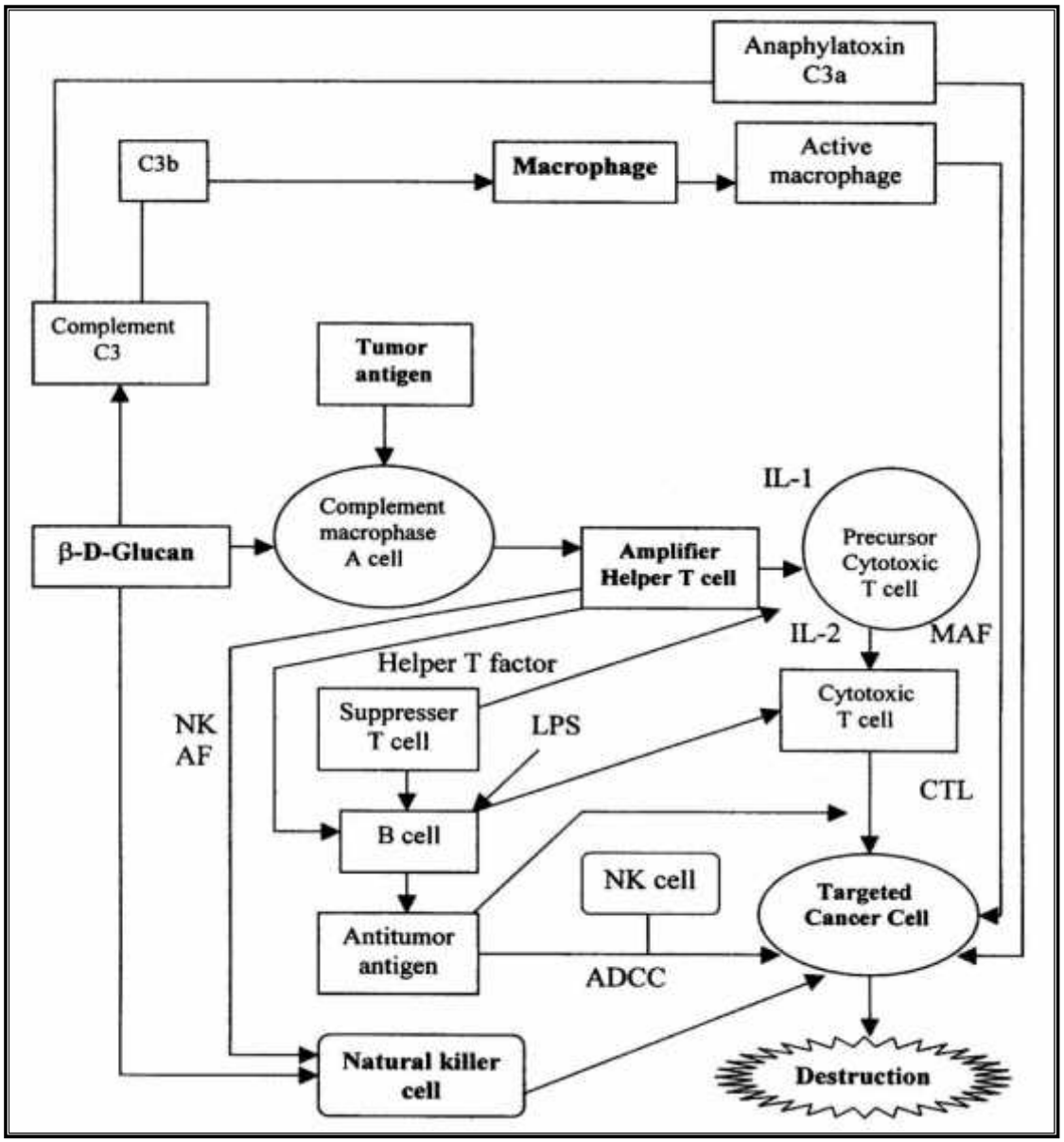

Figure 8. Schematic representation showing the mode of action of polysaccharide, β-glucan as biological response modifier to target cancer cell.

[NK: Natural Killer cell; AF: Antibody Formation; LPS: Liver Protein Serum; ADCC: Antibody Dependent Cell mediated Cytotoxicity; CTL: Cytotoxic T-Lymphocyte; MAF: Macrophage Activating Factor; IL-1: Interlukine 1; IL-2: Interlukine 2].

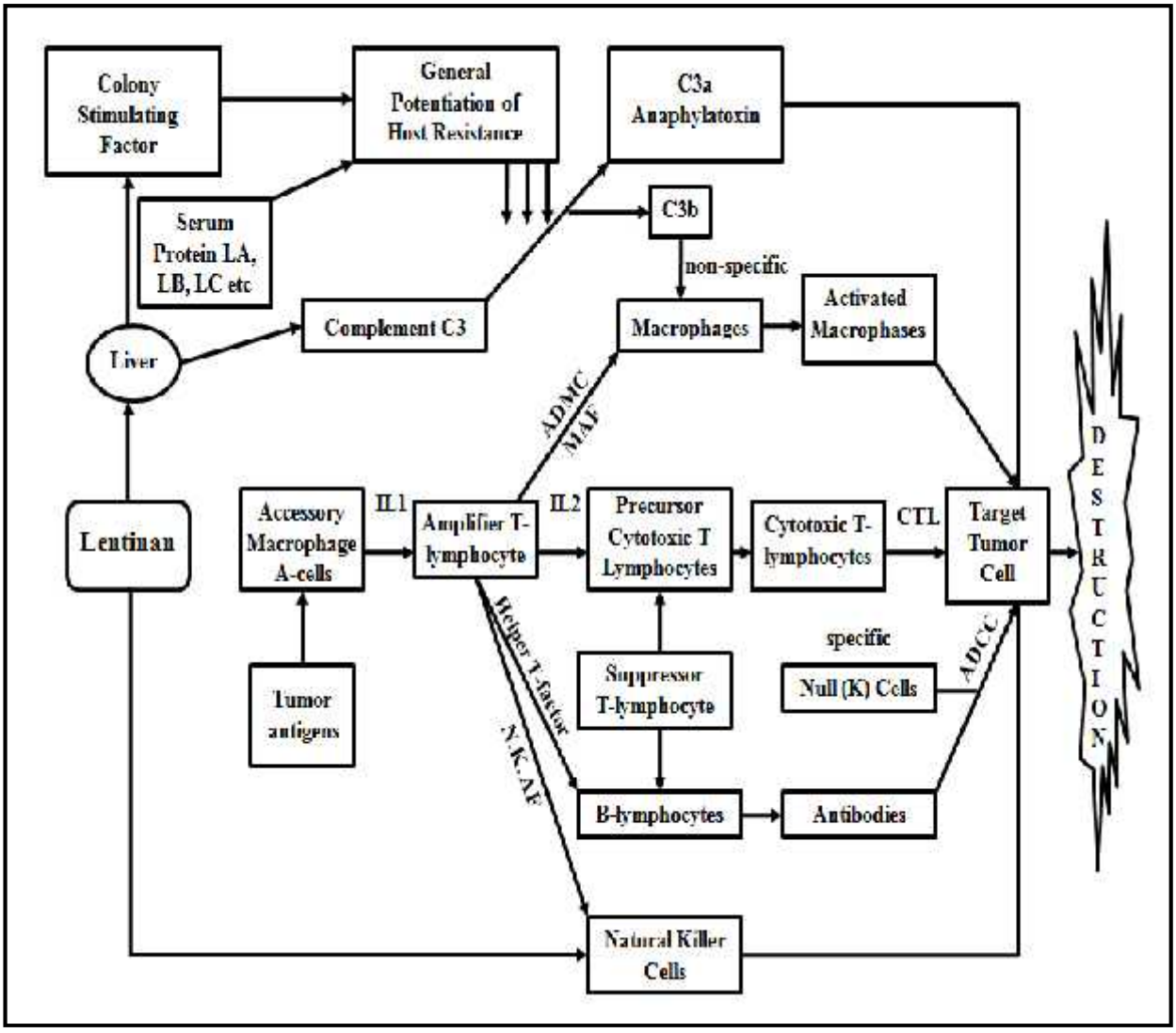

Figure 9. The schematic presentation showing mode of action of Lentinan.

[NK: Natural Killer cell; AF: Antibody Formation; LPS: Liver Protein Serum; ADCC: Antibody Dependent Cell mediated Cytotoxicity; CTL: Cytotoxic T-Lymphocyte; MAF: Macrophage Activating Factor; IL-1: Interlukine 1; IL-2: Interlukine 2].

1.A.4. References

[1] Robyt, J. F. *Essentials of Carbohydrate Chemistry*, Spinger Advanced Texts in Chemistry. Spinger-Verlag, New York. **1998**.

[2] Tolstoguzov, V. *Food Hydrocolloid*. **2004**, *18*, 873-877.

[3] Fukushima, M.; Ohashi, T.; Fujiwara, Y.; Sonoyama, K.; Nakano, M. *Exp. Biol. Med.* **2001**, *226*, 758-785.

[4] Klemm, D.; Brigitte, H.; Fink, H.; Bohn, A. *Angew. Chem. Int. Ed.* **2005**, *44*, 3358-3393.

[5] Crawford, R. L. *Lignin biodegradation and transformation*. New York: John Wiley and Sons. **1981**, ISBN 0-471-05743-6.

[6] Lee, Y. L.; Yen, M. T.; Mau, J. T. *Food Chem*. **2007**, *104*, 1-9.

[7] Smania, E. F. A.; Delle, M. F.; Smania, J. A.; Yunes R. A. *Fitoterapia*. **2003**, *74*, 375-377.

[8] Lunn, J.; Buttriss, J. L. *Nutr. Bull*. **2007**, *32*, 21-64.

[9] Gupta, B.; Arorab, A.; Saxenaa, S.; Alam, M. S. *Polym. Advan. Technol*. **2008**, *20*, 58-65.

[10] Chang, S. T.; Miles, P. G. *The Mycologist.* **1992**, *6*, 64-65.

[11] Wasser, S. P.; Weis, A. L. *Int. J. Med. Mushrooms.* **1999**, *1*, 31-62.

[12] Reshetnikov, S. V.; Wasser, S. P.; Tan, K. K. *Int. J. Med. Mushrooms.* **2001,** *3*, 361-394.

[13] Breene, W. M. *J. Food Procect*. **1990**, *53*, 883-894.

[14] Anderson, E. E.; Fellers, C. R. *Proc. Am. Soc. Hort. Sci*. **1942**, *41*, 301-304.

[15] Gilbert, F. A.; Robinson, R. F. *Econ. Botany*. **1957**, *11*, 126-145.

[16] Giacomini, V. *Sci. Aliment.* **1957**, *3*, 103-108.

[17] Pandey, N. Chemical Analysis of Mushroom of Kathmandu Valley. A paper submitted to UGC, University of Kathmandu, Nepal. **2004**.

[18] Brochers, A. T.; Stern, J. S.; Hackman, R. M.; Keen, C. L.; Gershwin, M. E. *Proc. Soc. Exp. Biol. Med.* **1999**, *221*, 281-293.

[19] Peberdy, J. F.; Fox, H. M. Protoplast technology and edible mushrooms. In: Chang ST, Buswell, J. A., Miles, P. G. (eds) Genetics and breeding of edible mushrooms. Gordon and Breach Science Publishers, The Netherlands. **1999**, 125-155.

[20] Chakraborty, U.; Sikdar, S. R. *World J. Microb. Biotechnol*. **2010**, *26*, 213-225.

[21] Chakraborty, U.; Sikdar, S. R. *World J. Microb. Biotechnol*. **2008**, *24*, 1481-1492.

[22] Mallick, P.; Sikdar, S. R. *Int. J. Pharm. Bio. Sci.* **2015**, *6*, 301-314.

[23] Tzianabos, A. O. *Clin. Microbiol. Rev.* **2000**, *1*, 523-533.

[24] Mizuno, T. *Int. J. Med. Mushrooms.* **1999**, *1*, 9-29.

[25] Lorenzen, K.; Anke, T. *Curr. Org. Chem.* **1998**, *2*, 329-364.

[26] Mizuno, T. *Int. J. Med. Mushrooms.* **1999**, *1*, 105-119.

[27] Ooi, V. E. C.; Liu, F. *Int. J. Med. Mushrooms.* **1999**, *1*, 195-206.

[28] Cui, J.; Chisti, Y. *Biotech. Adv.* **2003**, *21*, 109-122.

[29] Gao, Y.; Zhou, S.; Chen, G.; Dai, X.; Ye, J. A. *Int. J. Med. Mushrooms*. **2002**, *4*, 207-214.

[30] Gao, Y.; Zhou, S. H.; Huang, M.; Xu, A. *Int. J. Med. Mushrooms*. **2003**, *5*, 235-246.

[31] Gao, Y.; Lan, J.; Dai, X.; Ye, J.; Zhou, S. H. *Int. J. Med. Mushrooms*. **2004**, *6*, 96-107.

[32] Didukh, M. Y.; Wasser, S. P.; Nevo, E. *Int. J. Med. Mushrooms*. **2003**, *5*, 133-152.

[33] Rowan, N. J.; Smith, J. E.; Sullivan, R. *Int. J. Med. Mushrooms*. **2003**, *5*, 95-110.

[34] Sullivan, R.; Smith, J. E.; Rowan, N. J. *Perspect. Biol. Med*. **2006**, *49*, 159-170.

[35] Zhang, M.; Cui, S. W.; Cheung, P. C. K. *Trends Food Sci. Technol*. **2007**, *18*, 4-19.

[36] Dai, Y. C.; Zang, Z. L.; Ui, B. K.; Yu, C. J.; Zhou, L. W. *Int. J. Med. Mushrooms*. **2009**, *11*, 287-302.

[37] Wasser, S. P. *Int. J. Med. Mushrooms*. **2010**, *12*, 1-16.

[38] Morikawa, K.; Takeda, R.; Yamazaki, M.; Mizuno, D. *Cancer Res.* **1985**, *45*, 1496-1501.

[39] Mansell, P. W.; Ichinose, H.; Reed, R. J.; Krementz, E. T.; McNamee, R.; Di Luzio, N. R. J. *Natl. Cancer Inst.* **1975**, *54*, 571-580.

[40] Miura, N. N.; Ohno, N.; Aketagawa, J.; Tamura, H.; Tanaka, S.; Yadomae, T. *FEMS Immunol. Med. Microbiol.* **1996**, *13*, 51-57.

[41] Zhang, P.; Cheung, P. C. K. *Biosci. Biotechnol. Biochem.* **2002**, *66*, 1052-1056.

[42] Mizuno, T.; Hagiwara, T.; Nakamura, T.; Ito, H.; Shimura, K.; Sumiya, T.; Asakura A. *Agric. Biol. Chem.* **1990**, *54*, 2889-2896.

[43] Wang, T.; Deng, L.; Li, S.; Tan, T. *Carbohydr. Polym.* **2007**, *67*, 133-137.

[44] Rout, D.; Mondal, S.; Chakraborty, I.; Pramanik, M.; Islam, S. S. *Med. Chem. Res.* **2004**, *13*, 509-517.

[45] Ghoneum, M.; Wimbley, M.; Salem, F.; McKlain, A.; Attallah, N.; Gill, G. *Int. J. Immunother.* **1995**, *11*, 23-28.

[46] Kiho, T.; Yoshida, I.; Katsuragawa, M.; Sakushima, M.; Ukai, S. *Biol. Pharm. Bull*. **1994**, *17*, 1460-1462.

[47] Mizuno, T.; Saito, H.; Nishitoba, T.; Kawagashi, H. *Food Rev. Int.* **1995**, *11*, 23-61.

[48] Matsushita, K.; Kuramitsu, Y.; Ohiro Y.; Obara, M.; Kobayashi, M.; Li, Y. Q. *Anti-Cancer Drug*. **1998**, *9*, 343-350.

[49] Gao, Q. P.; Seljelid, R.; Chen, H. Q.; Jiang, R. *Carbohydr. Res*. **1996**, *288*, 135-142.

[50] Kawagishi, H.; Kanao, T.; Inagaki, R.; Mizuno, T.; Shimura, K.; Ito, H.; Hagiwara, T.; Hakamura, T. *Carbohydr. Polym*. **1990**, *12*, 393-404.

[51] Zhuang, C.; Mizuno, T.; Shimada, A.; Ito, H.; Suzuki, C.; Mayuzumi, Y.; Okamoto, H.; Ma, Y. Li, J. *Biosci. Biotechnol. Biochem.* **1993**, *57*, 901-906.

[52] Wasser, S. P. *Appl. Microbiol. Biotechnol.* **2002**, 60, 258-274.

[53] Mizuno, T.; Yeohlui, P.; Kinoshita, T.; Zhuang, C.; Ito, H.; Mayuzumi, Y. *Biosci. Biotechnol. Biochem.* **1996**, *60*, 30-33.

[54] Mizuno, T.; Zhuang, C.; Abe, K.; Okamoto, H.; Kiho, T.; Ukai, S.; Leclerc, S.; Meijer, L. *Int. J. Med. Mushrooms*. **1999**, *1*, 301-316.

[55] Yoshida, I.; Kiho, T.; Usui, S.; Sakushima, M.; Ukai, S. *Biol. Pharm. Bull.* **1996**, *19*, 114-121.

[56] Harada, T.; Misaki, A.; Saito, H. *Arch. Biochem. Biophys*. **1968**, *124*, 292-298.

[57] Sia, G. M.; Candlish, J. K. *Phytother*. *Res.* **1999**, *13*, 133-137.

[58] Yang, P.; Liang, M.; Zhang, Y.; Shen, B. *Adv Ther.* **2008**, *25*, 787-794.

[59] Nimura, H.; Mitsumori, N.; Takahashi, N. *Gan to Kagaku Ryoho.* **2006,** *33*, 106-109.

[60] Hazama, S.; Watanabe, S.; Ohashi, M.; Yagi, M.; Suzuki, M.; Matsuda, K.; Yamamoto, T.; Suga, Y.; Suga, T.; Nakazawa, S.; Oka, M. *Anticancer Res.* **2009,** *29*, 2611-2617.

[61] Hobbs, C. *Medicinal mushrooms: an exploration of traition, healing and culture.* Botanical Press, Santa Cruz, Calif. **1999**.

[62] Furue, H. *Int. J. Immunopharmacol.* **1985**, *7*, 333-336.

[63] Kimura, Y.; Tojima, H.; Fukase, S.; Takeda, S. *Acta Otolargynzol*. **1994**, *511*, 192-195.

[64] Okamura, K.; Suzuki, M.; Yajima, K.; Chihara, T.; Fujiwara, A.; Fukuda, T.; Goto, S.; Ichinohe, K.; Jimi, S.; Kasamatsu, T.; Kawai, N.; Mizuguchi, K.; Mori, S.; Nakano, H.; Noda, K.; Sekiba, K.; Suzuki, K.; Suzuki, T.; Takahashi, K.; Takeuchi, K.; Takeuchi, S.; Ogawa, N. *Cancer*. **1986**, *58*, 865-872.

[65] Wasser, S. P. *J. Am. Bot. Co.* **2002**, *56*, 28-33.

[66] Hobbs, C. Botanica Press, Santa Cruz, Calif. **1995**.

[67] Stamets, P. Ten Speed press, Berkeley, Calif. **2000**.

[68] Sugimachi, K.; Maechara, Y.; Ogawa, M.; Kakegawa, T.; Tomira, M. *Cancer Chemother. Pharmacol.* **1997**, *40*, 233-238.

[69] Mizuno, T.; Morimoto, M.; Minato, K. I.; Tsuchida, H. *Biosci. Biotechnol. Biochem.* **1998**, *62*, 434-437.

[70] Itoh, H.; Ito, H.; Amano, H.; Noda, H. *Jpn. J. Pharmacol.* **1994**, *66*, 265-271.

[71] Fujimiya, Y.; Kobori, H.; Oshiman, K. I.; Soda, R.; Ebina, T. *Nippon Shokuhin Kagaku Kaishi.* **1998**, 45, 246-252.

[72] Mizuno, T.; Hagiwara, T.; Nakamura, T.; Ito, H.; Shimura, K.; Sumiya, T.; Asakura, A. *Agri. Biol. Chem.* **1990**, *54*, 2889-2896.

[73] Nishida, I.; Nanba, H.; Kuroda, H. *Chem. Pharm. Bull.* **1988**, *36*, 1819-1827.

[74] Fulleroton, S. A.; Samadi, A. A. *Mol. Urol.* **2000**, *4*, 7-13.

[75] Luzio, D.; McNamee, N. R. R.; Jones, E.; Cook, J. A.; Hoffman, E. O. *The Macrophage in Neoplasia.* Academic Press, New York. **1976**, 181.

[76] Scaringi, L.; Marconi, P.; Boccanera, M.; Tissi, L.; Bistoni, F.; Cassone. A. *J. Gen. Microbiol.* **1988**, *134*, 1265-1274.

[77] Suzuki, M.; Kikuchi, T.; Takatsuki, F.; Hamuro. *J. Biotherapy*. **1993**, *7*, 345.

[78] Ross, G. D.; Veˇtvicˇka, V.; Yan, J.; Xia, Y.; Veˇtvicˇkova´, J. *Immunopharmacol.* **1999**, *42*, 61-74.

[79] Chihara, G.; Hamuro, J.; Maeda,Y. Y.; Shiio, T.; Suga, T.; Takasuka, N.; Sasaki, T. *Cancer Detect. Prev. Suppl.* **1987**, *1*, 423-443.

[80] Chihara, G. Excerpta. *Med. Int. Congr. Ser.* Elsevier, Amsterdam, **1981**, 576.

.

Chapter – I: PART-B

Introduction to nanoparticles and polysaccharide based nanoparticles

1.B.1. Introduction to nanoparticles

Nanoscience and its applied aspect Nanotechnology is a broad and interdisciplinary area of research that has been growing explosively in the past decades. It deals with manipulation of matter at the atomic or molecular scale and defined as "the study of process and fine tuning of requisites at atomic, molecular and macromolecular scales where premises differ profoundly from those at a large proportion" [1]. Nanoparticles are defined as "a discrete entity with at least one dimension being 100 nm or less" [2]. Much attention has been focused on the preparation of metal nanoparticles due to their unique properties and wide ranging application in a variety of areas including physics, chemistry, material science, and biomedical science [3-6]. Nanoparticles act a bridge between bulk materials and atomic or molecular structures. The bulk materials should have constant physical properties regardless of its size; however properties of nanomaterial exhibit strong dependence on its size. The unusual properties of nanomaterial compared to bulk material are due to size confinement, surface effects and quantum phenomena [7]. Materials at nanoscale have a larger surface area to volume ratio as compared to bulk materials that show a major impact on the mechanical response [8,9]. On the other hand, the quantum effect also plays a dominant role at the nanoscale affecting their optical, electrical, and magnetic properties [10]. Thus, the properties of nanomaterials which depend on their size and shape can be tuned via synthetic techniques.

1.B.2. Synthesis of Nanoparticles

Generally, there are two approaches for the synthesis of metal nanoparticles namely "top-down" and "bottom-up" [10]. In "top-down'' approach, the bulk material is broken down into nano-sized particles. The reduction in size in "top down'' approach can be achieved by the processes like vapour deposition, mechanical milling, laser ablation, grinding etc. In "bottom up" approach, nanoparticles are synthesized by assembling the atoms and smaller particles. The "bottom up" synthesis is based on chemical methods e.g. chemical reduction, photochemical reduction, co-precipitation, thermal decomposition, hydrolysis, etc. Since, surface chemistry and other physical properties of the nanoparticles are highly dependent on the surface structure of nanomaterials, "top down'' approach is not appropriate for synthesis of nanoparticle because the surface structure of the nanomaterials is damaged in this method.

1.B.2.1. Green synthesis of nanoparticles

Numerous methods for the synthesis of nanoparticles are reported, amongst them, most conventional is the reduction of metal salt solution by means of reducing agent like sodium borohydride, N,N- dimethyl formamide, trisodium citrate, or other organic compounds [11-14]. But the use of such reducing agents may be associated with environmental toxicity or biological hazards. Currently integration of 'green chemistry' principles into nanotechnology is one of the key issues in nanoscience research. Utilization of nontoxic chemicals, environmentally benign solvents, and renewable materials are some of key issues for a green synthesis strategy. Now a days, biomolecules and bioorganisms are also used in the synthesis of metal nanoparticles [15-17]. Synthesis of metal nanoparticles using green renewable entities is low cost effective and therefore can be used as an economic and valuable alternative for the large-scale production of metal nanoparticles.

1.B.3. Polysaccharide based nanoparticles

Polysaccharides are the most abundant biopolymer on earth. Polysaccharides offer a number of advantages for nanoparticle synthesis as they have hemiacetal end to reduce metal salt precursors and lot of hydroxyl group and other functionalities to stabilize the synthesized metal NPs. The hydroxyl groups of polysaccharides also play an important role in the reduction of gold salts [18]. Polysaccharides with hydroxyl and amino groups bind tightly to the surface of the metal nanoparticles giving them a hydrophilic surface [19]. There are series of reports where hyaluronic acid (HA), alginic acid, chitosan as well as plant polysaccharides like starch, cellulose, dextran were used in the synthesis of metal nanoparticles.

- **Starch capped Au NPs**

  Starch can act as both reducing and stabilizing agent for the synthesis of metal nanoparticles. Starch capped Au NPs having an average size of 3.5 nm has been synthesized by Hussain et al. [20]. Engelbrekt et al. used starch as a protecting agent for synthesis of Au NPs [21]. Parida et al. also synthesized Au NPs stabilized and labeled with starch and gum arabic [22]. These synthesized Au NPs have various biomedical applications. Deka et al. used starch for the preparation of Au nanoparticle-starch composites [23]. The composite was used for studying α-amylase digestion rate.

- **Cellulose capped Au NPs**

  Cellulose is the main component of plant cell walls consisting of a linear chain of β-(1, 4)-linked D-glucose. Cai et al. reported the preparation of nanoporous cellulose gels obtained from an aqueous alkali hydroxide-urea solution [24]. The gels were immersed in precursor salt solutions, $AuCl_4.3H_2O$ to synthesize Au NPs. These Au NPs-carrying gels provided high surface area, transmittance, porosity, good mechanical strength and moderate thermal stability. These nanomaterials find many potential applications in catalysis, electro-optical devices and as antibacterial agents.

- **Dextran capped Au NPs**

  Dextran was employed both as reducing and stabilizing agent for the preparation of biocompatible Au NPs [25]. Aminodextran was also used as reducing and protecting agent for the preparation of Au NPs. Morrow et al. showed the morphology of Au NPs can be controlled by altering the pH of aminodextran solution [26]. In alkaline pH (p^H~12) aminodextran solution yields spherical Au NPs of mean size of 20 nm while acidic pH favors the formation of large Au NPs of other shapes.

- **Chitosan capped Au NPs**

  Chitosan-capped Au NPs was first reported by Huang and Yang in 2004 [27]. The primary amine group of chitosan effectively supports the immobilization of metallic nanoparticles. In another report, the catalytic activity of Au nanoparticle-chitosan bioconjugates was assessed for the reduction of 4-nitrophenol in the presence of $NaBH_4$ [28]. In an earlier report it has been observed that the size, shape and crystalline structure of Au-chitosan nanocomposites can be controlled by controlling the reaction temperature [29]. These nanocomposites were successfully employed for detection of trace amount of amino acids by surface-enhanced Raman spectroscopy (SERS). Bhumkar et al. reported another important nanomedicinal application of chitosan stabilized Au NPs [30]. They have employed Au nanoparticles-chitosan composites for facile transport of insulin across the intestinal track of diabetic rats.

- **Hyaluronic acid capped Au NPs**

  Hyaluronic acid (HA) is a linear, high molecular weight polysaccharide commonly found in soft tissues of animals. HA was used for the preparation of Au NPs with sizes ranging from 5 to 30 nm by thermal treatment, where it played the role of both the reducing and stabilizing agent [31].

- **Alginic acid capped Au NPs**

  Alginic acid is an acidic polysaccharide widely distributed in the cell walls of brown algae [32]. Alginic acid has many applications including in drug industry as drug delivery agent and in the food industry as stabilizer and thickener [32,33]. Photochemical synthesis of Au NPs was done using calcium alginate both as reducing and stabilizing agent [34]. The resulting nanoparticles were spherical with a size of less than 10 nm. The catalytic activity of nanoparticles were assessed by the reduction of 4-nitrophenol to 4-aminophenol implying that it can be used as solid-phase heterogeneous catalyst for industrial applications [34].

1.B.4. MORPHOLOGY OF NANOPARTICLES

Nanoparticles have different morphologies such as zero, one, two and three dimensional structures.

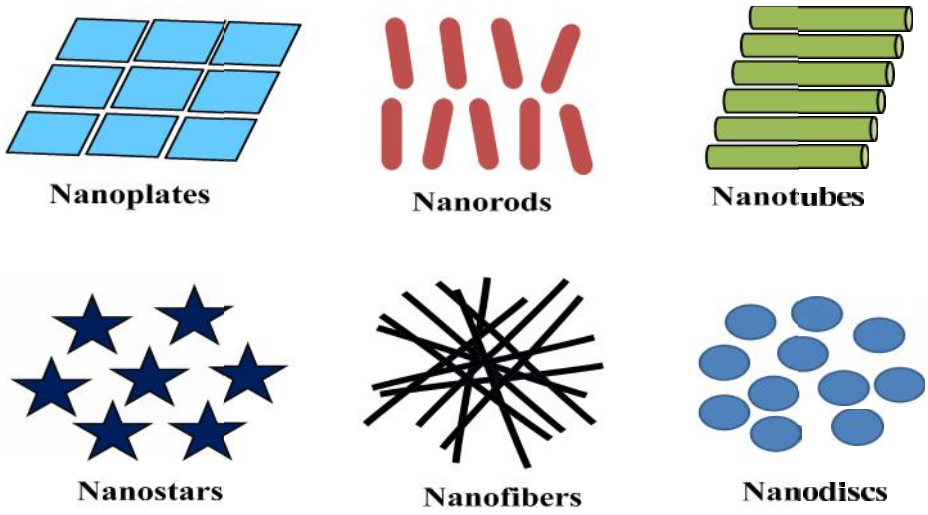

Figure 1. Various morphology of metal nanoparticles

- **Zero dimensional nanostructures**

  A variety of physical and chemical methods have been developed for producing zero dimensional (0D) nanostructures. 0D nanostructures such as quantum dots, core–shell quantum dots, hollow spheres, onions and nano-lenses have been synthesized and reported by several research groups [35-39]. Amongst all 0D nanostructures, quantum

dots has been studied extensively in light emitting diodes (LEDs) [40], solar cells [41], single-electron transistors [42] and lasers [43].

- **One dimensional nanostructures**

  In the last decade, one dimensional (1D) nanostructures have inspired an increasing interest due to their wide range of potential applications. It is established that 1D nanostructures are ideal systems for exploring novel phenomena at the nanoscale and investigating the variation of functional properties on size and dimensionality. Several 1D nanostructures such as nanowires, nanorods, nanotubes, nanobelts, nanoribbons, and hierarchical nanostructures have profound application in nanoelectronics, nanodevices, nanocomposite materials and alternative energy resources etc. [44-50].

- **Two dimensional nanostructures**

  In recent years, considerable research attention has been focused on the development of syntheses of two dimensional (2D) nanostructures. 2D nanostructures with certain geometries exhibit exceptional shape-dependent characteristics and ensuing utilization as building blocks for the key components of nanodevices [51,52]. 2D nanostructures such as nanoprisms, nanoplates, nanosheets, nanowalls, and nanodisks are particularly interesting for developing novel applications in sensors, photocatalysts, nanoreactors, etc. [53-58].

- **Three dimensional nanostructures**

  3D nanostructures such as nanoballs, nanocoils, nanocones, and nanoflowers have attracted intensive research interests because of their large surface area which have enough absorption sites to be used as catalyst [59]. On the other hand, such materials with porosity in three dimensions could be used for transport of molecules [60,61]. Nanocages possessing hollow interiors and porous walls are useful for colorimetric sensing and biomedical applications [62].

1.B.5. Application of nanoparticles

Nanomaterials having wide range of applications in the field of gene therapy, sensing, imaging of cancer cells, drug delivery, degradation of pesticides, antimicrobial agent, catalysis etc. [Figure 2].

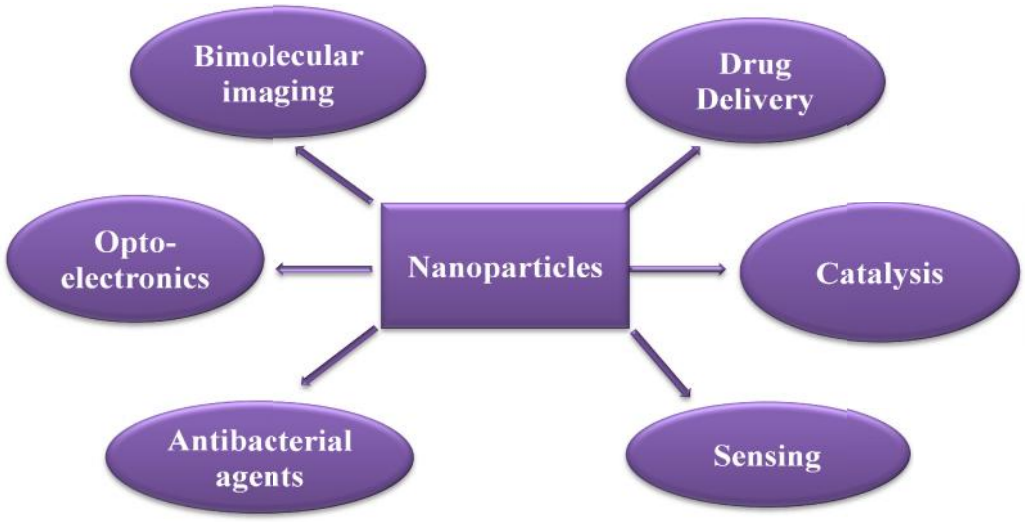

Figure 2. Metal nanoparticles and their various potential applications.

1.B.5.1. Catalytic activity

The increasing proportion of surface atoms of nanoparticles with decreasing particle size makes nanoparticles become highly reactive catalysts as surface atoms possess more energy than bulk atoms. Au NPs serve as an effective catalyst in the reduction of various pollutants like 4-NP, the most common organic pollutant in industrial and agricultural waste water [63]. Now it is also widely used as catalyst for various types of organic transformation reactions such as: selective hydrogenation reaction, aromatic ring hydrogenation, selective oxidation reaction of alkanes, epoxidation reaction, oxidation of alcohols, oxidation of polyols, and selective oxidation of amines [64-70].

1.B.6. REFERENCES

[1] Commission of the European Communities, **2009**. Nanoscience and Nanotechnologies: An action plan for Europe. Second Implementation Report 2007-2009 (SEC 1468).

[2] García. M.; Forbe, T.; Gonzalez, E. *Ciênc. Tecnol. Aliment*. **2010**, *30*, 573-581.

[3] Pradhan, N.; Pal, A.; Pal, T. *Langmuir*. **2001**, *17*, 1800-1802.

[4] Pradhan, N.; Pal, A.; Pal, T. *Colloids. Surf. A.* **2002**, *196*, 247-257.

[5] Cao, Y. W.; Jin, R.; Mirkin, C. A. *J. Am. Chem. Soc.* **2001**, *123*, 7961-7962.

[6] Hayward, R. C.; Saville, D. A.; Aksay, I. A. *Nature*. **2000**, *404*, 56-59.

[7] Esaki, L. *Nanostructured. Mater*. **1999**, *12*, 1-8.

[8] Park, H. S.; Klein, P. A. *Comput. Methods. Appl. Mech. Eng.* **2008**, *197*, 3249-3260.

[9] Park, H. S.; Klein, P. A.; Wagner, G. J. *Int. J. Numer. Methods. Eng*. **2006**, *68*, 1072-1095.

[10] Nirmala, M. J.; Shiny, P. J.; Ernest, V.; Dhas, S. P.; Samundeeswari, A. *Int. J. Pharm. Pharm. Sci.* **2013**, *5*, 23-29.

[11] Zhang, Z.; Wu, Y. *Langmuir*. **2010**, *26*, 9214-9223.

[12] Rivas, L.; Sanchez-Cortes, S.; Garcia-Ramos, J. V.; Morcillo, G. *Langmuir*. **2001**, *17*, 574-577.

[13] Wang, T.; Zhang, D.; Xu, W.; Yang, J.; Han, R.; Zhu, D. *Langmuir*. **2002**, *18*, 1840-1848.

[14] Pastoriza-Santos, I.; Liz-Marzan, L. M. *Langmuir*. **1999**, *15*, 948-951.

[15] Esumi, K.; Takei, N.; Oshimura, T. Y. *Colloids. Surf. B.* **2003**, *32*, 117-123.

[16] Mucic, R. C.; Storhoff, J. J.; Mirkin, C. A.; Letsinger, R. L. *J. Am. Chem. Soc.* **1998**, *120*, 12674-112675.

[17] Mukherjee, P.; Ahmad, A.; Mandal, D.; Senapati, S.; Sankar, S. R.; Khan, M. I.; Ramani, R.; Parischa, R.; Ajaykumar, P. V.; Alam, M.; Sastry, M.; Kumar, M. *Angew. Chem. Int. Ed.* **2001**, *40*, 3585- 3588.

[18] Mata, Y. N.; Torres, E.; Blazquez, M. L.; Ballester, A.; Gonzalez, F.; Munoz, J. A. *J. Hazard. Mater.* **2009**, *166*, 612-618.

[19] Kemp, M. M.; Kumar, A.; Mousa, S.; Dyskin, E.; Yalcin, M.; Ajayan, P.; Linhardt, R. J.; Mousa, S. A. *Nanotechnology*. **2009**, *20*, 455104 (7 pp).

[20] Hussain, S. T.; Muhammad, I.; Mazhar, M. *J. Nanopart. Res.* **2009**, *11*, 1383-1391.

[21] Engelbrekt, C.; Sørensen, K. H.; Zhang, J.; Welinder, A. C.; Jensen, P. S.; Ulstrup, J. *J. Mater. Chem*. **2009**, *19*, 7839-7847.

[22] Parida, U. K.; Nayek, P. L. *World Journal of Nanoscience and technology*. **2012**, *1*, 10-25.

[23] Deka, J.; Paul, A.; Ramesh, A.; Chattopadhyay, A. *Langmuir*. **2008**, *24*, 9945-9951.

[24] Cai, J.; Kimura, S.; Wada, M.; Kuga, S. *Biomacromolecules*. **2009**, *10*, 87-94.

[25] Wang, Y.; Zhan, L.; Huang, C. Z. *Anal. Methods.* **2010**, *2*, 1982-1988.

[26] Morrow, B. J.; Matijevic, E.; Goia, D. V. *J. Colloid. Interface. Sci.* **2009**, *335*, 62-69.

[27] Huang, H.; Yang, X. *Carbohydr. Res.* **2004**, *339*, 2627-2631.

[28] Wei, D.; Ye, Y.; Jia, X.; Yuan, C.; Qian, W. *Carbohydr. Res.* **2010**, *345*, 74-81.

[29] Potara, M.; Maniu, D.; Astilean, S. *Nanotechnology*. **2009**, *20*, 315602 (7 pp).

[30] Bhumkar, D. R.; Joshi, H. M.; Sastry, M.; Pokharkar, V. B. *Pharm. Res.* **2007**, *24*, 1415-1426.

[31] Kemp, M. M.; Kumar, A.; Mousa, S.; Park, T. J.; Ajayan, P.; Kubotera, N.; Mousa, S. A.; Linhardt, R. J. *Biomacromolecules*. **2009**, *10*, 589-595.

[32] George, M.; Abraham, T. E. *J. Control. Release*. **2006**, *114*, 1-14.

[33] Tonnesen, H. H.; Karlsen, J. *Drug. Dev. Ind. Pharm*. **2002**, *28*, 621-630.

[34] Saha, S.; Pal, A.; Kundu, S.; Basu, S.; Pal, T. *Langmuir*. **2010**, *26*, 2885-2893.

[35] Kim, Y. T.; Han, J. H.; Hong, B. H.; Kwon, Y. U. *Adv. Mater.* **2010**, *22*, 515-518.

[36] Zhang, G.; Wang, D. *J. Am. Chem. Soc.* **2008**, *130*, 5616-5617.

[37] Wang, J.; Lin, M.; Yan, Y.; Wang, Z.; Ho, P. C.; Loh, K. P. *J. Am. Chem. Soc.* **2009**, *13*, 11300-11302.

[38] Gautam, U. K.; Vivekchand, S. R. C.; Govindaraj, A.; Kulkarni, G. U.; Selvi, N. R.; Rao, C. N. R. *J. Am. Chem. Soc.* **2005**, *127*, 3658-3659.

[39] Lee, J. Y.; Hong, B. H.; Kim, W. Y.; Min, S. K.; Kim, Y.; Jouravlev, M. V.; Bose, R.; Kim, K. S.; Hwang, I. C.; Kaufman, L .J.; Wong, C. W.; Kim, P.; Kim, K. S. *Nature.* **2009**, *460*, 498-501.

[40] Stouwdam, J. W.; Janssen, R. A. J. *J. Mater. Chem.* **2008**, *18*, 1889-1894.

[41] Lee, W.; Kang, S. H.; Kim, J. Y.; Kolekar, G. B.; Sung, Y. E.; Han, S. H. *Nanotechnology*. **2009**, *20*, 335706 (7 pp).

[42] Mokerov, V. G.; Fedorov, Y. V.; Velikovski, L. E.; Scherbakova, M. Y. *Nanotechnology*. **2001**, *12*, 552.

[43] Ustinov, V. M.; Zhukov, A. E.; Kovsh, A. R.; Mikhrin, S. S.; Maleev, N. A.; Volovik, B. V.; Musikhin, Y. G.; Shernyakov, Y. M.; Kondat'eva, E. Y.; Maximov, M. V.; Tsatsul'nikov, A. F.; Ledentsov, N. N.; Alferov, Z. I.; Lott, J. A.; Bimberg, D. *Nanotechnology*. **2000**, *11*, 397.

[44] Huang, L.; Wang, H.; Wang, Z.; Mitra, A.; Zhao, D.; Yan, Y. *Chem. Mater.* **2002**, 14 876-880.

[45] Li, G. R.; Feng, Z. P.; Zhong, J. H.; Wang, Z. L.; Tong, Y. X. *Macromolecules.* **2010**, *43*, 2178-2183.

[46] Yoon, S. M.; Hwang, I. C.; Kim, K. S.; Choi, H. C. *Angew. Chem. Int. Ed.* **2009**, *48*, 2506-2509.

[47] Wang, Y.; Lee, J. Y.; Kim, J. S.; Kim, G. H.; Kim, K. S. *Chem. Mater.* **2007**, *19*, 3912-3916.

[48] Hong, B. H.; Bae, S. C.; Lee, C. W.; Jeong, S.; Kim, K. S. *Science.* **2001**, *294*, 348-351.

[49] Hong, B. H.; Lee, J. Y.; Lee, C. W.; Kim, J. C.; Bae, S. C.; Kim, K. S. *J. Am. Chem. Soc.* **2001**, *123*, 10748-10749.

[50] Hong, B. H.; Lee, J. Y.; Beetz, T.; Zhu, Y.; Kim, P.; Kim, K .S. *J. Am. Chem. Soc.* **2005**, *127*, 15336-15337.

[51] Jun, Y. W.; Seo, J. W.; Oh, S. J.; Cheon, J. *Coord. Chem. Rev.* **2005**, *249*, 1766-1775.

[52] Kim, K. S.; Zhao, Y.; Jang, H.; Lee, S. Y.; Kim, J. M.; Kim, K. S.; Ahn, J. H.; Kim, P.; Choi, J. Y.; Hong, B. H. *Nature*. **2009**, *457*, 706-710.

[53] Pradhan, D.; Leung, K. T. *J. Phys. Chem. C*. **2008**, *112*, 1357-1364.

[54] Tiwari, J. N.; Pan, F. M.; Tiwari, R. N.; Nandi, S. K. *Chem. Commun.* **2008**, 6516-6518.

[55] Dong, X.; Ji, X.; Jing, J.; Li, M.; Li, J.; Yang, W. *J. Phys. Chem. C.* **2010**, *114*, 2070-2074.

[56] Mann, A. K. P.; Skrabalak, S. E. *Chem. Mater.* **2011**, *23*, 1017-1022.

[57] Siril, P. F.; Ramos, L.; Beaunier, P.; Archirel, P.; Etcheberry, A.; Remita, H. *Chem. Mater.* **2009**, *21*, 5170-5175.

[58] Lee, H.; Habas, S. E.; Kweskin, S.; Butcher, D.; Somorjai, G. A.; Yang, P. D. *Angew. Chem. Int. Ed.* **2006**, *45*, 7824-7828.

[59] Shen, Q.; Jiang, L.; Zhang, H.; Min, Q.; Hou, W.; Zhu, J. J. *J. Phys. Chem. C*. **2008**, *112*, 16385-16392.

[60] Teng, X. W.; Liang, X. Y.; Maksimuk, S.; Yang, H. *Small*. **2006**, *2*, 249-253.

[61] Lee, H.; Habas, S. E.; Kweskin, S.; Butcher, D.; Somorjai, G. A.; Yang, P. D. *Angew. Chem. Int. Ed.* **2006**, *45*, 7824-7828.

[62] Skrabalak, S. E.; Chen, J.; Sun, Y.; Lu, X.; Au, L.; Cobley, C. M.; Xia, Y. *Acc. Chem. Res.* **2008**, *41*, 1587-1595.

[63] Sen, I. K.; Mandal, A. K.; Chakraborti, S.; Dey, B.; Chakraborty, R.; Islam, S. S. *Int. J. Biol. Macromol.* **2013**, *62*, 439-449.

[64] Qi, S. T.; Cheney, B. A.; Zheng, R. Y.; Lonergan, W. W.; Yu, W. T.; Chen, J. G. G. *Appl. Catal. A: Chem.* **2011**, *393*, 44-49.

[65] Primo, A.; Concepcion, P.; Corma, A. *Chem. Commun.* **2011**, *47*, 3613-3615.

[66] Lawrence, S. A. *Amines: Synthesis, Properties and Applications*, Cambridge University Press, New York. **2004**.

[67] Navarro, R. M.; Pawelec, B.; Trejo, J. M.; Mariscal, R.; Fierro J. L. G. *J. Catal.* **2000**, *189*, 184-194.

[68] Backvall, J. E. *In Modern Oxidation Methods*, Wiley-VCH, New York. **2004**.

[69] Porta, F.; Rossi, M.; *J. Mol. Catal. A: Chem.* **2003**, *204-205*, 553-559.

[70] Barbaro, G.; Battaglia, A.; Giorgianni, P. *J. Org. Chem*. **1988**, *53*, 5491-5501.

Chapter – II: PART-A

Methodology for structural analysis and biological studies of polysaccharide

2. A.1. STRUCTURAL ANALYSIS OF POLYSACCHARIDES

For determination of the exact structure of the polysaccharide it is of prime importance to purify the polysaccharide as much as possible. Different techniques like chromatography, ultra centrifugation, dialysis, precipitation, and re-precipitation etc. are adopted for this purpose. The course of determination of structure of polysaccharides fundamentally stands on two kinds of methods; one is chemical method and another is spectroscopic method. Chemical method includes acid hydrolysis, methylation, periodate oxidation studies and spectroscopic method includes 1D (^{1}H, ^{13}C, DEPT-135) and 2D (TOCSY, DQF-COSY, NOESY, ROESY, HSQC, HMBC) NMR analyses. A schematic diagram of the methodology adopted for structure determination of a polysaccharide has been presented in Figure 1.

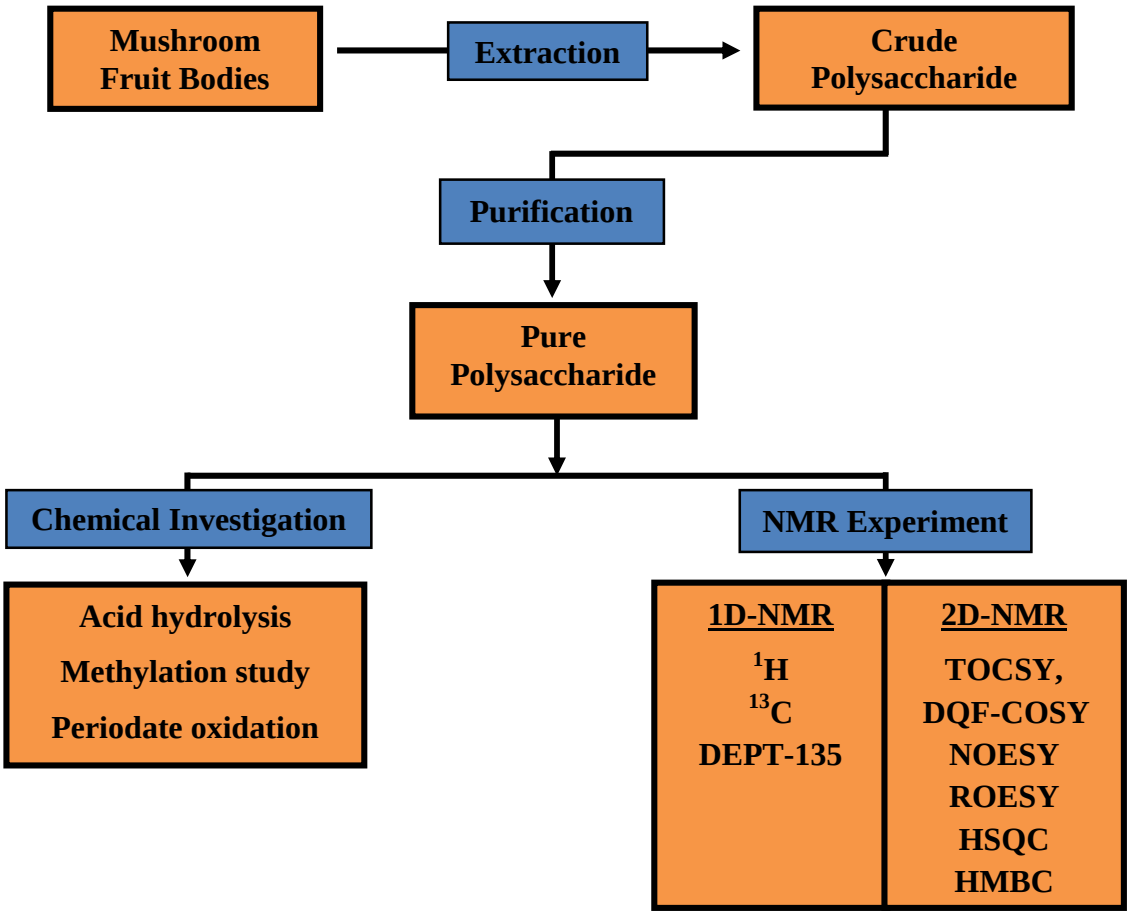

Figure 1. Schematic diagram of structural analysis of polysaccharide

2.A.2. Isolation of polysaccharide from mushroom

The fresh fruit bodies of the hybrid mushrooms were washed with distilled water, followed by boiling with hot water for 8 h. The aqueous extract was kept overnight at 4 °C and then filtered through linen cloth. The filtrate was centrifuged at 8000 rpm (using a Heraeus Biofuge stratus centrifuge) for 45 min at 4 °C. The supernatant was precipitated in 1:5 (v/v) EtOH, kept overnight at 4 °C. The precipitated polysaccharide was collected through centrifugation and then dissolved in a minimum volume of distilled water and dialyzed through cellulose membrane (D9652, Sigma-Aldrich, retaining MW >12,000 Da) against distilled water for 48 h. The material retained inside the cellulose bag was then centrifuged as mentioned above. The residue was rejected and the filtrate (water soluble part) was freeze dried to obtain crude polysaccharide

2.A.3. Purification of polysaccharides

Purification of a polysaccharide is crucial for determination of the structure of its repeating unit. The technique of gel-permeation chromatography (GPC) is widely used to separate a mixture of polysaccharides. In this technique molecules are separated on the basis of size relative to the pores in the packing particles. This technique is also known as size exclusion chromatography (SEC). The crude polysaccharide was purified through Sepharose 6B column (fractionation range 10,000-10,00,000 Da) in water as eluant using a Redifrac fraction collector. Eluent was collected in test tubes and monitored spectrophotometrically at 490 nm with the phenol-sulfuric acid reagent [1] using Shimadzu UV-vis spectrophotometer, model 1601. A chromatogram of sample distribution was obtained by plotting the test tube number against the carbohydrate concentration. The purification procedure was carried out in several lots. Fractions were collected and freeze dried. . A schematic diagram of the isolation and purification of crude polysaccharide from fruit body of mushroom has been presented in Figure 2.

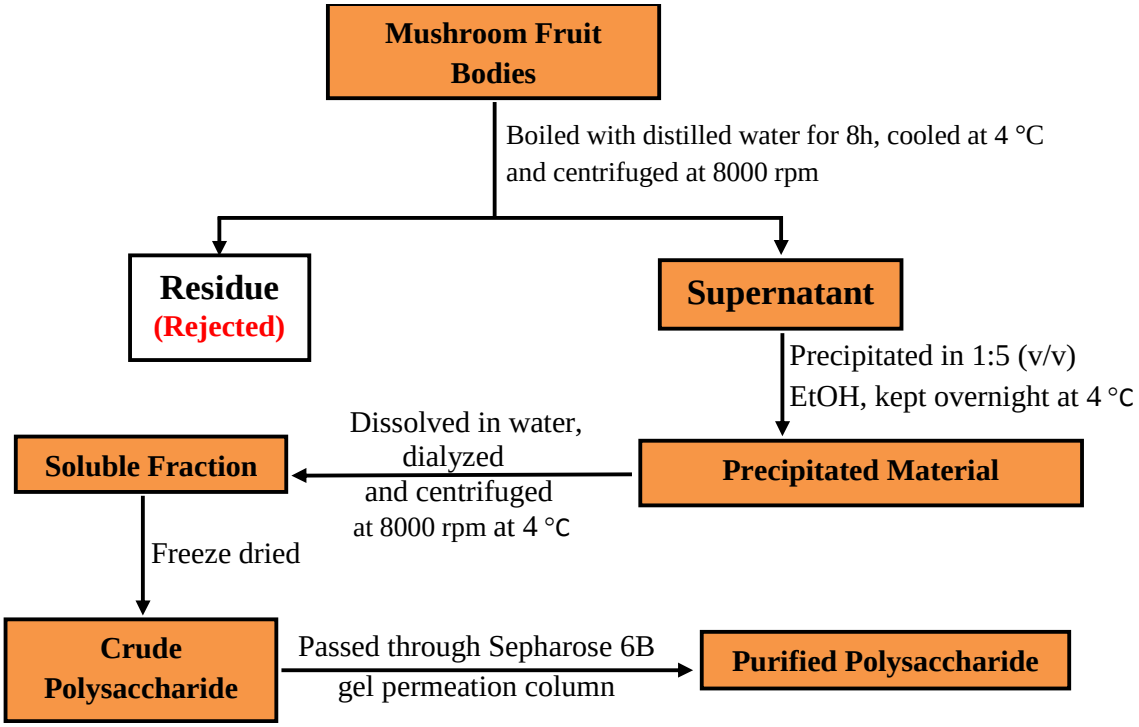

Figure 2. Schematic diagram of isolation and purification of polysaccharide from mushroom fruit body

2.A.4. Determination of physical properties

2.A.4.1. Optical rotation measurement

Purified polysaccharide (5 mg) was dissolved in 5 mL distilled water and then optical rotation was measured on a Jasco Polarimeter (Model P-1020) at room temperature.

2.A.4.2. Molecular weight determination

The molecular weights of the polysaccharides were determined by gel-chromatographic technique [2]. Standard dextrans T-250, T-200, T-70, and T-40 were passed through a Sepharose-6B column using water as an eluant, and then the elution volumes were plotted against the logarithms of their respective molecular weights. The elution volume of the polysaccharide was then plotted on the same graph, and the average molecular weight of the polysaccharide was determined.

2.A.4.3. Estimation of total carbohydrate

Phenol-sulfuric acid method [1] has been used for the estimation of total carbohydrate of polysaccharide. At first, different concentrations (20 µg, 40 µg, 80 µg, 100 µg and 200 µg) of standard glucose solutions were prepared. The 1000 µg sample solution was prepared by dissolving 5 mg sample in 5 mL distilled water and two different concentrations (100 µg and 80 µg) from that solution were prepared. Then 1 mL of each standard glucose solution was pipetted out into five test tubes. 1 mL of different concentration sample solution was pipetted out into two test tubes and 1mL water was added into a test tube for blank test. Now 1 mL of 5% phenol solution was added into each test tube, and then 5 mL of concentrated H_2SO_4 was also added to each test tube. All test tubes were shaken well using cyclomixture and kept for 20 min. Finally absorptions of each test tube solution were recorded at 490 nm in UV-vis spectrophotometer. Concentrations of standard solution were plotted against absorption in a graph and a straight line was obtained. The absorption values of the sample solution were plotted on the same graph paper and exact carbohydrate percentage of the sample was estimated.

2.A.5. Chemical analysis

2.A.5.1. Monosaccharide analysis

The monosaccharide composition is essential to determine the complete structure of the polysaccharide. In this process the glycosidic bonds between monosaccharide residues present in the polysaccharide are cleaved and therefore different monosaccharide residues present in polysaccharide are released. Polysaccharide (3 mg) was hydrolyzed with 2 M CF_3COOH (2 mL) in a round-bottomed flask at 100 ºC for 18 h in a boiling water bath. The excess acid was completely removed by co-distillation with water. Then the hydrolyzed product was reduced with $NaBH_4$ (9 mg) followed by acidification with dilute CH_3COOH, and then co-distillation with pure CH_3OH to remove excess boric acid. The reduced sugars (alditol) were acetylated with 1:1 pyridine-Ac_2O in a boiling water bath for 1 h to give alditol acetates [Figure 3], which were analyzed by Gas Chromatography (GC). A gas chromatograph Hewlett-Packard model 5730 A was used, with flame ionization detector and glass columns (1.8 m x 6 mm) packed with 3% ECNSS-M (A) on Gas Chrom Q (100-120 mesh) and 1% OV-225 (B) on Gas Chrom Q (100-120 mesh). All GC analyses were performed at 170 ºC.

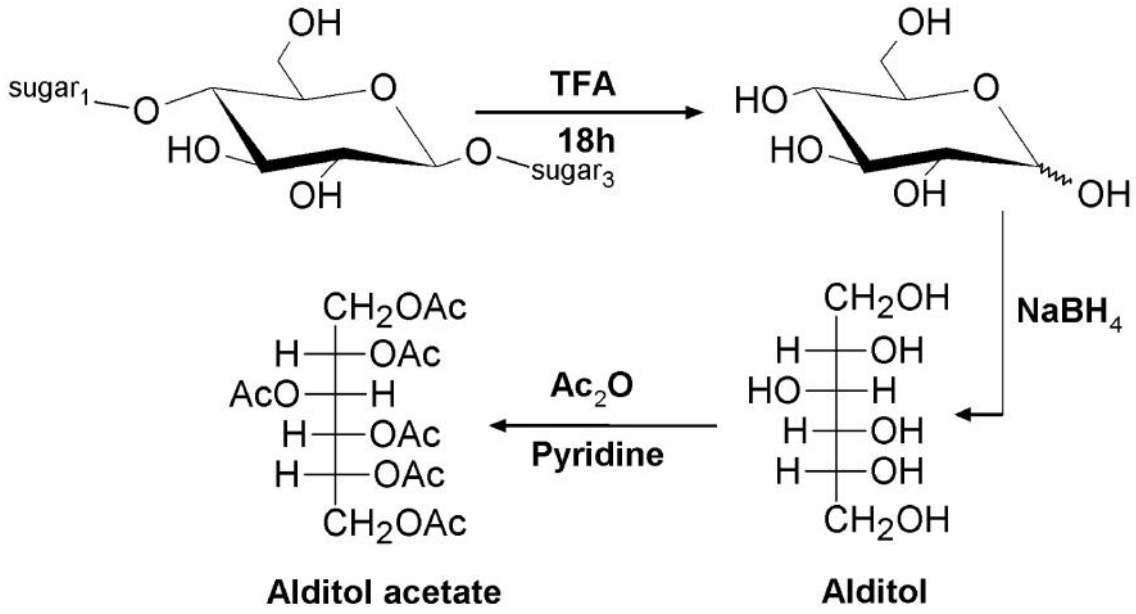

Figure 3. Schematic diagram of preparation of alditol acetates.

2.A.5.2. Determination of the absolute configuration of the monosaccharide

Sugars can either have the D or L configuration. In the present thesis absolute configuration were determined by method described by Gerwig et al. [3,4]. The polysaccharide (1.0 mg) was hydrolyzed with CF_3COOH, and then the acid was removed by co-distillation with distilled water. A solution of 250 µL of 0.625 M HCl in R-(+)-2-butanol was added and heated at 80 ºC for 16 h. Then the reactants were evaporated and TMS-derivatives were prepared with N, O-bis (trimethylsilyl) trifluroacetamide (BSTFA). The products were analyzed by GLC using a capillary column SPB-1 (30 m × 0.26 mm), a temperature program (3 ºC /min) from 150 to 210 ºC. The 2,3,4,6-tetra-*O*-TMS-(+)-2-butylglycosides obtained were identified by comparison with those prepared from the D and L enantiomers of different monosaccharide.

2.A.5.3. Methylation analysis

Methylation analysis has been used to determine the mode of linkages of each monosaccharide units. Methylation analysis includes conversion of all free hydroxyl groups into methoxyl groups followed by hydrolysis. Acidic hydrolysis of the resulting poly-methyl-ethers only cleaves the inter-glycosidic linkages, leaving the methyl ether bonds intact. The hydrolyzed monomers are reduced and acetylated to produce volatile partially methylated alditol acetates (PMAA) as shown in Figure 4. The substitution pattern of the *O*-acetyl group of the PMAA reflects the linkage patterns of the

corresponding sugars in the original polymer. There are several methods for methylation, but the most popular one is the method adopted by ciucanu and kerek [5]. In this method the polysaccharide (4.0 mg) were treated with finely powdered sodium hydroxide (NaOH) in DMSO (1mL) to de-protonate the hydroxyl groups yielding polyanion (alkoxide ions) followed by addition of methyl iodide (1 mL) in stirring condition. The methylated polysaccharide was isolated by making a partition between $CHCl_3$ and water (5:2, v/v). The organic layer containing product was washed with water for several times and dried. The methylated polymer was hydrolyzed with 90% HCOOH (1 mL) at 100 ºC for 1 h, and excess HCOOH was removed by co-distillation with distilled water. The hydrolyzed product was then reduced with $NaBH_4$ and acetylated with pyridine and Ac_2O [Figure 4]. The alditol acetates of the methylated sugars were analyzed by Gas Chromatography-Mass Spectroscopy (GC-MS). GC-MS analysis was performed on Shimadzu GC-MS Model QP-2010 Plus automatic system, using ZB-5MS capillary column (30 m x 0.25 mm). The program was isothermal at 150 ºC; hold time 5 min, with a temperature gradient of 2 ºC /min up to a final temperature of 200 ºC.

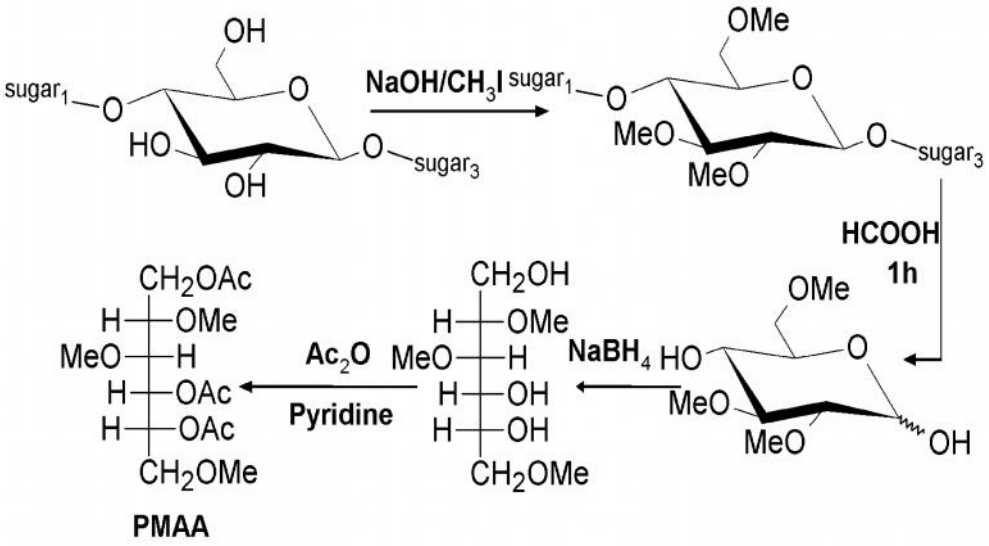

Figure 4. Schematic diagram of preparation of partially methylated alditol acetates (PMAA) of a polysaccharide.

2.A.5.4. Periodate oxidation study

The different mode of linkages of monosaccharide units in a polysaccharide is finally confirmed with the help of periodates oxidation study. The free hydroxyl groups present in the polysaccharides have the potential to react with oxidizing agents such as periodic acid

or its salts. 1,2-diols react with periodic acid or its salt to form two aldehydes groups due to the cleavage of the carbon-carbon sigma bond between them. Non-reducing end sugar residues and (1→6)-linked hexopyranose residues have three adjacent hydroxyl groups. In these cases double cleavage will occur forming one molar equivalent of formic acid and two molar equivalent of periodate is consumed as shown in Figure 5. (1→2) and (1→4)-linked hexopyranose units consume one equivalent of periodate per mole yielding a dialdehyde, whereas (1→3)-linked hexopyranose residues will not be affected by this reaction because of absence of vicinal OH groups. Polysaccharide was treated with sodium metaperiodate, kept in dark for 48 h and the excess periodate was consumed by adding 1,2-ethane diol. The solution was dialyzed against distilled water for 1 h followed by reduction with $NaBH_4$ [6,7]. The periodate oxidized-reduced product was divided into two portions. One portion was hydrolyzed with 2 M CF_3COOH for 18 h to prepare alditol acetates and subjected to GC analysis. Another portion was methylated by the method of Ciucanu and Kerek [5] and the alditol acetate of this methylated product (PMAA) was analyzed by GC-MS.

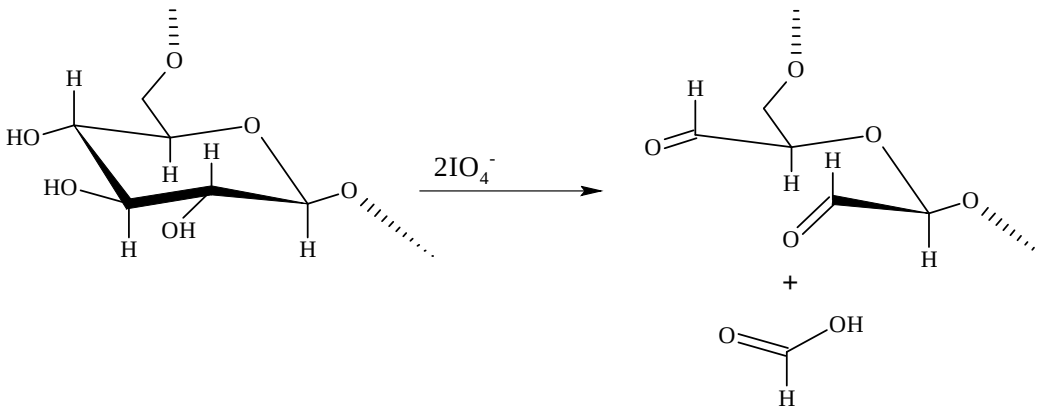

Figure 5. Schematic diagram of periodate oxidation of (1→6)-linked hexopyranoside.

2.A.6. Nuclear magnetic resonance (NMR) spectroscopy

Nuclear Magnetic Resonance (NMR) spectroscopy is widely used for structural analysis of polysaccharides. It is used for identification of monosaccharide composition, elucidation of α or β anomeric configurations, establishment of linkage patterns, and sequence of the

sugar units in the repeating unit of the polysaccharide. For complete elucidation of the structure of a polysaccharide different types of 1D (^{1}H, ^{13}C, and DEPT-135) and 2D (DQF-COSY, TOCSY, NOESY, ROESY, HSQC, and HMBC) NMR techniques have been applied as shown in the following diagram [Figure 6].

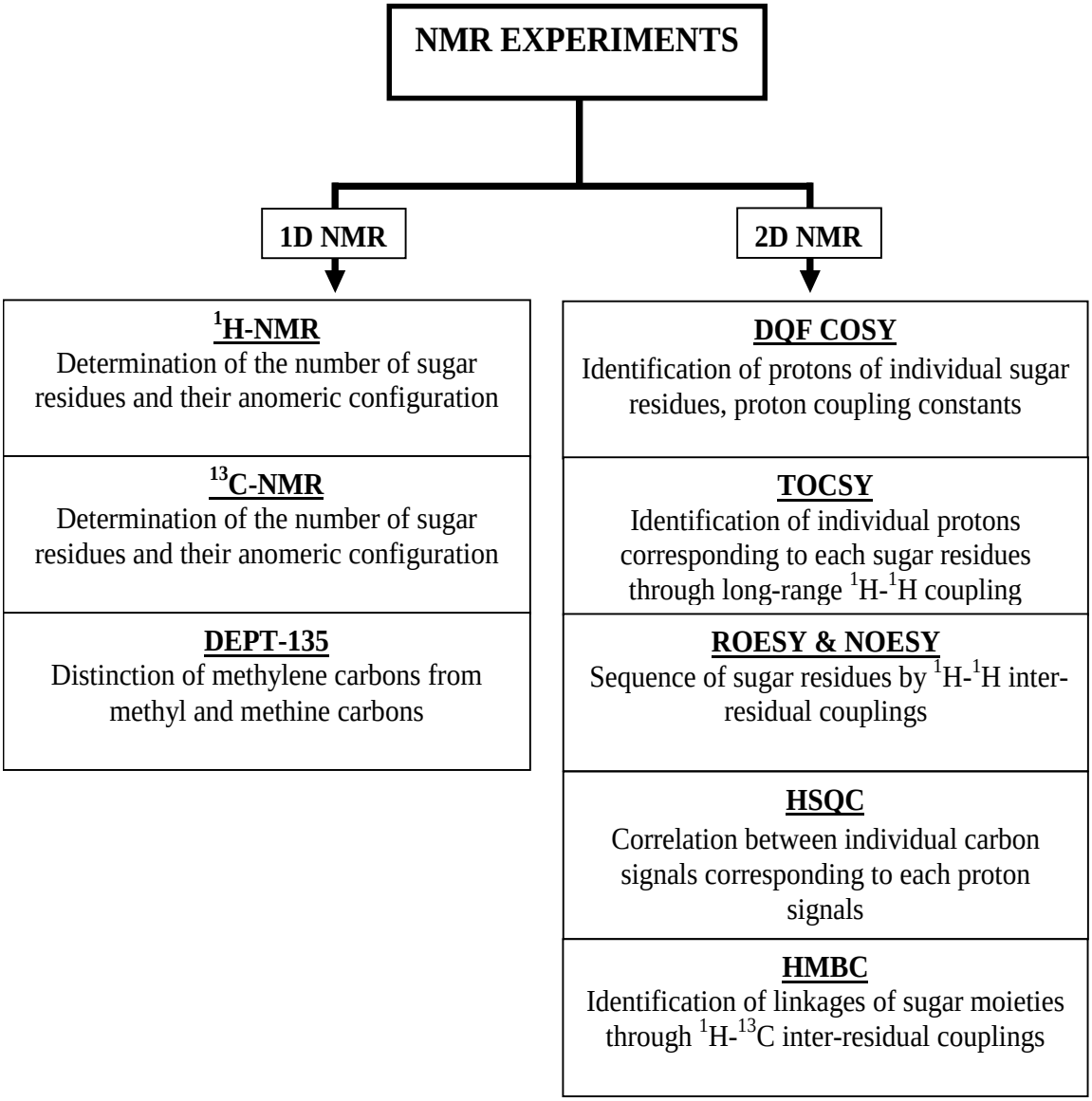

Figure 6. Schematic diagram of determination of structure of a polysaccharide by NMR spectroscopic methods.

2.A.6.1. Preparation of NMR sample and instrumentation

In ^{1}H NMR a major problem is that the OH protons of sugar units and the proton signals from residual water appear in the region of the ring protons, and thereby creates a definite

interference for peak identification. In order to overcome this problem, the samples were kept over P_2O_5 in vacuum for several days to free it from water and deuterium exchanged by repeated lyophilization with D_2O (99.96%. atom ^2H, Aldrich). The ^1H NMR and ^{13}C NMR experiments were performed with a Bruker Avance DPX-500 instrument at 30 °C. The ^1H NMR spectrum was recorded by suppressing the HOD signal (fixed at δ ~ 4.70) using the presaturation method. The DQF-COSY experiment was carried out using standard pulse sequence at 30 °C. The NOESY and ROESY mixing delay were 300 ms. The delay time in the HMBC experiment was 80 ms. The ^{13}C NMR experiments of the polysaccharide were carried out taking acetone as the internal standard, fixing the methyl carbon signal at δ 31.05 by using D_2O as the solvent.

2.A.6.2. One-dimensional NMR

The number of sugar residues (monosaccharide units) and their anomeric configuration can be determined by ^1H NMR. The anomeric proton resonances are generally found in the range of δ 4.4-5.5. The remaining ring proton resonances are found in the range of δ 3-4.2.

The anomeric protons from each monosaccharides give recognizable signals depending upon their α or β anomeric configurations. Normally the α-anomer resonates downfield compared to the β-anomer in D pyranoses. The vicinal coupling constant between the anomeric H-1 and the H-2 (J_{1-2}) indicates the relative orientation of two protons. If both of them are in an axial configuration in pyranose structures, a large coupling constant (7-8 Hz) is observed, whereas if they are in equatorial-axial orientation, the coupling constant is smaller (J_{1-2} ~4 Hz) [8]. Different sugars are identified from their characteristic coupling pattern.

Although ^{13}C NMR signals are much weaker than ^1H, it has significant advantages over the ^1H NMR spectroscopy because in the former the signals are spread out over a wide range. In the ^{13}C NMR spectrum, signals for anomeric carbons appear in the region of δ 90-110, and the non-anomeric carbons in the region of δ 60-90. In case of deoxy sugars the methyl carbons appear in the region of δ 15-20. The α-anomeric carbon signals appear generally in the range of δ 95-103 whereas most of the β-anomeric carbons appear in the region of δ 101-105. Unsubstituted ring carbons usually appear in the region of δ 65-75 [9]. If there is any linkage at any carbon, the signal for that carbon will suffer a downfield shift by δ 4-10, and the carbon next to that one will appear in a little upfield region (by δ

0.7-4.7) [9,10]. Signals for carbonyl carbons are generally observed between δ 165-185. Sometimes the ^{1}H J_{1-2} values are not sufficient to determine the anomeric configurations of the sugars. If the glycosyl residue has the *manno*-configuration, the distinction between the two anomeric forms is very difficult since the coupling costant values for α (J_{1-2} ~1.8 Hz) and β (J_{1-2} ~1.5 Hz) are too close to be differentiated. The one bond ^{13}C-^{1}H coupling constants are useful for determination of the anomeric configuration of sugar residues [11]. For D sugars a $^{1}J_{C1,H1}$ ~170 Hz indicates an α-anomeric sugar configuration whereas $^{1}J_{C1,H1}$ ~160 Hz indicates a β-anomeric sugar configuration [12]. This is reversed for the L sugars. C-1, H-1 coupling constants were determined from proton coupled ^{13}C NMR experiment.

A very useful pulse sequence in ^{13}C spectroscopy is employed in the experiment called Distortionless Enhancement by Polarization Transfer (DEPT). This experiment determines multiplicity of carbon atom substitution with hydrogens. In a DEPT-135 spectrum, methyl and methine carbons give rise to positive peaks, whereas methylene carbons appear as negative peaks.

2.A.6.3. Two-dimensional NMR

The connectivity between the nuclei in a residue and the cross connectivity between the nuclei of different residues can be obtained from 2D NMR. In the present thesis different 2D NMR experiments such as TOCSY, DQF-COSY, NOESY, ROESY, HMQC, and HMBC have been used.

TOCSY (Total correlation spectroscopy)

A TOCSY spectrum correlates protons that are in the same spin system and yields both short range and long-range correlations. It is useful for establishing the scalar connectivity if the proton signals are within a spin system, especially when the multiplets overlap, or there is extensive second order coupling. TOCSY is very powerful tool to confirm the assignments of ^{1}H spectrum. The TOCSY experiment was recorded at mixing time of 300 ms, and complete assignment required several TOCSY experiments having mixing times ranging from 60 to 300 ms.

DQF-COSY (Double quantum filtered correlation spectroscopy)

It gives the information about the protons of an individual sugar residue through a three-bond coupling. The strategy of assigning a COSY spectrum is to find one unmistakable characteristic signal from which to begin the tracing of a spin system or network. An anomeric proton is often chosen as the starting point because it is connected with the other proton atoms of that residue. Coupling constants can also be measured from DQF-COSY spectrum.

NOESY (Nuclear overhauser enhancement spectroscopy)

The NOESY experiment gives information on linkages and sequence of sugar residues in a polysaccharide. It provides information on through space rather than through bond couplings. NOE connectivies are often observed between the anomeric protons of a particular sugar residue to protons of another sugar residue that is glycosidically linked to the former.

ROESY (Rotating frame overhauser enhancement spectroscopy)

ROESY spectrum is used to determine signals arisen from protons, which are close in space but not closely connected by chemical bonds. A ROESY spectrum yields through space correlations via the Rotational nuclear overhauser effect (ROE). ROESY is especially useful for cases where NOESY signals are weak because they are near the transition between negative and positive. ROESY cross peaks are always negative. The ROESY experiment also yields cross peaks arisen from chemical exchange.

HSQC (Heteronuclear single quantum coherence)

This NMR spectrum represents a direct correlation between a carbon and a proton. All the ^{13}C chemical shifts of the sugar residues are here assigned from the individual proton signals assigned from DQF-COSY and TOCSY spectrum as they are directly correlated.

HMBC (Hetero multiple bond coherence spectroscopy)

An HMBC spectrum detects long range coupling between proton and carbon (two or three bonds away) with high sensitivity. Once all the carbon signals are assigned, especially the anomeric and glycosidically linked carbons, unambiguous glycosidic linkages and sequences of the sugar residues can be established through the long-range ^{13}C-^{1}H correlations. HMBC experiments establish multiple-bond correlation through the

glycosidic bonds, and this together with NOESY/ROESY experiments provides necessary information on linkages and sequences of a polysaccharide.

2.A.7. Immunological Studies

2.A.7.1. Test for macrophage activity by nitric oxide assay

RAW 264.7 growing in Dulbecco's modified Eagle's medium (*DMEM*) was seeded in 96 well flat bottom tissue culture plate at 5 x 10^5 cells/mL concentration (180 µL) [13]. Cells were left overnight for attachment and different concentrations (12.5, 25, 50, 100 or 200 µg/mL) of polysaccharides were added. After 48 hrs of treatment, culture supernatant of each well was collected and NO content was estimated using Griess Reagent [14]. Lipopolysaccharide (LPS), L6511 of Salmonella enterica serotype typhimurium (Sigma, St. Louis, USA) was used as positive control where as PBS (Phosphate Buffer Saline, 10 mM, pH-7.4) and soluble starch were used as negative control.

2.A.7.2. Splenocyte and thymocyte proliferation assay

A single cell suspension of spleen and thymus were prepared from the normal mice under aseptic conditions by homogenization in Hank's balanced salt solution (HBSS). The suspension was centrifuged to obtain cell pellet. The contaminating red blood cells (RBC) were removed by hemolytic Gey's solution. After washing two times in HBSS, the cells were resuspended in complete Roswell Park Memorial Institute (RPMI) medium. Cell concentration was adjusted to 1×10^6 cells/mL and the viability of splenocyte and thymocyte (as tested by trypan blue dye exclusion) was always over 90%. The cells (180 µL) were plated in 96-well flat-bottom tissue culture plates and incubated with 20 µL of different concentrations of polysaccharides. PBS (Phosphate Buffer Saline, 10 mM, pH-7.4) is taken as carrier control whereas lipopolysaccharide (LPS, L6511 of Salmonella enterica serotype typhimurium, Sigma, 4 µg/mL) and Concanavalin A (Con A, Himedia, 10 µg/mL, used for only thymocyte proliferation assay for hybrid mushroom *pfle 1p)* served as positive controls. All cultures were set up at 37 °C for 72 h in a humidified atmosphere of 5% CO_2. Proliferation of splenocyte (% Splenocyte Proliferation Index or % SPI) and thymocyte (% Thymocyte Proliferation Index or %TPI) were checked by MTT assay method [15]. All the experiments were done twice with several replicates. The data are reported as the mean ± standard deviation and compared against PBS control [14,16].

2.A.8. References

[1] York, W. S.; Darvill, A. K.; McNeil, M.; Stevenson, T. T.; Albersheim, P. *Methods Enzymol.* **1985**, *118*, 33-40.

[2] Hara, C.; Kiho, T.; Tanaka, Y.; Ukai, S. *Carbohydr. Res.* **1982**, *110*, 77-87.

[3] Gerwig, G. J.; Kamerling, J. P.; Vliegenthart, J. F. G. *Carbohydr. Res.* **1978**, *62*, 349-357.

[4] Gerwig, G. J.; Kamerling, J. P.; Vliegenthart, J. F. G. *Carbohydr. Res.* **1979**, *77*, 1-7.

[5] Ciucanu, I.; Kerek, F. *Carbohydr. Res.* **1984**, *131*, 209-217.

[6] Hay, G. W.; Lewis, B. A.; Smith, F. *Methods Carbohydr. Chem.* **1965**, *5*, 357- 361.

[7] Goldstein, I. J.; Hay, G. W.; Lewis, B. A.; Smith, F. *Methods Carbohydr. Chem.* **1965**, *5*, 361-370.

[8] Jansson, P. E.; Kenne, L.; Widmalm, G. *Carbohydr. Res.* **1987**, *168*, 67-77.

[9] Agrawal, P. K. *Phytochemistry*. **1992**, *31*, 3307-3330.

[10] Gruter, M.; Leeflang, B. R.; Kuiper, J.; Kamerling, J. P.; Vliegenthart, J. F. G. *Carbohydr. Res.* **1993**, *239*, 209-226.

[11] Bock, K.; Pedersen, C.; Pedersen, H. *Adv. Carbohydr. Chem. Biochem.* **1984**, *42*, 193-225.

[12] Bock, K.; Pedersen, C. *J. Chem. Soc. Perkin Trans.* **1974**, *2*, 293-297.

[13] Mallick, S. K.; Maiti, S.; Bhutia, S. K.; Maiti, T. K. *Cell. Biol. Int.* **2011**, *35*, 617-621.

[14] Green, L. C.; Wagner, D. A.; Glogowski, J.; Skipper, P. L.; Wishnok, J. S.; Tannenbaum, S. R. *Anal. Biochem.* **1982**, *126*, 131-138.

[15] Sarangi, I.; Ghosh, D.; Bhutia, S. K.; Mallick, S. K.; Maiti, T. K. *Int. Immunopharmacol.* **2006**, *6*, 1287-1297.

[16] Maiti, S.; Bhutia, S. K.; Mallick, S. K.; Kumar, A.; Khadgi, N.; Maiti, T. K. *Environ. Toxicol. Pharmacol.* **2008**, *26*, 187-191.

CHAPTER – II: PART-B

Methodology for synthesis of gold nanoparticles

2.B.1. Synthesis of gold nanoparticles (Au NPs)

2.B.1.1. Isolation and purification of polysaccharide from *Cochlospermum religiosum* (Katira gum)

Katira gum was washed with methanol, dried, and made powder and then soxhletted using different solvents. The crude material was then dissolved in water, dialyzed, centrifuged, and the filtrate was precipitated in alcohol to get crude polysaccharide which was further purified through Sepharose 6B column as reported by Ojha et al. [1]. The structure of the pure polysaccharide was confirmed by NMR studies [1] as

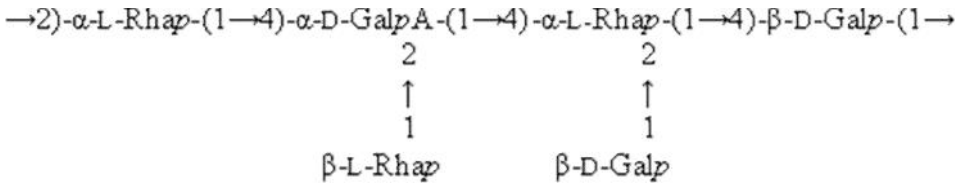

2.B.1.2. Synthesis of polysaccharide based Au NPs

The pure polysaccharide isolated from katira gum was used for the synthesis of Au NPs. For the synthesis of Au NPs, 2 mL aqueous solution of $HAuCl_4$ with a concentration of 10^{-3} M was added to 6 mL 0.2 % (w/v) aqueous polysaccharide solution. The mixture was then heated at 70 °C, 6 h with continuous stirring on a magnetic stirrer and UV-vis spectra of the reaction mixture were recorded at different time interval till the completion of the reaction.

2.B.2. Characterization of Au NPs

2.B.2.1. UV-vis spectroscopic analysis

The UV-vis absorption spectra were taken at room temperature on a Shimadzu UV-1601 spectrometer using a quartz cuvette with a 1 cm optical path. 1 ml of each solution was diluted with equal volume of water for taking spectra. Double distilled water was used as the blank

2.B.2.2. High resolution-transmission electron microscopy (HR-TEM) analysis

The shape, morphology, and size distribution of the Au NPs were analyzed using high resolution transmission electron microscopy (HR-TEM). HRTEM is a powerful instrument for studying properties of materials on the atomic scale. Transmission electron microscopic images were recorded in a JEOL-JEM-2100 HRTEM operated at 200 kV. For

the TEM analysis a droplet of aqueous solution of synthesized Au NPs was spread onto a carbon coated copper grid (300 meshes) and dried under IR lamp. Micrographs were taken in both in the transmission mode and diffraction mode.

2.B.2.3. X-ray diffraction (XRD) analysis

XRD data of NPs generally provide information about crystallinity, crystallite size, orientation of the crystallites. For XRD analysis, a thin film of the sample was prepared on a microscopic glass slide using the aqueous solution of Au NPs and dried under vacuum. The measurements were carried out with a Rigaku Miniflex II X-ray diffractometer, using Ni-filtered Cu Kα (λ=0.15406 nm) radiation. The diffraction intensities were recorded from 30° to 80° 2θ angle.

2.B.2.4. Fourier transform-infrared spectra (FT-IR) analysis

In order to investigate the interaction of Au NPs with the polysaccharide, FT-IR experiment of both the polysaccharide and Au NPs polysacharide bioconjugates were carried out. The aqueous solution of the synthesized Au NPs was freeze-dried and the dried sample was used for FT-IR analysis. FT-IR analysis was performed in an FTIR-8400S (Shimadzu) instrument between 4000 and 400 cm^{-1} using KBr pellet technique.

2.B.3. Catalytic properties of Au NPs for 4-nitrophenol reduction

The reduction of 4-nitrophenol (4-NP) was studied as a model reaction to prove the catalytic activity of synthesized Au NPs. The catalytic reaction was performed in a standard quartz cuvette with a 1 cm path length. 2 mL double distilled water was mixed with 120 µL of 2 mM 4-NP solution followed by the addition of 1mL of 15 mM freshly prepared $NaBH_4$ solution. Thereafter 3.5 mg of solid freeze dried Au NPs-polysaccharide bioconjugates were added to the above reaction mixture as heterogeneous catalyst. Immediately after the addition of Au NPs, the absorption spectra were recorded in 2 min interval in the range of 200-600 nm at room temperature.

2.B.4. References

[1] Ojha, A. K.; Maiti. D.; Chandra, K, Mondal, S.; Das, D.; Roy, S. K.; Ghosh, K.; Islam, S. S. Carbhydr. Res. **2008**, *343*, 1222-1231.

CHAPTER – III

Structural and immunological studies of polysaccharide from an edible hybrid mushroom *pfle 1q*

3.1. Introduction and review on earlier work

Mushrooms have been consumed globally as tasty food and nutritional supplements. Mushroom polysaccharides have been recognized as the most potent antitumor and immunostimulating materials [1-3]. Currently development of new hybrid mushroom through para-sexual mating is well established. Several somatic edible hybrid mushrooms were developed through polyethylene glycol-mediated protoplast fusion between *Pleurotues florida* and *Volvariella volvacea* [4], *Pleurotues florida and Calocybe indica var.* APK2 [5] *Pleurotues florida* and *Lentinus squarrosulus* [6]. A variety of immunoenhancing glycans and heteroglycans have been isolated from hybrid mushrooms. Immunostimulating polysaccharides from fruit bodies of the strain *PCH9FB* (hybrid of *P. florida* and *C. indica var.* APK2) were isolated and reported [7,8]. Two different polysaccharides were isolated from aqueous [9] and alkaline [10] extract of another hybrid mushroom obtained through back cross mating of a somatic hybrid mushroom *PfloVv12* (sterile line) with *V. volvacea*. Different immunoenhancing glucans from somatic hybrid *PfloVv5FB* [11,12] and heteroglycan from somatic hybrid *PfloVv1aFB* [13,14] were isolated and reported by our group. These two hybrid mushrooms *PfloVv5FB* and *PfloVv1aFB* were obtained through protoplast fusion between the strains of *P. florida* and *V. volvacea*.

3.1.1. The hybrid mushroom *pfle 1q*

Pleurotues florida is a common oyster mushroom in India, having good nutritive values and can be commercially cultivated in the sub-tropical climate (temperature range 22-26 ^{o}C). Compositional analyses revealed that *P. florida* is highly rich in protein, carbohydrate, fibre, and essential fatty acids [15]. Different immunostimulating polysaccharides such as (1→6)-α-D-glucan [16], (1→3), (1→6)-α, β-D-glucan [17], (1→3), (1→6)-β-D-glucan [18] and heteroglycan composed of glucose, mannose, and galactose [19] were isolated from *Pleurotus florida*.

Lentinula *edodes*, the shiitake mushroom native to East Asia, requires low temperature (10-18 ^{o}C) and specific substrate (oak log) for fruiting. It is a rich source of nutrients and fibers. Lentinan, a water insoluble (1→3)-, (1→6)-β-glucan isolated from *Lentinula edodes* is well known for its high antitumor activity [20]. A water soluble glucan having potent antitumor activity also isolated from *Lentinula edodes* [21].

Intergeneric protoplast fusion between the strains of *Pleurotus florida* and *Lentinula edodes* produced nine new hybrid out of which six strains *i.e., pfle 1o, pfle 1p, pfle 1q, pfle 1r, pfle 1s,* and *pfle 1v* produced fruit bodies [22]. Hybrid strains were selected based on double selection method and afterwards maintained in Potato-Dextrose-Agar medium. Spawn of the hybrid strain was produced on paddy grain and mushroom was produced on paddy straw substrate [22]. Aqueous extract of the fruit bodies of hybrid strain, *pfle 1q* yielded single polysaccharide through Sepharose 6B gel purification. The present polysaccharide is a mannogalactan consisting of a main chain of $(1\rightarrow6)$-linked D-galactopyranosyl moieties with terminal D-mannopyranosyl linked at C-2 of the D-galactopyranosyl residue, which was not obtained from any of the parent mushrooms. The detailed structural characterization and the immunoenhancing properties of this polysaccharide isolated from aqueous extract of the fruit bodies of the hybrid mushroom strain *pfle 1q* were carried out and discussed in this chapter.

Figure 1. Photograph of hybrid mushroom *pfle 1q* [22].

3.2. Present work

3.2.1. Isolation, purification, and physical characterization of PS

The hybrid mushroom of *pfle 1q* was cultivated and collected from Falta experimental farm, Bose Institute. The fresh mushroom fruit bodies (500 g) were washed thoroughly and then boiled with distilled water for 8 h followed by filtration, centrifugation, precipitation in ethanol, dialysis, centrifugation and freeze drying to yield 315 mg of crude polysaccharide. Purification of this water soluble crude polysaccharide (25 mg) through Sepharose 6B column yielded single fraction [Figure 2] which was then collected and

freeze-dried, yielding 10 mg purified polysaccharide (PS). The purification process was carried out in several lots.

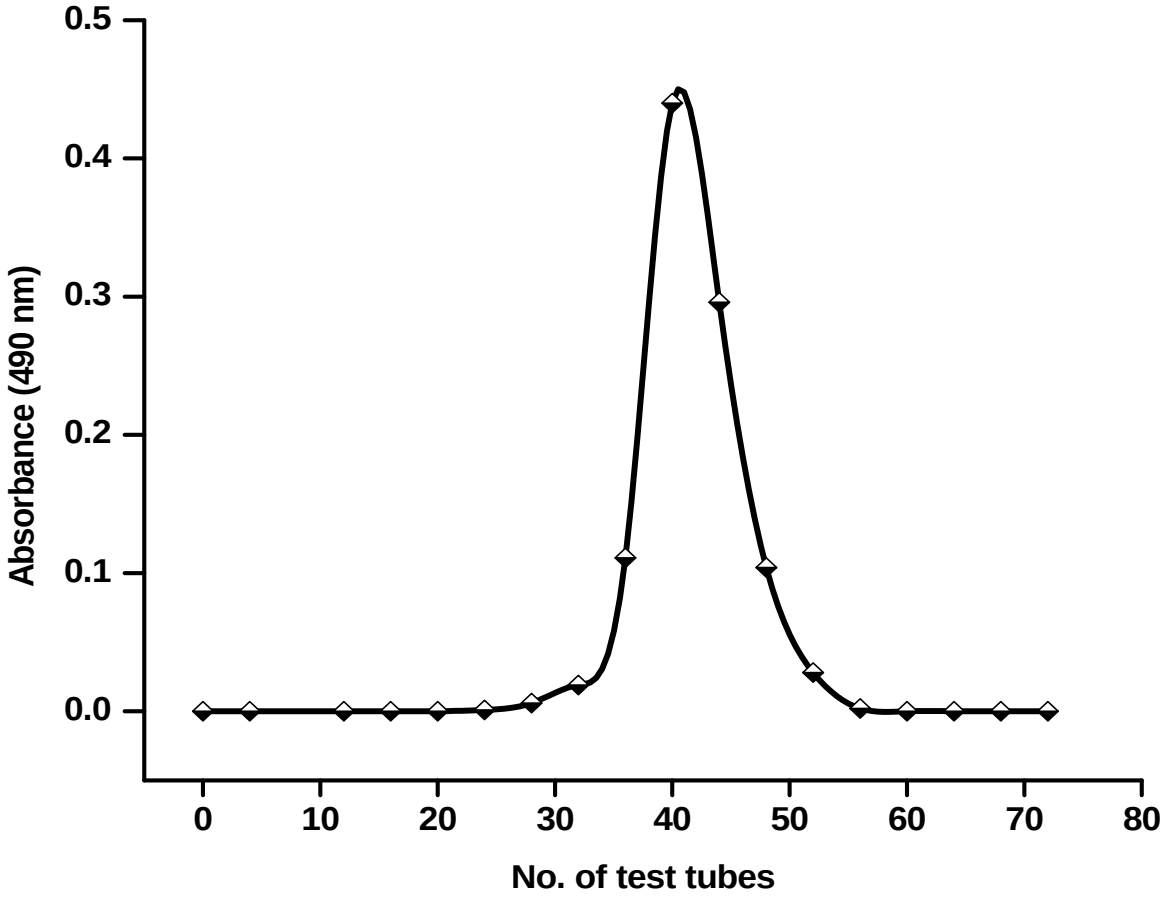

Figure 2. The gel permeation chromatogram of the crude polysaccharide fractionated through Sepharose 6B column.

The total carbohydrate of the PS was estimated to 98 % using sulfuric acid-phenol method [23]. In order to check the presence of protein, UV analysis was monitored at 280 nm but lack of absorbance at 280 nm in the UV spectrum indicated that the sample was free from protein. The PS showed a specific rotation of $[\infty]_D^{30.9}$ + 50.08 (*c* 0.09, water). The apparent average molecular weight [24] of the PS fraction was estimated as 1.55×10^5 Da, as determined from the calibration curve using dextrans of known molecular weight [Figure 3].

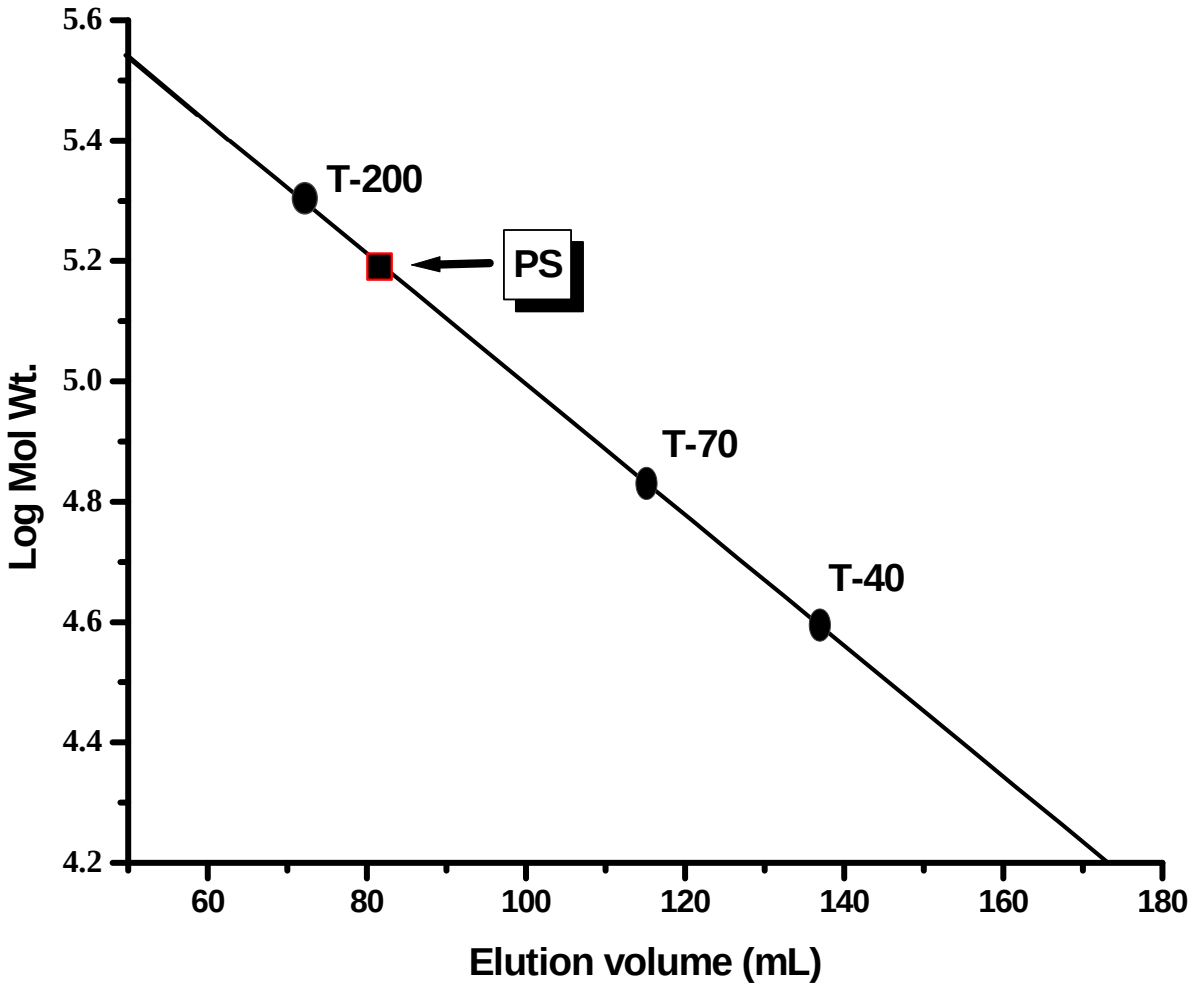

Figure 3. Determination of molecular weight of the PS isolated from the hybrid mushroom *pfle 1q*.

3.2.2. Strutural analysis of PS

3.2.2.1. Chemical analysis

Hydrolysis of PS was carried out with 2 M TFA for 18 h. The hydrolyzed product was then reduced and ultimately converted to alditol acetates. The GLC analysis of the alditol acetates of the hydrolyzed product of PS confirmed the presence of mannose and galactose in a molar ratio of nearly 1:2. The absolute configuration of the monosaccharides was determined by the method of Gerwig et al. [25] and it was found all the monosaccharides had D-configuration. The PS was methylated adopting the method of Ciucanu and Kerek [26] as given in methodology section (chapter II, part A, 2.A.5.3.) followed by hydrolysis, reduction and then alditol acetate preparation. The partially methylated alditol acetate was analyzed by GLC-MS.

The GLC-MS analysis revealed the presence of 1,5-di-*O*-acetyl-2,3,4,6-tetra-*O*-methyl-D-mannitol, 1,5,6-tri-*O*-acetyl-2,3,4-tri-*O*-methyl-D-galactitol, 1,2,5,6-tetra-*O*-acetyl-3,4-di-

O-methyl-D-galactitol in a molar ratio of nearly 1:1:1. Thus, PS was assumed to consist of terminal D-mannopyranosyl, (1→6)-linked D-galactopyranosyl, and (1→2,6)-linked D-galactopyranosyl moieties, respectively [Table 1, Figure 4]. These linkages were further confirmed by periodate oxidation experiment. The GLC-MS analysis of the alditol acetates of periodate oxidized, reduced, methylated [27,28] PS showed total disappearance of sugar residues. These results indicated that all the sugar residues were consumed during oxidation. Thus, the mode of linkages present in the PS was confirmed.

Table 1. GC-MS data for methylated PS isolated from the hybrid mushroom *pfle 1q*.

Methylated sugars	Linkages	Molar Ratio	Major Fragments (m/z)
2,3,4,6-Me_4-Man*p*	Man*p*-(1→	1	43, 45, 71, 87, 101, 117, 129, 145, 161, 205
2,3,4-Me_3-Gal*p*	→6)-Gal*p*-(1→	1	43,45,71,87,99,101,117,129,161, 173,189,233
3,4-Me_2-Gal*p*	→6,2)-Gal*p*-(1→	1	43,71,87,99,129,189

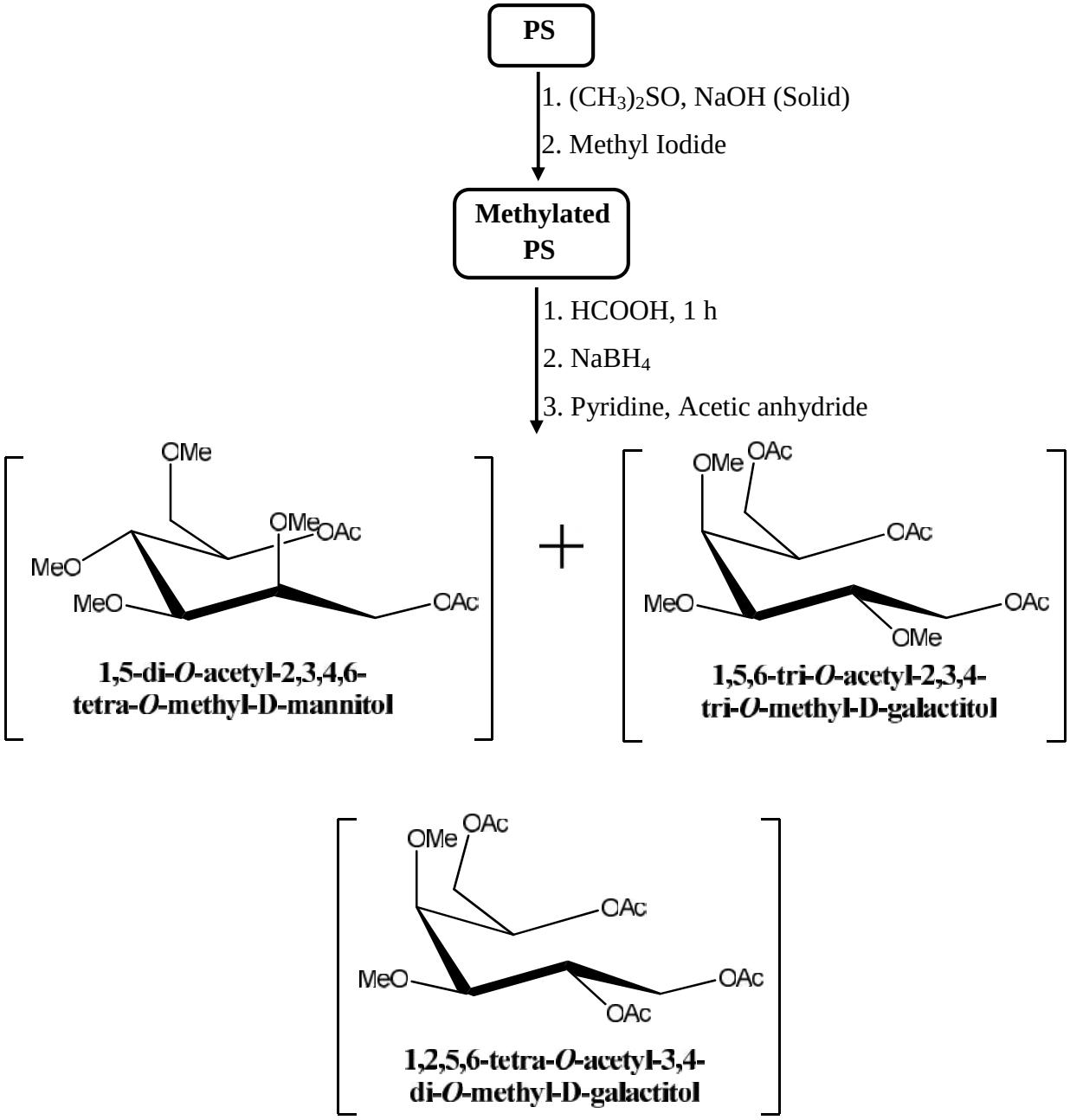

Figure 4. Schematic presentation of methylation experiment of PS isolated from hybrid mushroom *pfle 1q*.

3.2.2.2. NMR analysis

The ^{1}H NMR spectrum [Figure 5] of PS showed the presence of three signals in the anomeric region at δ 5.14, 5.00, and 4.81 in a ratio of nearly 1:1:1. They were designated **A**, **B**, and **C** according to their decreasing proton chemical shifts. Three signals in the anomeric region of ^{13}C spectrum [Figure 6] at δ 101.6, 98.3, and 97.8 correlated to the residues **C**, **A**, and **B,** respectively from HSQC spectrum [Figure 7]. The rest of the ^{1}H and ^{13}C signals [Table 2] were assigned from DQF-COSY, TOCSY, and HSQC experiments. The proton coupling constants were measured from DQF-COSY experiment.

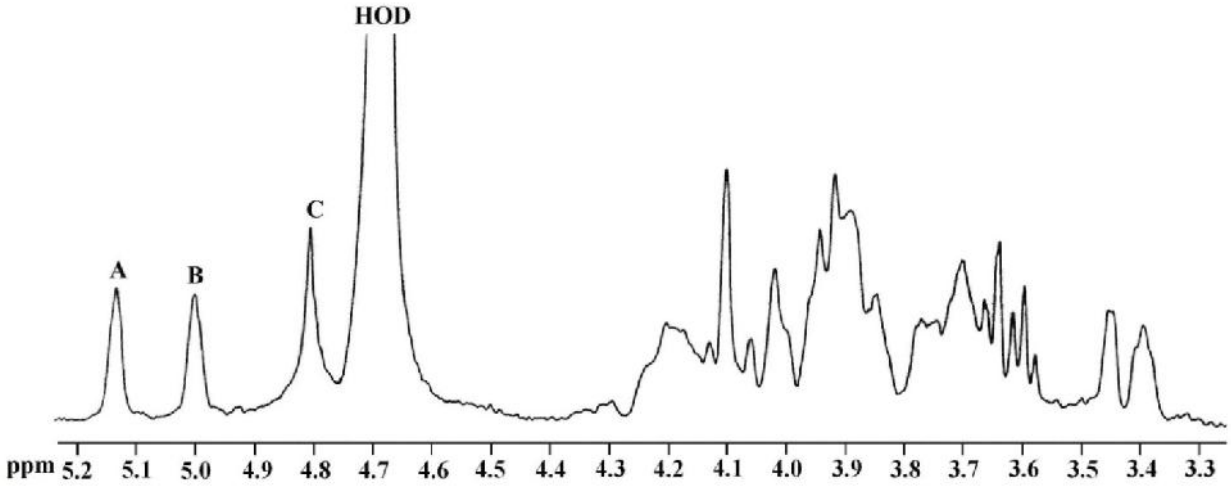

Figure 5. ^{1}H NMR spectrum (500 MHz, D_2O, 30 ºC) of the PS isolated from hybrid mushroom *pfle 1q*.

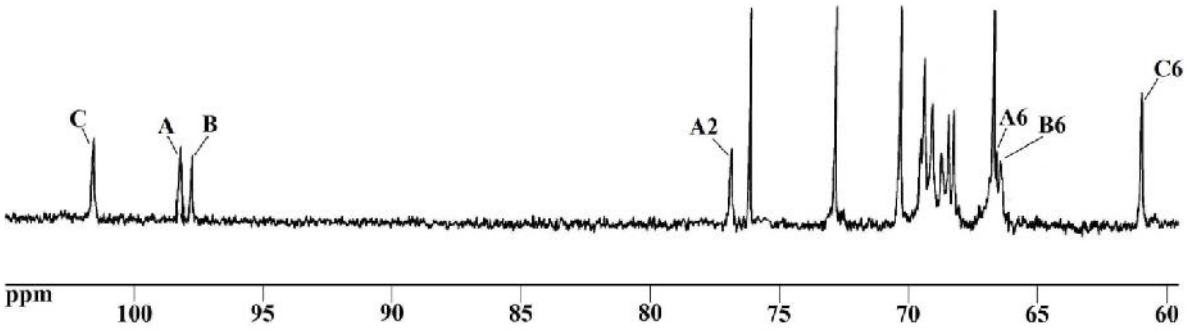

Figure 6. ^{13}C NMR spectrum (125 MHz, D_2O, 30 ºC) of the PS isolated from hybrid mushroom *pfle 1q*.

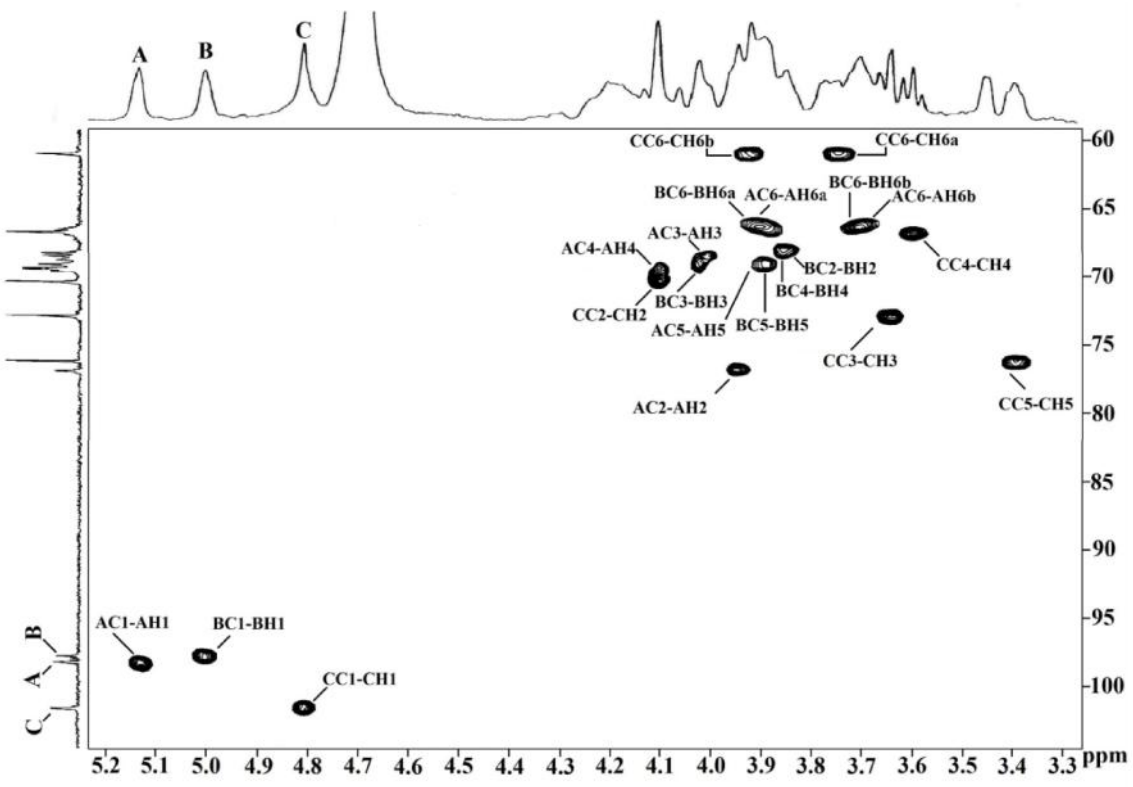

Figure 7. HSQC spectrum (D_2O, 30 ºC) of the PS isolated from hybrid mushroom *pfle 1q*.

Table 2. The ^{1}H and ^{13}C NMR chemical shifts for the PS isolated from *pfle 1q*[a,b] in D_2O at 30°C.

Glycosyl residue	H-1/C-1	H-2/C-2	H-3/C-3	H-4/C-4	H-5/C-5	H-6a, H-6b/C-6
→2,6)-α-D-Gal*p*-(1→ **A**	5.14	3.95	4.01	4.12	3.90	3.70[c], 3.90[d]
	98.3	76.9	68.5	69.5	69.1	66.6
→6)-α-D-Gal*p*-(1→ **B**	5.00	3.85	4.02	3.86	3.89	3.71[c], 3.91[d]
	97.8	68.3	68.8	68.3	69.1	66.5
β-D-Man*p*-(1→ **C**	4.81	4.11	3.64	3.60	3.39	3.74[c], 3.92[d]
	101.6	70.4	72.9	66.7	76.2	61.0

[a] Values of the ^{1}H chemical shifts were recorded with respect to the HOD signal fixed at δ 4.70 at 30 °C. [b] Values of the ^{13}C chemical shifts were recorded with reference to acetone as the internal standard and fixed at δ 31.05 at 30 °C. [c,d] Interchangeable.

Among these three residues, residues **A** and **B** had coupling constant values of $J_{H\text{-}2,\ H\text{-}3}$ ~9 Hz and $J_{H\text{-}3,\ H\text{-}4}$ ~3.5 Hz and thus, they were confirmed as D-galactopyranosyl residues.

The anomeric proton (δ 5.14 for **A** and δ 5.00 for **B**) and anomeric carbon chemical shifts (δ 98.3 for **A** and δ 97.8 for **B**) as well as the coupling constant values ($J_{H\text{-}1,H\text{-}2}$ ~3.1 Hz and $J_{C\text{-}1,H\text{-}1}$ ~171 Hz) confirmed that these residues were present in α-configuration. In case of residue **A**, all the proton and carbon chemical shifts except C-2 and C-6 were nearly matched with the standard values of methyl glucosides [29,30]. The downfield shifts of C-2 (δ 76.9) and C-6 (δ 66.6) with respect to standard values indicated that it was linked at C-2 and C-6. The linkage at C-6 was also supported by DEPT-135 spectrum [Figure 8]. Thus, **A** was confirmed as (1→2,6)-linked α-D-galactopyranosyl residue. For residue **B**, the downfield shift of C-6 (δ 66.5) with respect to standard values of methyl glucosides confirmed that residue **B** contained C-6 linkage. The linkage at C-6 was further supported by DEPT-135 spectrum [Figure 8]. Therefore, **B** was confirmed as (1→6)-linked α-D-galactopyranosyl residue. The large coupling constant values ($J_{H\text{-}3,\ H\text{-}4}$ ~7.5 Hz and $J_{H\text{-}4,\ H\text{-}5}$ ~10 Hz) of residue **C** confirmed its mannopyranosyl configuration. The anomeric proton (δ 4.81) and anomeric carbon chemical shifts (δ 101.6) as well as the low coupling constant values ($J_{H\text{-}1,H\text{-}2}$ ~0, $J_{C\text{-}1,H\text{-}1}$ ~161) confirmed that residue **C** was present in β-configuration. All the proton and carbon chemical shifts of residue **C** corresponded nearly to the standard values of methyl glycosides of β-D-mannose. Thus, **C** was confirmed as terminal β-D-mannopyranosyl residue.

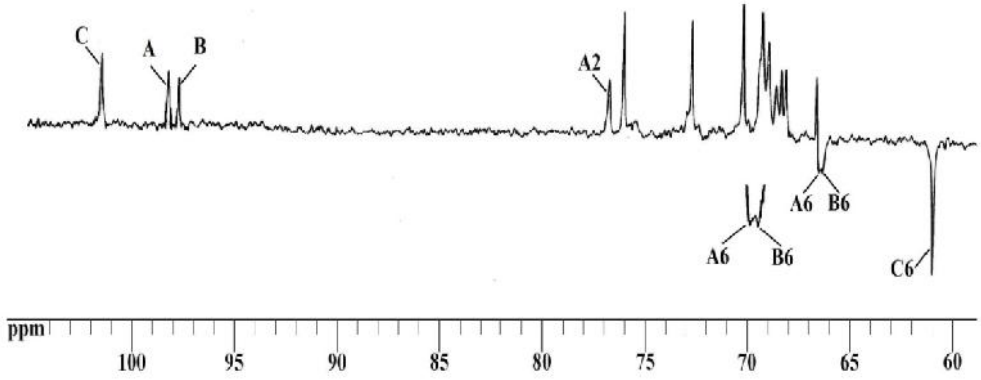

Figure 8. DEPT-135 spectrum (D_2O, 30 ºC) of the PS isolated from hybrid mushroom *pfle 1q*.

The different linkages that connected these three residues were determined from ROESY [Figure 9, Table 3] as well as NOESY (not shown) spectrum. In ROESY spectrum, the inter-residual connectivities were observed between **A**H-1/**B**H-6a and **B**H-6b, **B**H-1/**A**H-6a and **A**H-6b, and **C**H-1/**A**H-2 along with other intra-residual contacts.

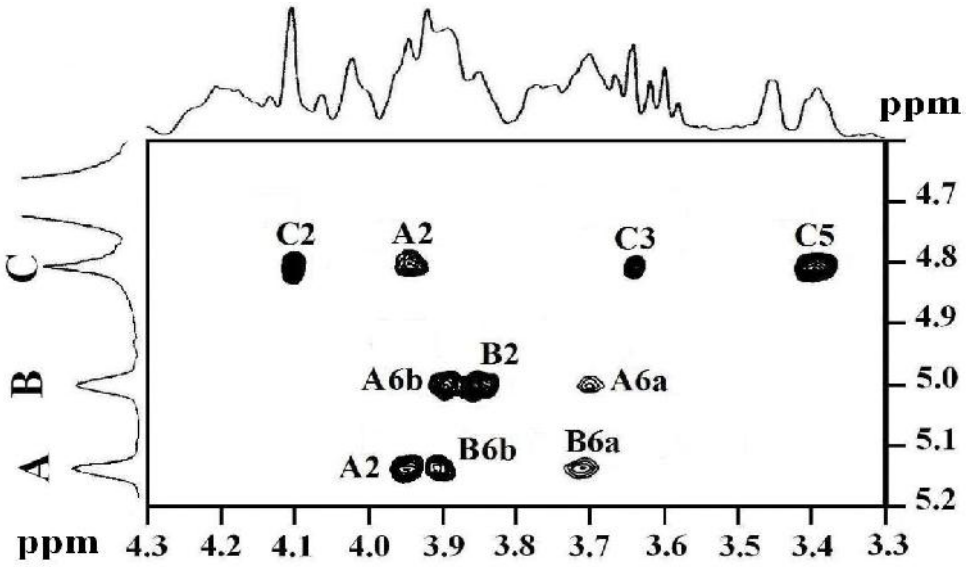

Figure 9. Part of the ROESY spectrum of the PS isolated from hybrid mushroom *pfle 1q*.

Table 3. ROESY data for the PS isolated from hybrid mushroom *pfle 1q*.

Glycosyl residue	Anomeric proton	ROE contact protons	
	δ	δ	**Residue**, Atom
→2,6)-α-D-Gal*p*-1→ **A**	5.14	3.95	**A** H-2
		3.71	**B** H-6a
		3.91	**B** H-6b
→6)-α-D-Gal*p*-(1→ **B**	5.00	3.85	**B** H-2
		3.70	**A** H-6a
		3.90	**A** H-6b
β-D-Man*p*-(1→ **C**	4.81	4.11	**C** H-2
		3.64	**C** H-3
		3.39	**C** H-5
		3.95	**A** H-2

Thus, from ROESY spectrum the following linkages were established.

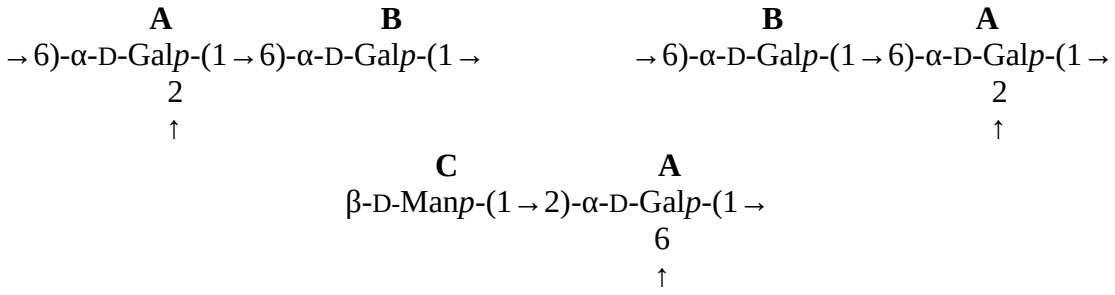

These connectivities were further confirmed from HMBC experiment [Figure 10, Table 4]. In HMBC spectrum the inter-residual cross-peaks were observed between **A**H-1/**B**C-6, **A**C-1/**B**H-6a and **B**H-6b, **B**H-1/**A**C-6, **B**C-1/**A**H-6a and **A**H-6b, **C**H-1/**A**C-2, and **C**C-1/**A**H-2.

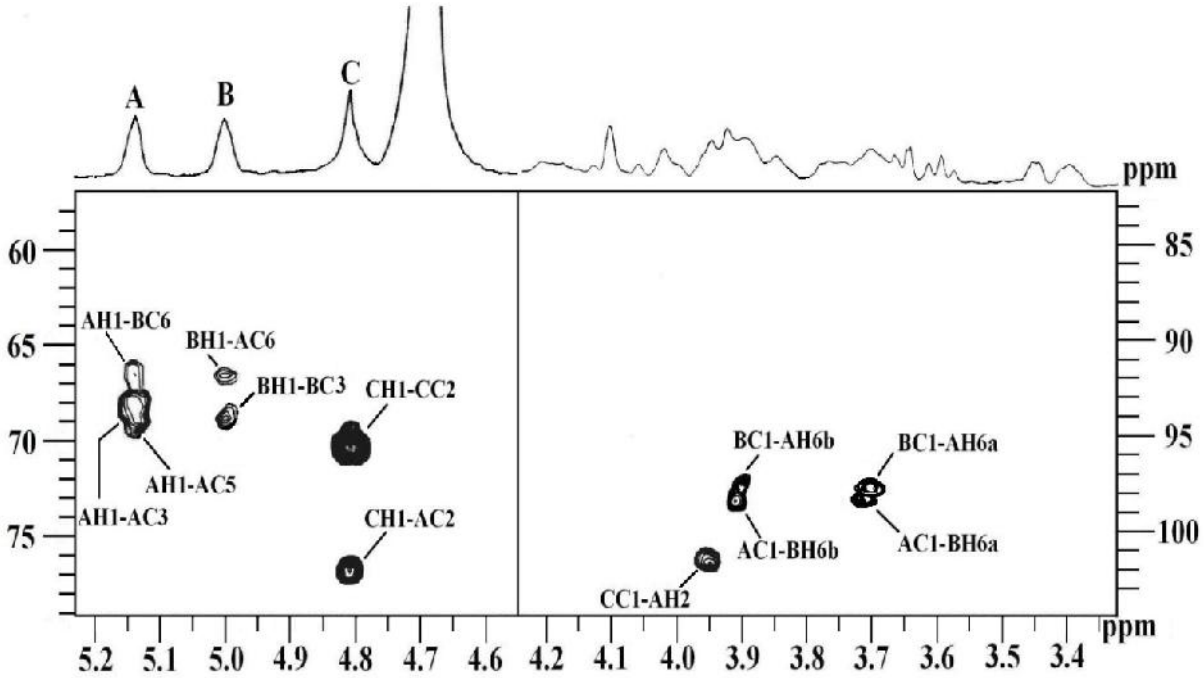

Figure 10. Part of the HMBC spectrum of the PS isolated from hybrid mushroom *pfle 1q*.

Table 4. The significant $^{3}J_{H,C}$ connectivities observed in an HMBC spectrum for the anomeric protons/carbons of the sugar residues of the PS isolated from hybrid mushroom *pfle 1q*.

Sugar residue	H-1/C-1	Observed connectivities		
	δ_H/δ_C	δ_H/δ_C	**Residue**	Atom
→2,6)-α-D-Gal*p*-(1→	5.14	68.5	**A**	C-3
A		69.1	**A**	C-5
		66.5	**B**	C-6
	98.3	3.71	**B**	H-6a
		3.91	**B**	H-6b
→6)-α-D-Gal*p*-(1→	5.00	68.8	**B**	C-3
B		66.6	**A**	C-6
	97.8	3.70	**A**	H-6a
		3.90	**A**	H-6b
β-D-Man*p*-(1→	4.81	70.4	**C**	C-2
C		76.9	**A**	C-2
	101.6	3.95	**A**	H-2

Thus, the HMBC and ROESY connectivities clearly supported the presence of the following repeating unit in the PS:

A **B**
→6)-α-D-Gal*p*-(1→6)-α-D-Gal*p*-(1→
2
↑
1
β-D-Man*p*
C

3.2.3. Biological studies

3.2.3.1. Assay for macrophage activity by NO

Mushroom polysaccharides function as immunostimulator by activating the macrophages [31]. Macrophages are white blood cells which play key roles in immune system defense. They usually engulf and destroy bacteria and viruses. Hence, macrophage activation induced by the PS was tested *in vitro*. On treatment with different concentrations of this PS it was observed that 25% to 34% of NO production increased up to 25 µg/mL. This was further increased by 87% to 114% at 50 and 100 µg/mL, respectively, but decreased at 200 µg/mL [Figure 11]. Hence, an enhanced production of NO i.e. the effective dose of this PS was observed at 100 µg/mL with optimum production of 12.8 µM NO per 5×10^5 macrophages.

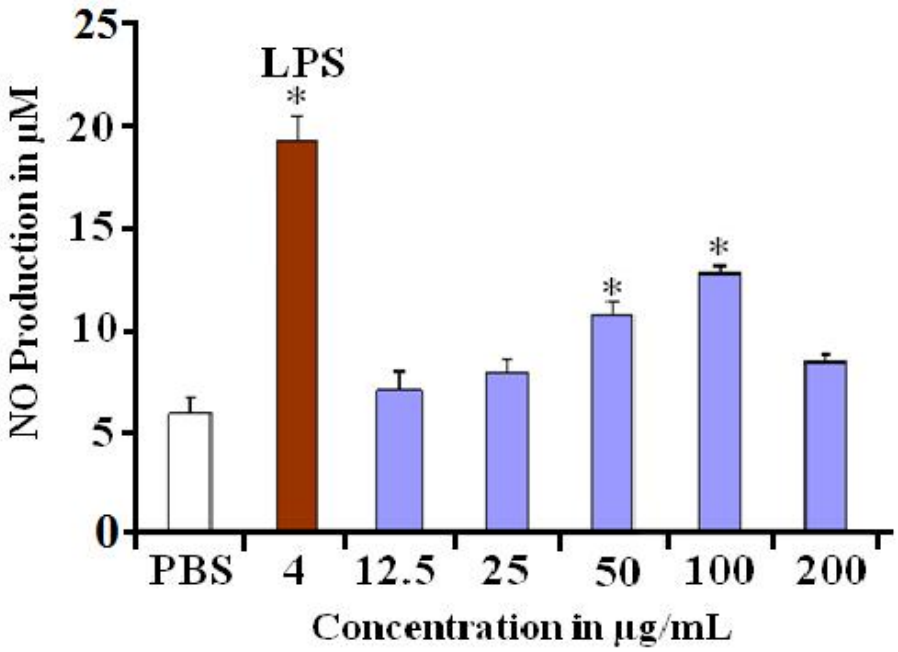

Figure 11. *In vitro* activation of macrophage stimulated with different concentrations of the PS isolated from hybrid mushroom *pfle 1q* in terms of NO production.

\

3.2.3.2. Splenocyte and thymocyte proliferation assay

Proliferation of splenocyte and thymocyte is an indicator of immunostimulation [31]. The splenocyte and thymocyte activation tests were carried out in mouse cell culture medium with the PS by the MTT [3-(4,5-dimethylthiazol-2-yl)-2,5-diphenyltetrazolium bromide] method [32]. The PS was tested to stimulate splenocyte and thymocyte and the results are shown in Figure 12 and 13, respectively. The asterisks on the columns indicated the statistically significant differences compared to phosphate buffer saline (PBS) control. The splenocyte and thymocyte proliferation indices as compared to PBS control if closer to 100 or below indicate low stimulatory effect on immune system. Both the splenocyte and thymocyte proliferation indices were found maximum at 50 µg/mL, above and below which it decreased. Hence, it can be concluded that 50 µg/mL is the optimum concentration of the PS for splenocyte and thymocyte proliferation.

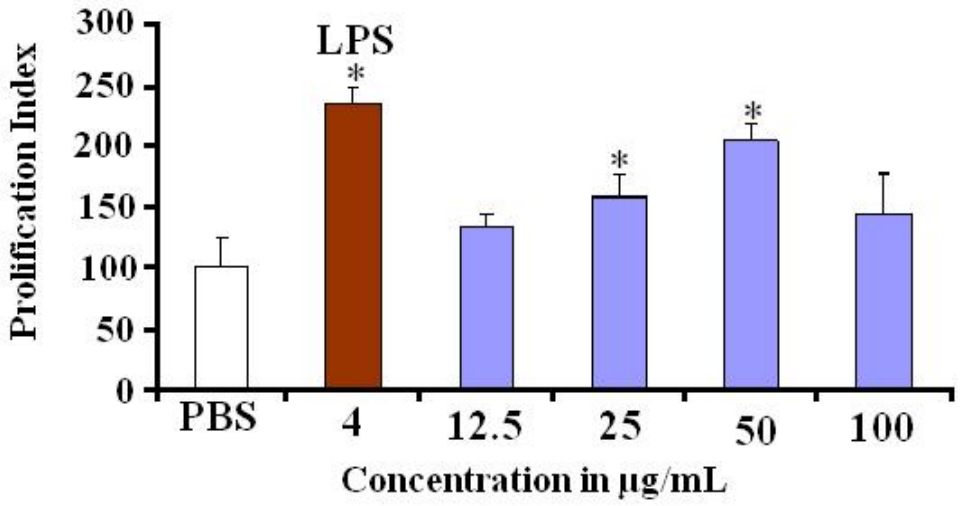

Figure 12. Effect of different concentrations of the PS isolated from hybrid mushroom *pfle 1q* on splenocyte proliferation ('*' means data is significant compared to the PBS control).

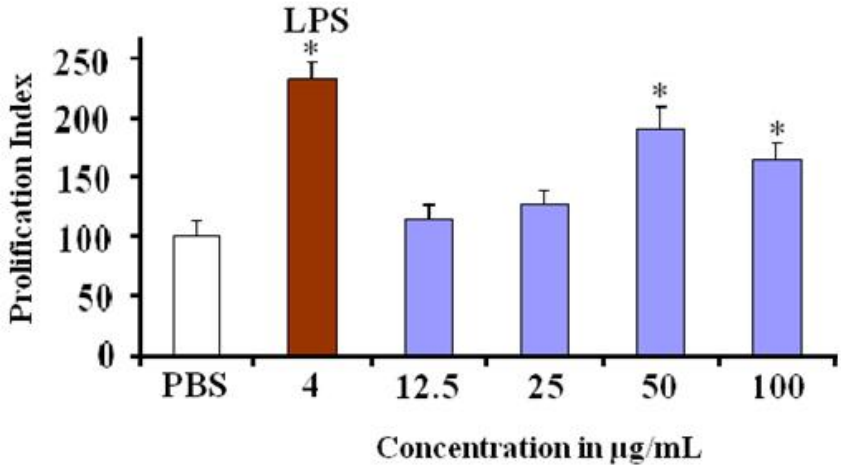

Figure 13. Effect of different concentrations of the PS isolated from hybrid mushroom *pfle 1q* on thymocyte proliferation. ('*' means data is significant compared to the PBS control).

Mushroom polysaccharides have been recognized as biological response modifiers (BRMs). Biological response modifiers (BRMs) are the compounds which are capable of interacting with the immune system to upregulate or downregulate the host immune response. BRMs affect different cell type involving hematopoietic stem cells, innate (nonspecific) and adaptive (specific) immune systems and cytokine networks and signaling pathways and the activities also depend on their mechanism of action or the site of activity [32]. The studies like NO production by macrophages, splenocyte and thymocyte proliferations are preliminary steps to explore whether the PS has any immunomodulating property or not. However, further studies are needed in order to identify the specific cells or cytokine pathway through which the PS exerts its action. It is expected that the PS showing immunomodulating properties *in vitro* may exhibit similar effect *in vivo* and help in combating microbial infection including tuberculosis, tumor cell eradication and autoimmune diseases.

3.3. References

[1] Borchers, A. T.; Stern, J. S.; Hackman, R. M.; Keen, C. L.; Gershwin, M. E. *P. Soc. Exp. Med.* **1999**, *221*, 281-293.

[2] Nanba, H.; Hamaguchi, A.; Kuroda, H. *Chem. Pharm. Bull*. **1987**, *35*, 1162-1168.

[3] Mizuno, T.; Inagaki, R.; Kanao, T.; Hagiwara, T.; Nakamura, T.; Ito, H.; Shimura, K.; Sumiya, T.; Asakura, A. *Agr. Biol. Chem.* **1990**, *54*, 2897-2905.

[4] Chakraborty, U.; Sikdar, S. R. *World J. Microbiol. Biotechnol.* **2008**, *24*, 1481-1492.

[5] Chakraborty, U.; Sikdar, S. R. *World J. Microbiol. Biotechnol.* **2010**, *26*, 213-225.

[6] Mallik, P.; Sikdar, S. R. *Int. J. Pharm. Bio. Sci.* **2015**, *6*, 301-314.

[7] Maity, K.; Kar, E.; Maity, S.; Gantait, S. K.; Das, D.; Maiti, S.; Maiti, T. K.; Sikdar, S. R.; Islam, S. S. *Int. J. Biol. Macromol.* **2011**, *48*, 304-310.

[8] Maity, K.; Kar, E.; Maity, S.; Gantait, S. K.; Das, D.; Maiti, S.; Maiti, T. K.; Sikdar, S. R.; Islam, S. S. *Int. J. Biol. Macromol*. **2011**, *49*, 555-560.

[9] Nandan, C. K.; Sarkar, R.; Bhanja, S. K.; Sikdar, S. R.; Islam, S. S. *Carbohydr. Res.* **2011**, *346*, 2451-2456.

[10] Sarkar, R.; Nandan, C. K.; Bhanja, S. K.; Maiti, S.; Maiti, T. K.; Sikdar, S. R.; Islam, S. S.
Carbohydr. Res. **2012**, *347*, 107-113.

[11] Das, D.; Mondal, S.; Roy, S. K.; Maiti, D.; Bhunia, B.; Maiti, T. K.; Sikdar, S. R.; Islam, S. S. *Carbohydr. Res.* **2010**, *345*, 974-978.

[12] Maity, K. K.; Patra, S.; Dey, B.; Bhunia, S. K.; Mandal, S.; Behera, B.; Maiti, T. K.; Sikdar,
S. R.; Islam, S. S. *Carbohydr. Res.* **2013**, *370*, 13-18.

[13] Patra, S.; Maity, K. K.; Bhunia, S. K.; Dey, B.; Mandal, S.; Maiti, T. K.; Sikdar, S. R.; Islam, S. S. *Carbohydr. Res.* **2012**, *354*, 110-115.

[14] Bhunia, S. K.; Dey, B.; Maity, K. K.; Patra, S.; Mandal, S.; Maiti, S.; Maiti, T. K.; Sikdar, S. R.; Islam, S. S. *Carbohydr. Res.* **2011**, *346*, 1967-1972.

[15] Crisan, E. V.; Sands, A.; Nutritional value. In: S. T. Chang, W.A. Hayes (eds.), *The biology*
and cultivation of edible mushrooms, New York Academic Press, New York. **1978**, 137-165.

[16] Rout, D.; Mondal, S.; Chakraborty, I.; Pramanik, M.; Islam, S. S. *Med. Chem. Res.* **2004**, *13*, 509-517.

[17] Rout, D.; Mondal, S.; Chakraborty, I.; Pramanik, M.; Islam, S. S. *Carbohydr. Res.* **2005**, *340*, 2533-2539.

[18] Rout, D.; Mondal, S.; Chakraborty, I.; Islam, S. S. *Carbohydr. Res.* **2008**, *343*, 982-987.

[19] Rout, D.; Mondal, S.; Chakraborty, I.; Islam, S. S. *Carbohydr. Res.* **2006**, *341*, 995-1002.

[20] Sasaki, T.; Takasuka, N. *Carbohydr. Res.* **1976**, *47*, 99-104.

[21] Yu, Z.; Ming, G.; Kaiping, W.; Zhixiang, C.; Liquan, D.; Jingyu, L.; Fang, Z. *Fitoterapia.* **2010**, *81*, 1163-1170.

[22] Mallik, P.; Sikdar, S. R. *World J. Microbiol. Biotechnol.* **2014**, *30*, 2283-2293.

[23] York, W. S.; Darvill, A. G.; McNeil, M.; Stevenson, T. T.; Albersheim, P. *Method. Enzymol.* **1986**, *118*, 3-40.

[24] Hara, C.; Kiho, T.; Tanaka, Y.; Ukai, S. *Carbohydr. Res.* **1982**, *110*, 77-87.

[25] Gerwig, G. J.; Kamerling, J. P.; Vliegenthart, J. F. G. *Carbohydr. Res.* **1978**, *62*, 349-357.

[26] Ciucanu, I.; Kerek, F. *Carbohydr. Res.* **1984**, *131*, 209-217.

[27] Goldstein, I. J.; Hay, G. W.; Lewis, B. A.; Smith, F. *Methods Carbohydr. Chem.* **1965**, *5*, 361-370.

[28] Hay, G. W.; Lewis, B. A.; Smith, F. *Methods Carbohydr. Chem.* **1965**, *75*, 357-361.

[29] Agrawal, P. K. *Phytochemistry.* **1992**, *31*, 3307-3330.

[30] Rinaudo, M.; Vincendon, M. *Carbohydr. Polym.* **1982**, *2*, 135-144.

[31] Wasser, S. P. *Appl. Microbiol. Biot.* **2002**, *60*, 258-274.

[32] Ohno, N.; Saito, K.; Nemoto, J.; Kaneko, S.; Adachi, Y.; Nishijima, M.; Miyazaki, T.; Yadomae, T. *Biol. Pharm. Bull.* **1993**, *16*, 414-419.

[33] Tzianabos, A. O. *Clin. Microbiol. Rev.* **2000**, *13*, 523-533.

CHAPTER – IV

Structural and immunological studies of polysaccharide from an edible hybrid mushroom *pfle 1p*

4.1. Introduction and review on earlier work

Mushrooms are enriched with various bioactive molecules. Among them, β-glucans have been extensively studied and considered as the most potent antitumor and immunostimulating materials [1-3]. Lentinan, a (1→3), (1→6)-β-glucan isolated from *Lentinula edodes* is well known for its high antitumor activity [4,5]. Different types of glucans from *Pleurotus florida* also exhibit significant immunostimulating properties [6,7]. In addition to the antitumor β-glucans, researchers have focused on heteroglycan which also have significant biological activities [2,3]. The structure of different heteroglycans may contain backbone of (1→6) and (1→3) or both (1→6), (1→3)- linked α-galactose, α-glucose or β-glucose with mainly fucose, mannose, or glucose as nonreducing residues [8-11]. Recently, Dey et al. and Patra et al. have isolated different immunostimulating heteroglycans from edible hybrid mushroom [12,13]. Protoplast fusion between the strains of *Pleurotus florida* and *Lentinula edodes* produced nine new hybrid strains out of which six strains *i.e. pfle 1o*, *pfle 1p*, *pfle 1q*, *pfle 1r*, *pfle 1s*, and *pfle 1v* produced fruit bodies [14]. Recently, a (1→3), (1→6)-β-D-glucan and a heteroglycan have been isolated from one such hybrid strain *pfle 1r* [15,16]. Two water soluble polysaccharides (PS-I and PS-II) were isolated from the fruit bodies of *pfle 1p*. PS-I was found to consist of D-glucose, D-galactose, and D-mannose in a molar ratio of nearly 4:2:1. In the chapter, the detailed structural investigation and study of immunostimulating properties of PS-I were discussed.

Figure 1. Photograph of hybrid mushroom *pfle 1p* [14].

4.2. Present work

4.2.1. Isolation, purification, and physical characterization of PS-I

The fresh mushroom fruit bodies were washed thoroughly and then boiled with distilled water for 10 h followed by filtration, centrifugation, and precipitation in ethyl alcohol (EtOH), dialysis, again centrifugation, and freeze drying to yield 290 mg of crude polysaccharide. Purification of this water soluble crude polysaccharide (25 mg) through Sepharose 6B column yielded two fractions. Fraction I and fraction II were collected and freeze dried, yielding purified polysaccharide of 11 mg PS-I and 8 mg PS-II, respectively [Figure 2].

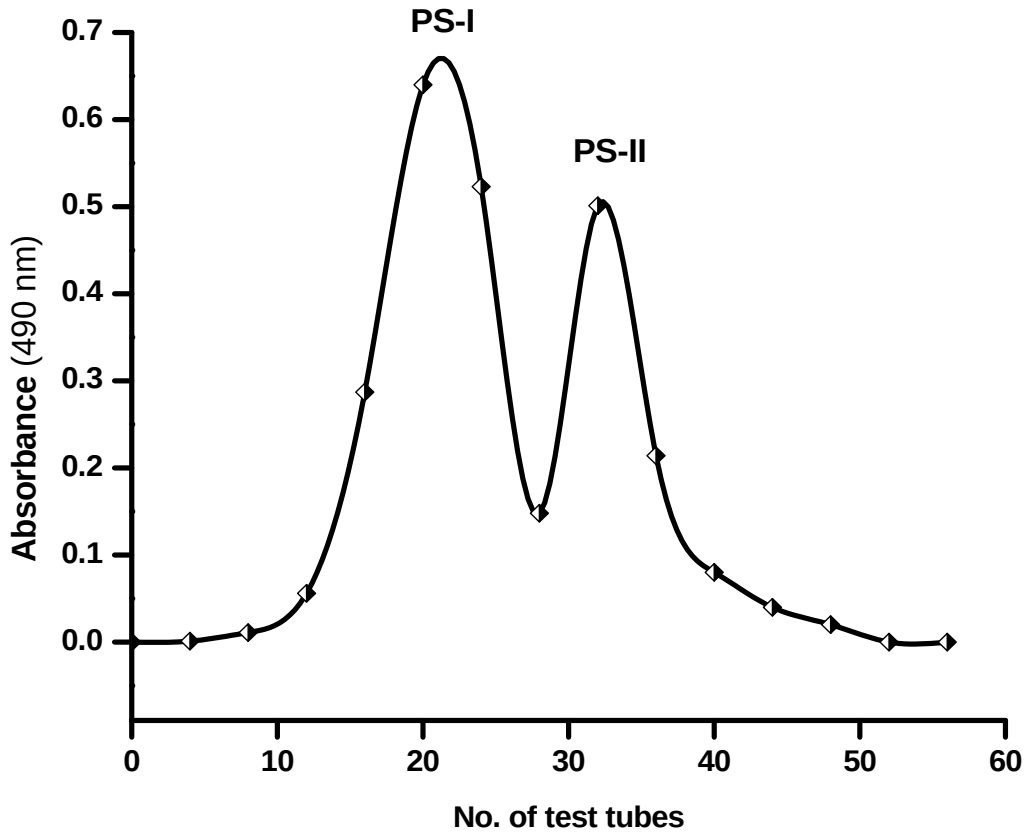

Figure 2. Separation graph of the crude polysaccharide isolated from hybrid mushroom *pfle 1p* through Sepharose 6B column.

The PS-I showed specific rotation $[\alpha]_D^{29.2}$ +32.6 (*c* 0.886, water). The average molecular weight of PS-I was estimated as ~2.1 × 10^5 Da [Figure 3] from a calibration curve prepared with standard dextrans [17].

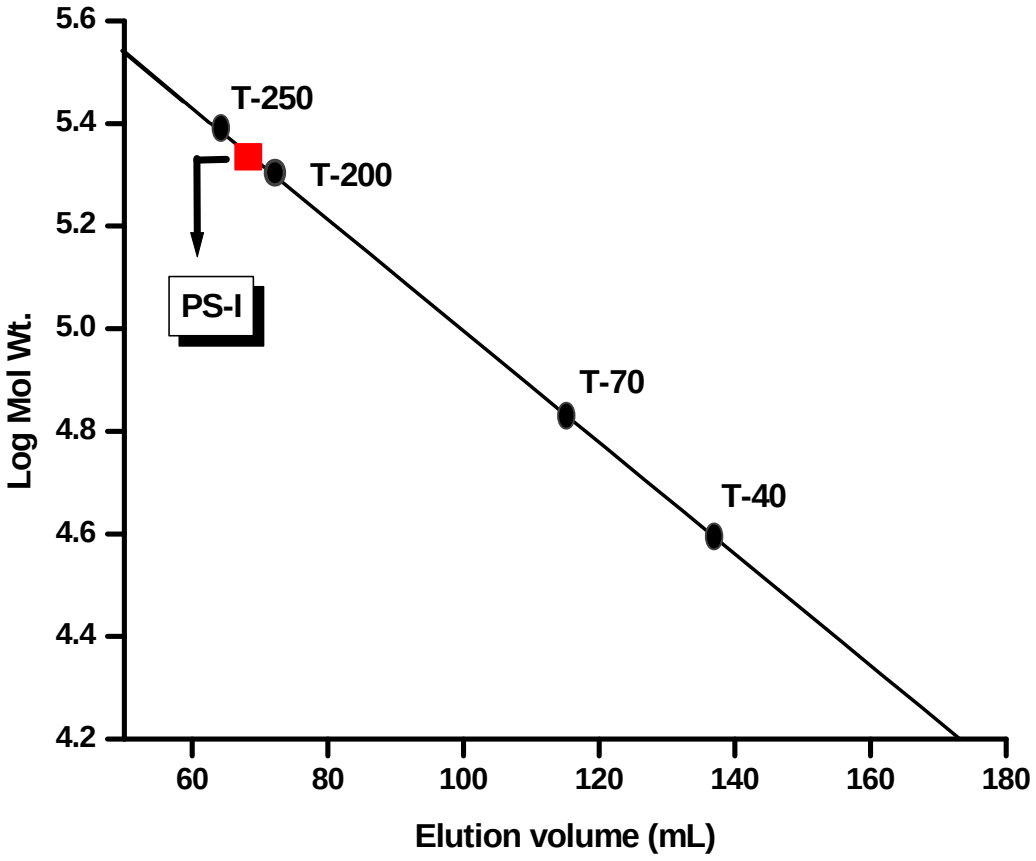

Figure 3. Determination of molecular weight of the PS-I isolated from hybrid mushroom *pfle 1p*.

4.2.2. Structural analysis of PS-I

4.2.2.1. Chemical analysis

Hydrolysis of PS was carried out with 2 M TFA for 18 h followed by reduction and alditol acetates preparation. GLC analysis of alditol acetates of hydrolyzed product of PS-I confirmed the presence of glucose, galactose, and mannose almost in a molar ratio of 4:2:1. The absolute configuration of the monosaccharides was determined by the method of Gerwig et al. [18] and it was found that all the monosaccharides had D-configuration. The PS-I was methylated by the method of Ciucanu and Kerek [19] as given in methodology section (chapter II, part A, 2.A.5.3.), followed by hydrolysis, reduction and then alditol acetate preparation. The alditol acetate was analyzed by GLC-MS. The GLC–MS analysis of partially methylated alditol acetates of PS-I revealed the presence of seven peaks in a molar ratio of nearly 1:1:1:1:1:1:1. The peaks were assigned as

1,5-di-*O*-acetyl-2,3,4,6-tetra-*O*-methyl-D-glucitol

1,5-di-*O*-acetyl-2,3,4,6-tetra-*O*-methyl-D-mannitol

1,5,6-tri-*O*-acetyl-2,3,4-tri-*O*-methyl-D-galactitol

1,5,6-tri-*O*-acetyl-2,3,4-tri-*O*-methyl-D-glucitol

1,3,5-tri-*O*-acetyl-2,4,6-tri-*O*-methyl-D-glucitol

1,3,4,5-tetra-*O*-acetyl-2,6-di-*O*-methyl-D-glucitol

1,2,5,6-tetra-*O*-acetyl-3,4-di-*O*-methyl-D-galactitol

Thus, PS-I was assumed to be consist of terminal D-glucopyranosyl and D-mannopyranosyl, (1→6)-linked D-galactopyranosyl, (1→6)-linked D-glucopyranosyl, (1→3)-linked D-glucopyranosyl, (1→3,4)-linked D-glucopyranosyl, and (1→2,6)-linked D-galactopyranosyl moieties, respectively. [Table 1, Figure 4].

Table 1. GC-MS data for methylated PS-I isolated from the hybrid mushroom *pfle 1p*.

Methylated sugars	Linkages	Molar Ratio	Major Fragments (m/z)
2,3,4,6-Me_4-Glc*p*	Glc*p*-(1→	1	43,45,71,87,101,117,129,145,161,205
2,3,4,6-Me_4-Man*p*	Man*p*-(1→	1	43, 45, 71, 87, 101, 117, 129, 145, 161, 205
2,3,4-Me_3-Gal*p*	→6)-Gal*p*-(1→	1	43,45,71,87,99,101,117,129,161, 173,189,233
2,3,4-Me_3-Glc*p*	→6)-Glc*p*-(1→	1	43,71,87,99,101,117,129,161,189 233
2,4,6-Me_3-Glc*p*	→3)-Glc*p*-(1→	1	43,71,87,101,117,129,161,233
2,6- Me_2-Glc*p*	→3,4)-Glc*p*-(1→	1	43,87,101,117,129,189
3,4-Me_2-Gal*p*	→6,2)-Gal*p*-(1→	1	43,71,87,99,129,189

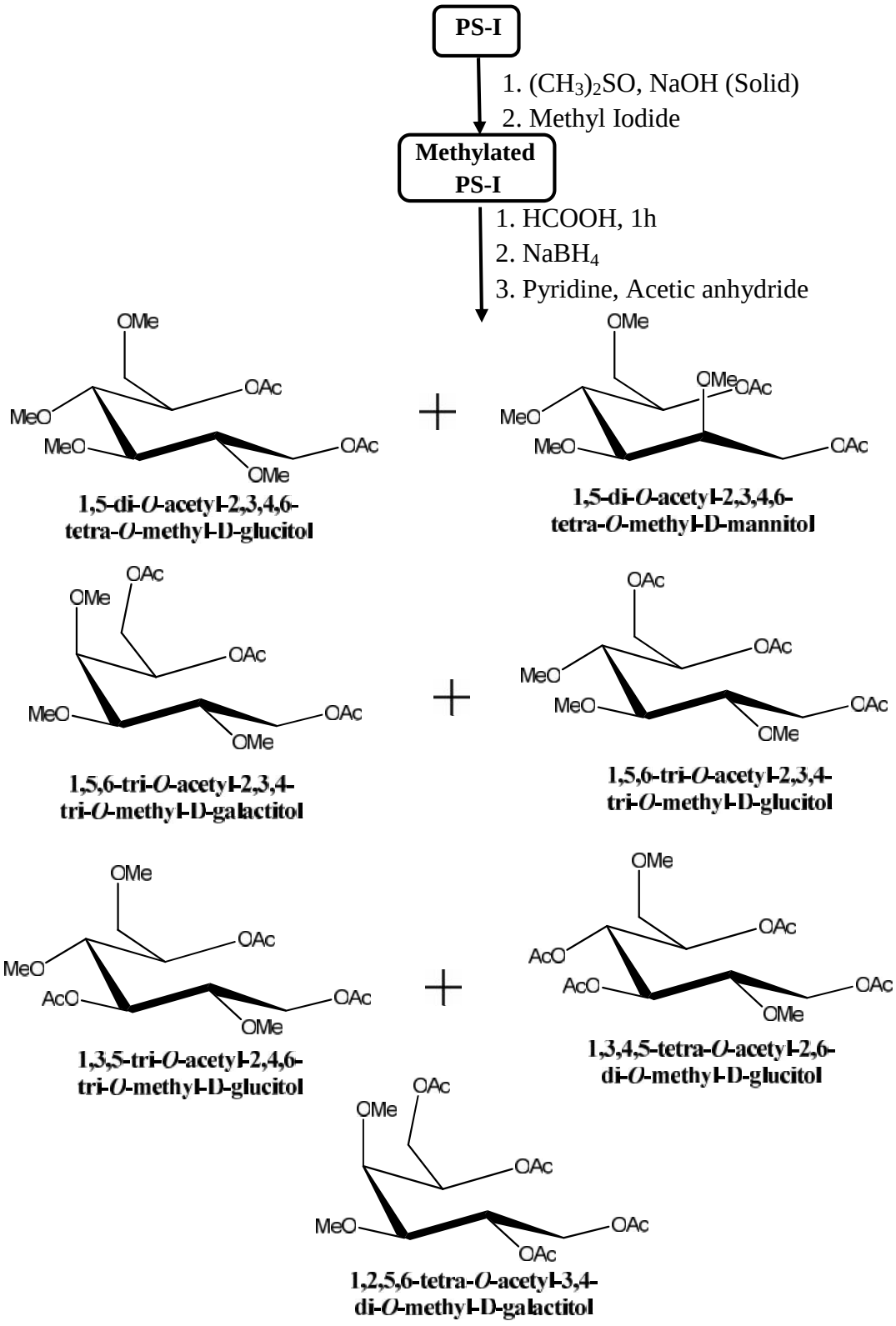

Figure 4. Schematic presentation of methylation experiment of PS-I isolated from hybrid mushroom *pfle 1p*.

These linkages were further confirmed by periodate oxidation experiment. The GLC-MS analysis of the alditol acetates of periodate oxidized [20,21], reduced PS-I was found to

contain glucose only and the periodate oxidized, reduced, methylated PS-I showed the presence of 1,3,4,5-tetra-*O*-acetyl-2,6-di-*O*-methyl-D-glucitol and 1,3,5-tri-*O*-acetyl-2,4,6-tri-*O*-methyl-D-glucitol in a molar ratio of nearly 1:1 [Table 2, Figure 5]. These results clearly indicated that the all other moieties except (1→3,4)-linked D-glucopyranosyl and (1→3)-linked D-glucopyranosyl were consumed during oxidation. Thus, the mode of linkages present in the PS-I were confirmed.

Table 2. GC-MS analysis of periodate oxidized methylated polysaccharide (PS-I) of hybrid mushroom strain *pfle 1p*.

Methylated sugars	Linkage types	Molar ratio	Major fragments (m/z)
2,6- Me_2-Glc*p*	→3,4)-Glc*p*-(1→	1	43,87,101,117,129,189
2,4,6-Me_3-Glc*p*	→3)-Glc*p*-(1→	1	43,71,87,101,117,129,161,233

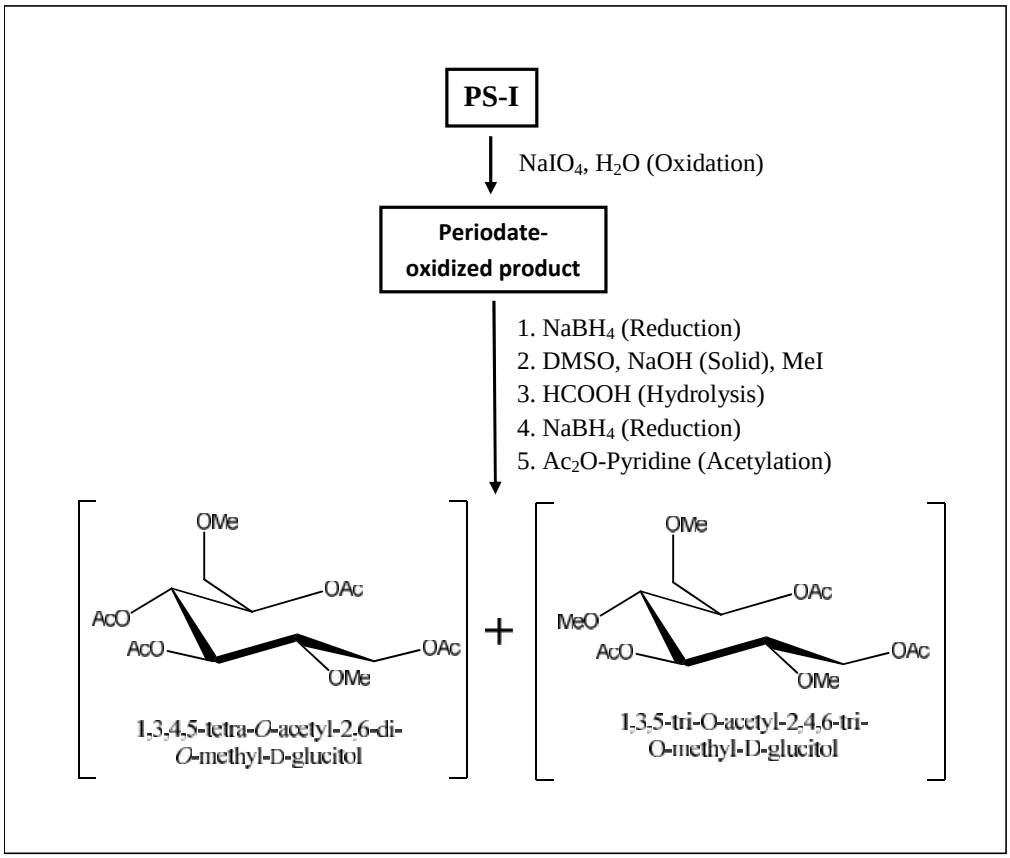

Figure 5. Schematic presentation of periodate-oxidation experiment of PS-I isolated from hybrid mushroom *pfle 1p*.

4.2.2.2. NMR analysis

The ^{1}H NMR spectrum [Figure 6] showed seven peaks in the anomeric region. The peaks were observed at δ 5.35, 5.12, 4.98, 4.78, 4.75, 4.51, and 4.49 in a ratio of nearly 1:1:1:1:1:1:1. They were designated as **A**, **B**, **C**, **D**, **E**, **F**, and **G** according to their decreasing proton chemical shifts.

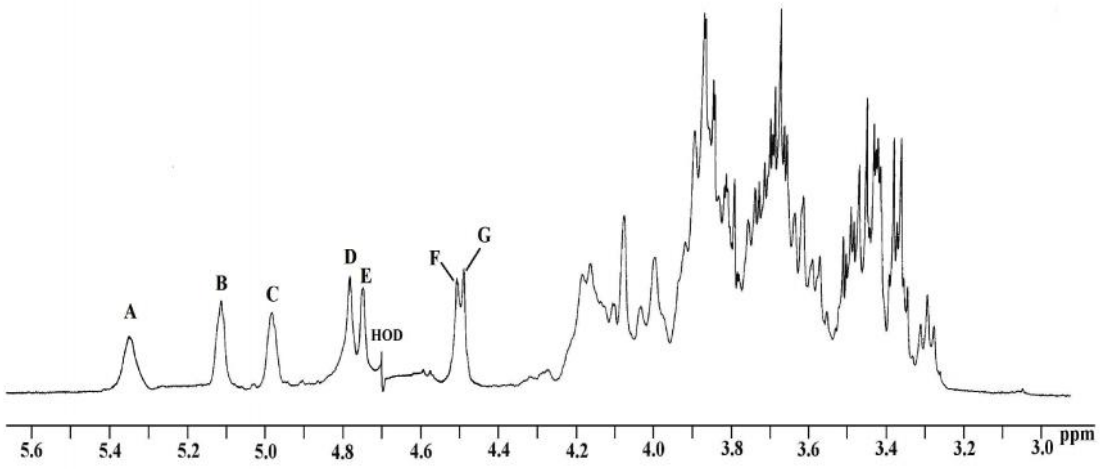

Figure 6. ^{1}H NMR spectrum of PS-I, isolated from hybrid mushroom *pfle 1p*.

Seven peaks in the anomeric region of ^{13}C spectrum [Figure 7a] at δ 97.8, 98.2, 99.7 101.7, 102.4, 102.5, and 102.8 correlated to the residues **C**, **B**, **A**, **D**, **E**, **F**, and **G**, respectively from the HSQC spectrum [Figure 8]. All the ^{1}H and ^{13}C signals were assigned using DQF-COSY, TOCSY, and HSQC experiments [Table 3].

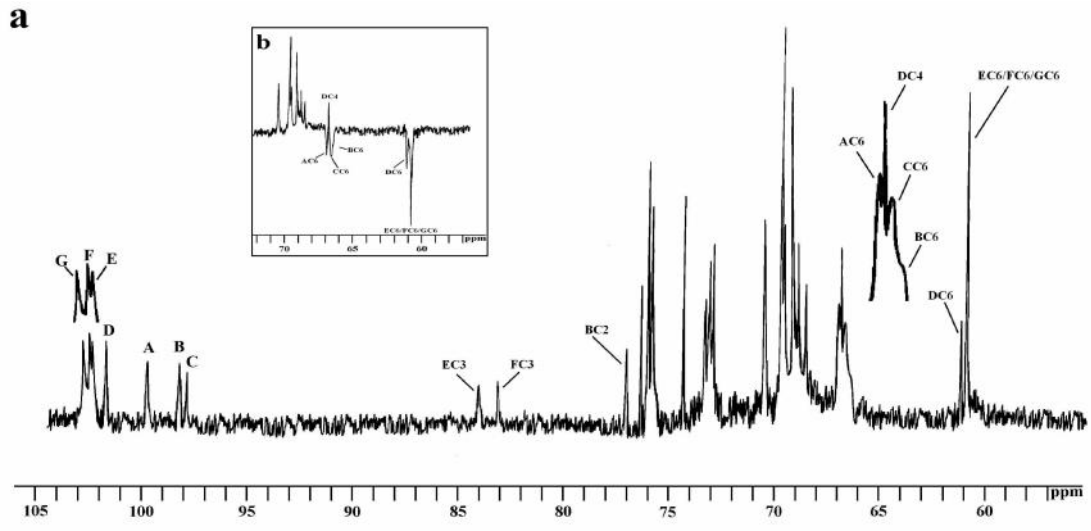

Figure 7. (a) ^{13}C NMR spectrum (b) with insert of the part of DEPT-135 spectrum of the PS-I, isolated from hybrid mushroom *pfle 1p*.

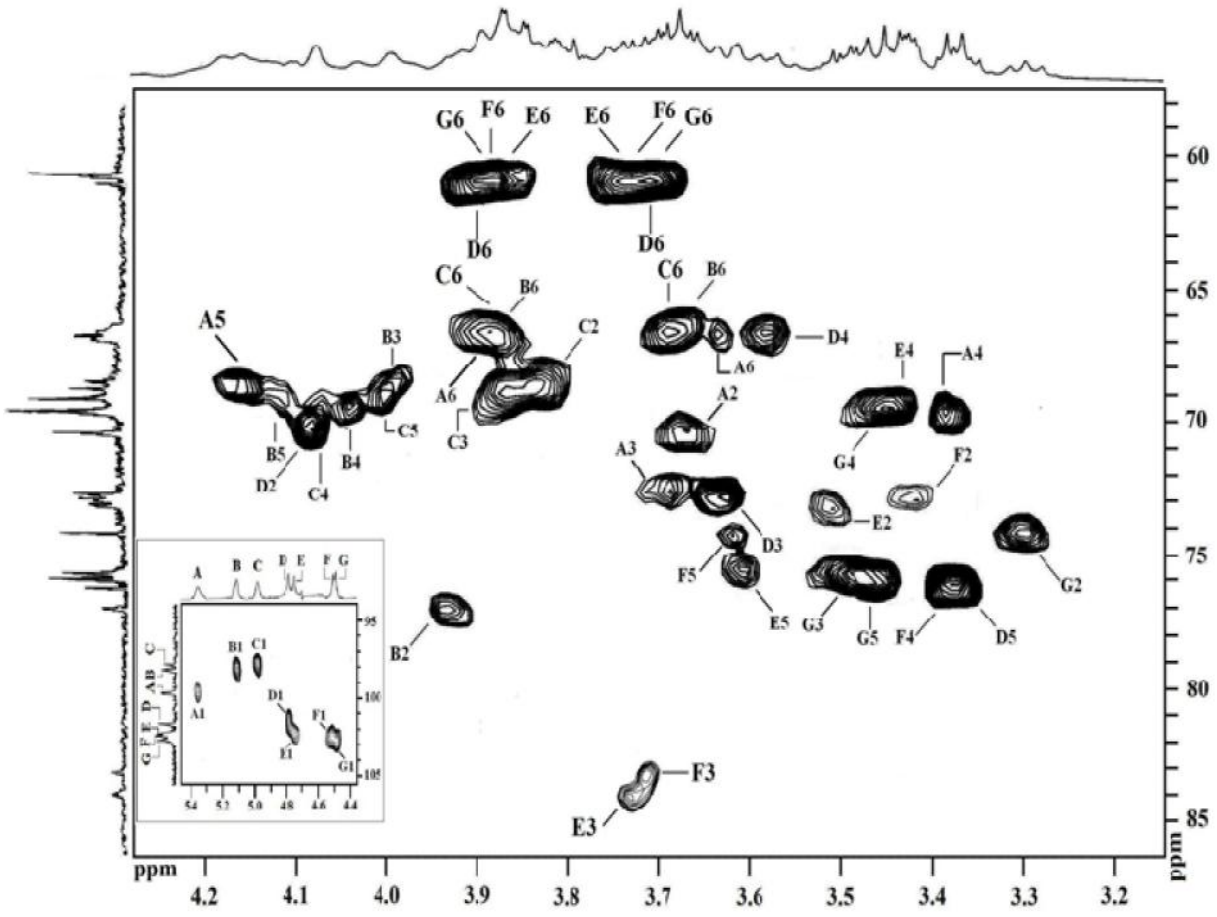

Figure 8. HSQC spectrum of PS-I, isolated from hybrid mushroom *pfle 1p*.

Table 3. The ^{1}H and ^{13}C NMR chemical shifts for the PS-I isolated from *pfle 1p*[a,b] .

Glycosyl residue	H-1/C-1	H-2/C-2	H-3/C-3	H-4/C-4	H-5/C-5	H-6a, H-6b/C-6
→6)-α-D-Glc*p*-(1→	5.35	3.67	3.69	3.38	4.16	3.88[c], 3.64[d]
A	99.7	70.4	72.8	69.6	68.8	66.9
→2,6)-α-D-Gal*p*-(1→	5.12	3.94	3.99	4.04	4.11	3.87[c], 3.66[d]
B	98.2	77.0	68.5	69.6	69.1	66.4
→6)-α-D-Gal*p*-(1→	4.98	3.83	3.87	4.08	4.01	3.88[c], 3.68[d]
C	97.8	68.8	69.1	70.4	69.1	66.6
β-D-Man*p*-(1→	4.78	4.09	3.63	3.58	3.37	3.90 [c], 3.71 [d]
D	101.7	70.4	73.0	66.8	76.3	61.1
→3)-β-D-Glc*p*-(1→	4.75	3.51	3.73	3.43	3.61	3.86[c], 3.73[d]
E	102.4	73.2	84.0	69.5	75.8	60.8
→3,4)-β-D-Glc*p*-(1→	4.51	3.42	3.71	3.38	3.62	3.88[c], 3.72[d]
F	102.5	73.0	83.1	76.3	74.2	60.8
β-D-Glcp-(1→	4.49	3.30	3.49	3.45	3.47	3.89[c], 3.70[d]
G	102.8	74.2	76.0	69.6	76.0	60.8

[a] Values of the ^{1}H chemical shifts were recorded with respect to the HOD signal set at δ 4.70 at 30 °C.

[b] Values of the ^{13}C chemical shifts were recorded with reference to acetone as the internal standard and set at δ 31.05 at 30 °C.

[c,d] Interchangeable.

The proton coupling constants were measured from DQF-COSY experiment. Among these seven residues, residues **A**, **E**, **F**, and **G** have large coupling constant values of $J_{H\text{-}2,H\text{-}3,}$ and $J_{H\text{-}3,H\text{-}4}$ (~10 H_Z) and thus they are confirmed as D-glucopyranosyl residues. Again, among these D-glucopyranosyl residues, residue **A** is the only α anomer ($J_{H\text{-}1,H\text{-}2}$ ~ 3.0 H_Z and $J_{H\text{-}1,C\text{-}1}$ ~170 H_Z) and the rest are β anomers ($J_{H\text{-}1,H\text{-}2}$ ~ 8.5 H_Z and $J_{H\text{-}1,C\text{-}1}$ ~161 H_Z). Similarly, from the coupling constant values, **B** and **C** are established as α-linked ($J_{H\text{-}1,H\text{-}2}$ ~3.1 and $J_{C\text{-}1,H\text{-}1}$ ~171 Hz) D-galactopyranosyl ($J_{H\text{-}2,\ H\text{-}3}$ ~9 Hz and $J_{H\text{-}3,\ H\text{-}4}$ ~3.5 Hz) moieties and **D** is determined as β-linked ($J_{H\text{-}1,H\text{-}2}$ ~0, $J_{C\text{-}1,H\text{-}1}$ ~161) mannopyranosyl ($J_{H\text{-}3,\ H\text{-}4}$ ~7.5 Hz and $J_{H\text{-}4,\ H\text{-}5}$ ~10 Hz) moiety. In case of residues **A** and **C**, all the proton and carbon chemical shifts except the C-6 were matched nearly with the standard values of methyl glycosides [22,23]. A downfield shift of C-6 (δ 66.9 for **A** and δ 66.6 for **C**) was observed. These observations confirmed that both the residues **A** and **C** contained C-6 linkages. Therefore, **A** was determined as (1→6)-linked α-D-glucopyranosyl residue and **C** as (1→6)-linked α-D-galactopyranosyl residue. Furthermore, the DEPT-135 spectrum [Figure 7b] confirmed the C-6 linkages in both of these residues. On the other hand, the downfield shifts of C-2 (δ 77) and C-6 (δ 66.4) of residue **B** with respect to standard values indicated that it was linked at C-2 and C-6. The linkage at C-6 of residue **B** was also supported by DEPT-135 spectrum. Thus, **B** was confirmed as (1→2,6)-linked α-D-galactopyranosyl residue. All the proton and carbon chemical shifts for residues **D** and **G** corresponded nearly to the standard values of methyl glycosides of mannose and glucose, respectively. Thus, **D** was confirmed as terminal β-D-mannopyranosyl residue and **G** as terminal β-D-glucopyranosyl residue. The downfield shift of C-3 (δ 84) of residue **E** in comparison to the standard values indicated that it was linked at C-3 position. Hence, **E** was established as (1→3)-linked β-D-glucopyranosyl residue. In case of residue **F,** downfield shifts at C-3 (δ 83.1) and C-4 (δ 76.3) were observed indicating that it was linked at C-3 and C-4. Thus, **F** was confirmed as (1→3,4)-linked β-D-glucopyranosyl residue. Since, residue **F** was present in the rigid part of the molecule, its C-3 (δ 83.1) appeared at the more upfield region in comparison to the C-3 (δ 84) of **E**.

The different linkages that connected these seven residues were determined from NOESY [Figure 9 and Table 4] as well as ROESY spectrum (not shown). In NOESY spectrum, the inter-residual connectivities were observed between **A**H-1/**B**H-6a; **A**H-1/**B**H-6b; **B**H-1/**C**H-6a; **B**H-1/**C**H-6b; **C**H-1/**E**H-3; **D**H-1/**B**H-2; **E**H-1/**F**H-3; **F**H-1/**A**H-6a; **F**H-1/**A**H-6b; **G**H-1/**F**H-4 along with other intra-residual contacts.

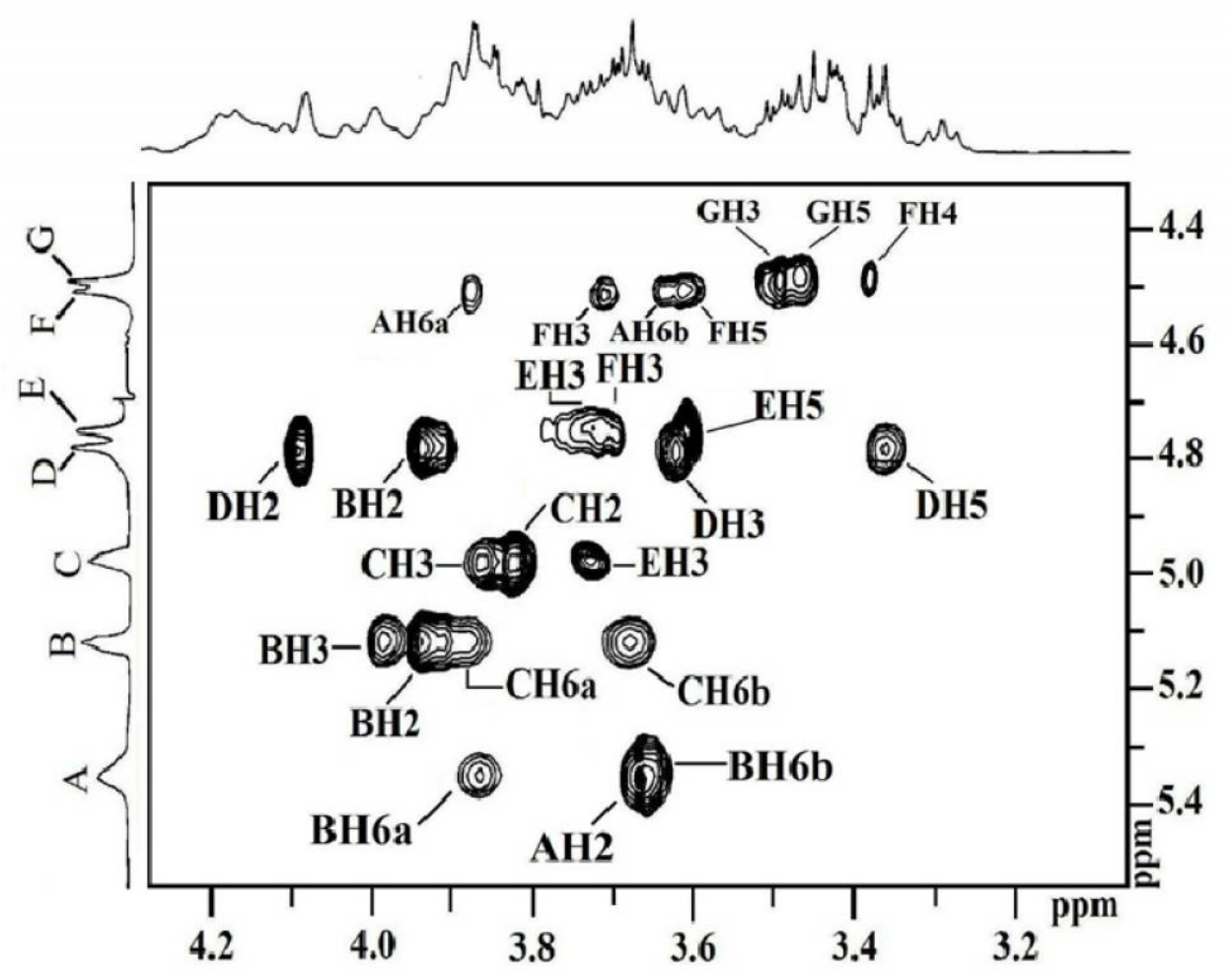

Figure 9. Part of NOESY spectrum of PS-I, isolated from hybrid mushroom *pfle 1p.*

Table 4. NOESY data for the PS-I isolated from hybrid mushroom *pfle 1p*.

Glycosyl residue	Anomeric proton	NOE contact protons	
	δ	δ	**Residue**,atom
→6)-α-D-Glc*p*-(1→	5.35	3.67	**A**H-2
A		3.87	**B**H-6a
		3.66	**B**H-6b
→2,6)-α-D-Gal*p*-(1→	5.12	3.94	**B**H-2
B		3.99	**B**H-3
		3.88	**C**H-6a
		3.68	**C**H-6b
→6)-α-D-Gal*p*-(1→	4.98	3.83	**C**H-2
C		3.87	**C**H-3
		3.73	**E**H-3
β-D-Man*p*-(1→	4.78	4.09	**D**H-2
D		3.63	**D**H-3
		3.37	**D**H-5
		3.94	**B**H-2
→3)-β-D-Glc*p*-(1→	4.75	3.73	**E**H-3
E		3.61	**E**H-5
		3.71	**F**H-3
→3,4)-β-D-Glc*p*-(1→	4.51	3.71	**F**H-3
F		3.62	**F**H-5
		3.88	**A**H-6a
		3.64	**A**H-6b
β-D-Glcp-(1→	4.49	3.49	**G**H-3
G		3.47	**G**H-5
		3.38	**F**H-4

Finally, these connectivities were confirmed from HMBC spectrum [Figure 10a and Figure 10b]. In this spectrum the inter-residual cross-peaks [Table 5] were observed between **A**H-1/**B**C-6; **A**C-1/**B**H-6a and **B**H-6b; **B**H-1/**C**C-6; **B**C-1/**C**H-6a and **C**H-6b; **C**H-1/**E**C-3; **C**C-1/**E**H-3; **D**H-1/**B**C-2; **D**C-1/**B**H-2; **E**H-1/**F**C-3; **E**C-1/**F**H-3; **F**H-1/**A**C-6; **F**C-1/**A**H-6a and **A**H-6b; **G**H-1/**F**C-4; and **G**C-1/**F**H-4.

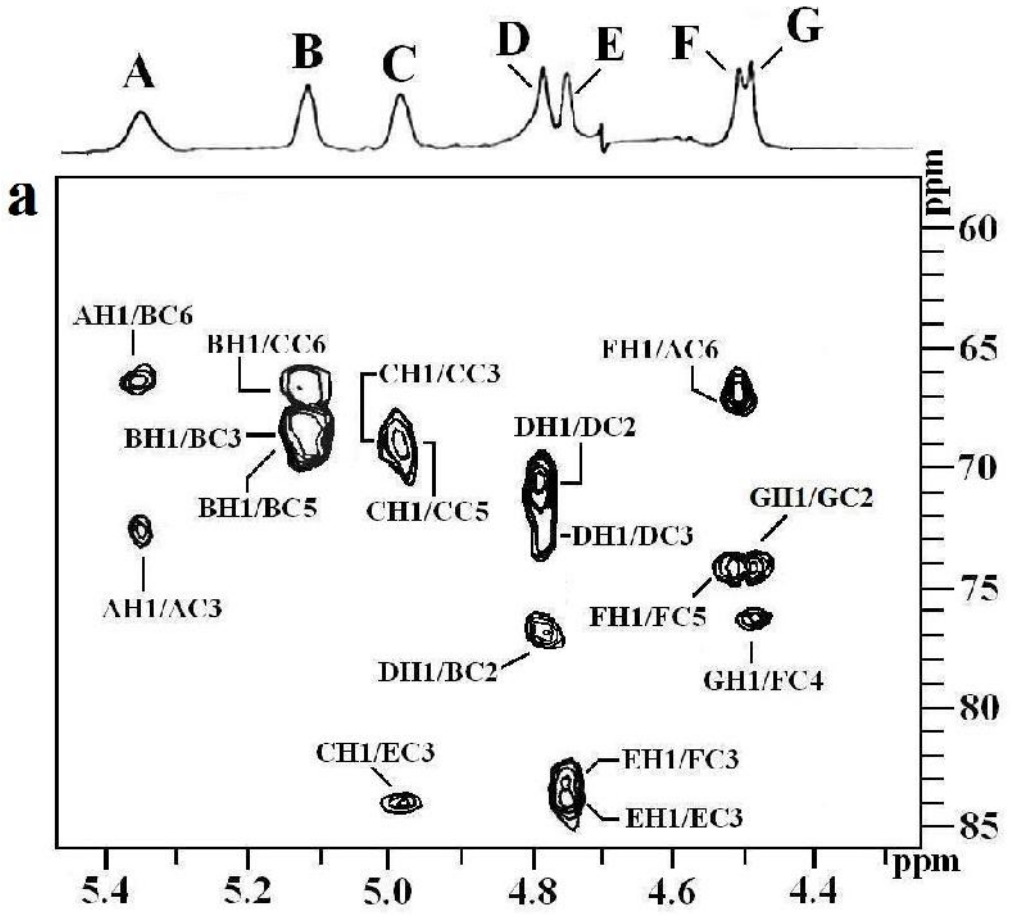

Figure 10. (a) The part of HMBC spectrum for anomeric protons, of PS-I, isolated from hybrid mushroom *pfle 1p*.

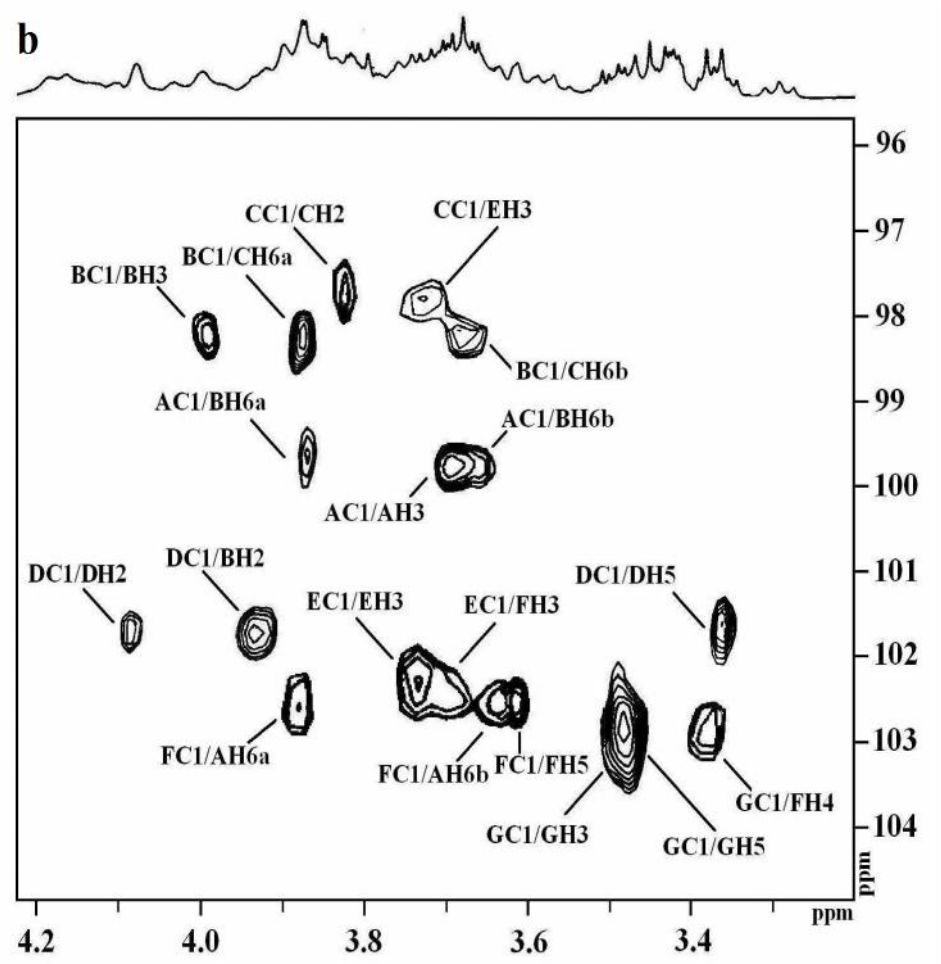

Figure 10. (b) The part of HMBC spectrum for anomeric carbons of PS-I, isolated from hybrid mushroom *pfle 1p*.

Table 5. The significant $^{3}J_{H,C}$ connectivities observed in an HMBC spectrum for the anomeric protons/carbons of the sugar residues of the PS-I isolated from hybrid mushroom *pfle 1p*.

Residue	Sugar linkage	H-1/C-1	Observed connectivities		
		δ_H/δ_C	δ_H/δ_C	Residue	Atom
A	→6)-α-D-Glc*p*-(1→	5.35	72.8	**A**	C-3
			66.4	**B**	C-6
		99.7	3.69	**A**	H-3
			3.87	**B**	H-6a
			3.66	**B**	H-6b
B	→2,6)-α-D-Gal*p*-(1→	5.12	68.5	**B**	C-3
			69.1	**B**	C-5
			66.6	**C**	C-6
		98.2	3.99	**B**	H-3
			3.88	**C**	H-6a
			3.68	**C**	H-6b
C	→6)-α-D-Gal*p*-(1→	4.98	69.1	**C**	C-3
			69.1	**C**	C-5
			84.0	**E**	C-3
		97.8	3.83	**C**	H-2
			3.73	**E**	H-3
D	β-D-Man*p*-(1→	4.78	70.4	**D**	C-2
			73.0	**D**	C-3
			77.0	**B**	C-2
		101.7	4.09	**D**	H-2
			3.37	**D**	H-5
			3.94	**B**	H-2
E	→3)-β-D-Glc*p*-(1→	4.75	84.0	**E**	C-3
			83.1	**F**	C-3
		102.4	3.73	**E**	H-3
			3.71	**F**	H-3

Table 5. The significant $^{3}J_{H,C}$ connectivities observed in an HMBC spectrum for the anomeric protons/carbons of the sugar residues of the PS-I isolated from hybrid mushroom *pfle 1p*.

Residue	Sugar linkage	H-1/C-1	Observed connectivities		
		δ_H/δ_C	δ_H/δ_C	Residue	Atom
F	→3,4)-β-D-Glc*p*-(1→	4.51	74.2	**F**	C-5
			66.9	**A**	C-6
		102.5	3.62	**F**	H-5
			3.88	**A**	H-6a
			3.64	**A**	H-6b
G	β-D-Glcp-(1→	4.49	74.2	**G**	C-2
			76.3	**F**	C-4
			3.49	**G**	H-3
			3.47	**G**	H-5
			3.38	**F**	H-4

Thus, the probable structural motif present in PS-I was established as:

E **F** **A** **B** **C**

→3)-β-D-Glc*p*-(1→3)-β-D-Glc*p*-(1→6)-α-D-Glc*p*-(1→6)-α-D-Gal*p*-(1→6)-α-D-Gal*p*-(1→

4 2

↑ ↑

1 1

β-D-Glc*p* β-D-Man*p*

G **D**

4.2.3. Biological studies of PS-I

4.2.3.1. Assay for macrophage activity by NO

To test immunomodulatory effects of PS-I, murine macrophages were incubated with PS-I in a humidified atmosphere of 5% CO_2 at 37 °C for 48 h and the production of nitric oxide (NO) was measured using Griess reagent (1:1 of 0.1% in 1-napthylethylenediamine in 5% phosphoric acid and 1% sulfanilamide in 5% phosphoric acid). On treatment with different concentrations of the PS-I, it was observed that NO production increased with increase in concentration up to 50 µg/mL with optimum production of 19.27 µM NO per 5×10^5 macrophages at 50 µg/mL which subsequently decreased with increase in concentration [Figure 11a]. Hence, the effective dose of the PS-I for macrophage activation was 50 µg/mL.

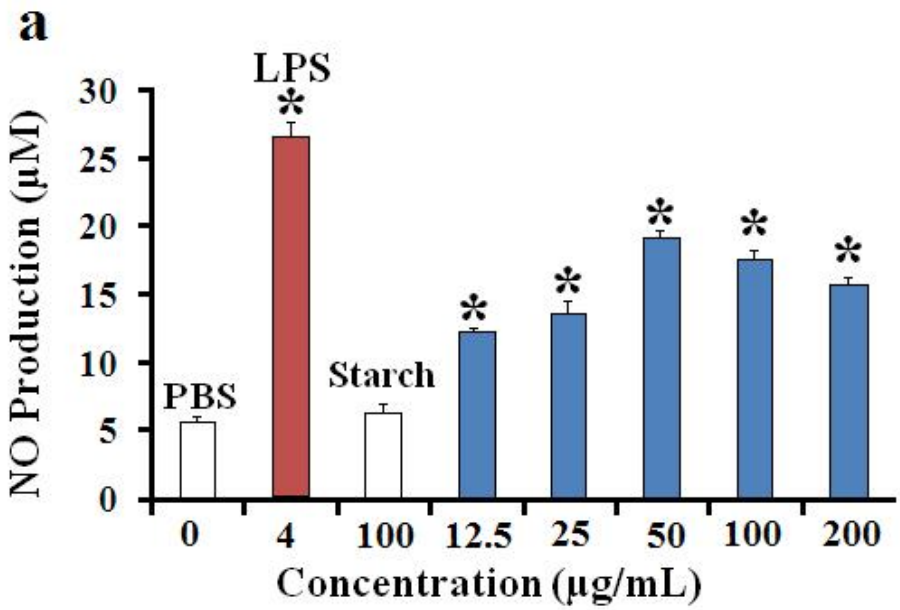

Figure 11. (a) In vitro activation of macrophage stimulated with different concentrations of PS-I isolated from hybrid mushroom *pfle 1p* in terms of NO production.

4.2.3.2. Splenocyte and thymocyte proliferation assay

Splenocyte is the cell present in the spleen that include T cells, B cells, dendritic cells etc. that stimulate the immune response in living organism whereas thymocyte is the hematopoietic cell present in thymus and the primary function of which is the generation of T cells. Proliferation of splenocyte and thymocyte is an indicator of immunostimulation [24]. Splenocyte and thymocyte proliferation in the presence of PS-I was used to evaluate cell stimulatory effects on the immune cell activation. The PS-I was tested to stimulate

splenocyte and thymocyte and the results are shown in Figure 11b and 11c, respectively. All the experiments were done twice with seven replicates and the result were represented as mean ± standard deviation using two tailed statistical analysis. The splenocyte and thymocyte proliferation indices as compared to PBS control if closer to 100 or below indicate low stimulatory effect on immune system. Difference in parameter between the treatment group and the control group was considered as statistically significant if $P < 0.05$ (indicated with a "*" mark). Both the splenocyte and thymocyte proliferation indices were found maximum at 50 µg/mL, above and below which it decreases. Hence, it can be concluded that 50 µg/mL is the optimum concentration of the PS-I for splenocyte and thymocyte proliferation.

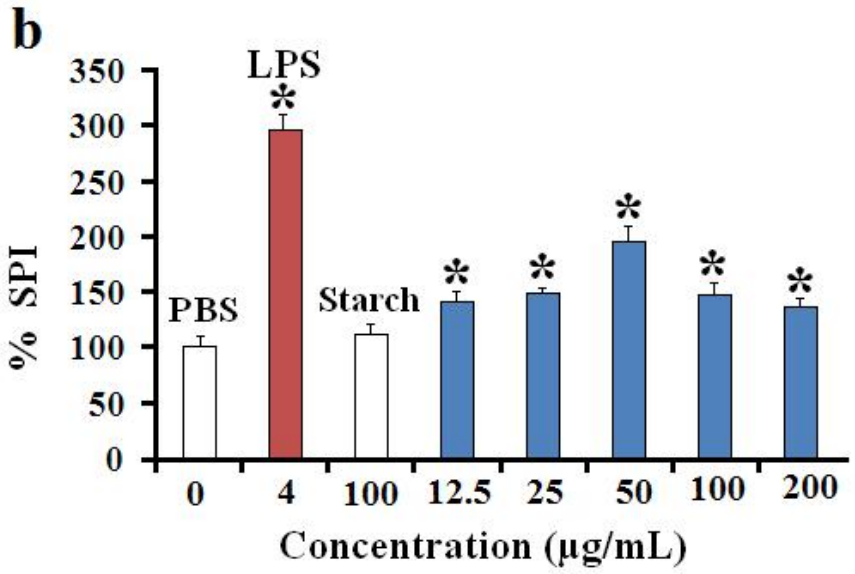

Figure 11. (b) Effect of different concentrations of PS-I, isolated from hybrid mushroom *pfle 1p* on splenocyte proliferation. ('*' means data is significant compared to the PBS control).

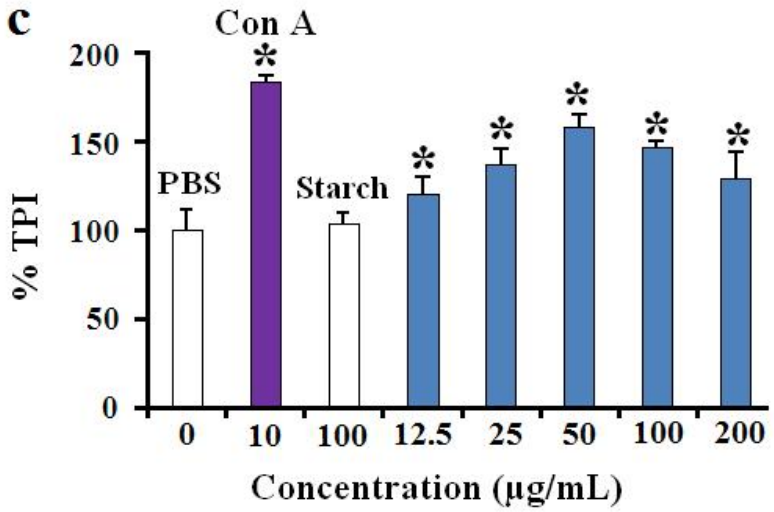

Figure 11. (c) Effect of different concentrations of PS-I, isolated from hybrid mushroom *pfle 1p* on thymocyte proliferation. ('*' means data is significant compared to the PBS control).

4.3. References

[1] Mizuno, T.; Inagaki, R.; Kanao, T.; Hagiwara, T.; Nakamura, T.; Ito, H.; Shimura, K.; Sumiya, T.; Asakura, A. *Agric. Biol. Chem.* **1990**, *54*, 2897-2905.

[2] Wasser, S. P. *Appl. Microbiol. Biotechnol.* **2002**, *60*, 258-274.

[3] Zhang, M.; Cui, S. W.; Cheung, P. C. K.; Wang, Q. *Trends Food Sci. Tech.* **2007**, *18*, 4-19.

[4] Sasaki, T.; Takasuka, N. *Carbohydr. Res.* **1976**, *47*, 99-104.

[5] Chihara, G.; Hamuro, J.; Maeda, Y. Y.; Arai, Y.; Fukuoka, F. *Cancer Res.* **1970**, *30*, 2776-2781.

[6] Rout, D.; Mondal, S.; Chakraborty, I.; Pramanik, M.; Islam, S. S. *Med. Chem. Res.* **2004**, *13*, 509-517.

[7] Rout, D.; Mondal, S.; Chakraborty, I.; Pramanik, M.; Islam, S. S. *Carbohydr. Res.* **2005**, *340*, 2533-2539.

[8] Bhunia, S. K.; Dey, B.; Maity, K. K.; Patra, S.; Mandal, S.; Maiti, S.; Maiti, T. K.; Sikdar, S. R.; Islam, S. S. *Carbohydr. Res.* **2010**, *345*, 2542-2549.

[9] Nandi, A. K.; Samanta, S.; Sen, I. K.; Devi, K. S. P.; Maiti, T. K.; Acharya, K.; Isalm, S. S. *Carbohydr. Polym.* **2013**, *94*, 918-926.

[10] Maity, K.; Kar (Mandal), E.; Maity, S.; Gantait, S. K.; Das, D.; Maiti, S.; Maiti, T. K.; Sikdar, S. R.; Islam, S. S. *Int. J. Biol. Macromol.* **2011**, *48*, 304-310.

[11] Bao, X.; Wang, X.; Dong, Q.; Fanj, J.; Li, X. *Phytochemistry.* **2002**, *59*, 175-181.

[12] Dey, B.; Bhunia, S. K.; Maity, K. K.; Patra, S.; Mandal, S.; Behera, B.; Maiti, T. K.; Sikdar, S. R.; Islam, S. S. *Int. J. Biol. Macromol.* **2013**, *52*, 312-318.

[13] Patra, S.; Maity, K. K.; Bhunia, S. K.; Dey, B.; Mandal, S.; Maity, T. K.; Sikdar, S. R.; Islam, S. S. *Carbohydr. Res.* **2011**, *346*, 1967-1972.

[14] Mallick, P.; Sikdar, S. R. *World J. Microbiol. Biotechnol.* **2014**, *30*, 2283-2293.

[15] Maji, P. K.; Sen, I. K.; Behera, B.; Maiti, T. K.; Mallick, P.; Sikdar, S. R.; Islam S. S. *Carbohydr. Res.* **2012**, *358*, 110-115.

[16] Maji, P. K.; Sen, I. K.; Devi, K. S. P.; Maiti, T. K.; Mallick, P.; Sikdar, S. R.; Islam S. S. *Carbohydr. Res.* **2013**, *368*, 22-28.

[17] Hara, C.; Kiho, T.; Tanaka, Y.; Ukai, S. *Carbohydr. Res.* **1982**, *110*, 77-87.

[18] Gerwig, G. J.; Kamerling, J. P.; Vliegenthart, J. F. G. *Carbohydr. Res.* **1978**, *62*, 349-357.

[19] Ciucanu, I.; Kerek, F. *Carbohydr. Res.* **1984**, *131*, 209-217.

[20] Hay, G. W.; Lewis, B. A.; Smith, F. *Methods Carbohydr. Chem.* **1965**, *5*, 357-361.

[21] Goldstein, I. J.; Hay, G. W.; Lewis, B. A.; Smith, F. *Methods Carbohydr. Chem.* **1965**, *5*, 361-370.

[22] Agrawal, P. K. *Phytochemistry*. **1992**, *31*, 3307-3330.

[23] Rinaudo, M.; Vincendon, M. *Carbohydr. Polym.* **1982**, *2*, 135-144.

[24] Ohno, N.; Saito, K.; Nemoto, J.; Kaneko, S.; Adachi, Y.; Nishijima, M.; Miyazaki, T.; Yadomae, T. *Biol. Pharm. Bull.* **1993**, *16*, 414-419.

CHAPTER – V

Green synthesis of gold nanoparticles using gum polysaccharide of *Cochlospermum religiosum* (katira gum) and its catalytic activity

5.1. Introduction and earlier work

Metal nanoparticles are important to researchers due to their unique properties and wide ranging application in a variety of areas including physics, chemistry, material science, and biomedical science. Numerous methods for the synthesis of nanoparticles are reported, amongst them, most conventional is the reduction of metal salt solution by means of reducing agent like sodium borohydride, N,N- dimethyl formamide, trisodium citrate, or other organic compounds [1-7]. But the use of such reducing agents may be associated with environmental toxicity or biological hazards. Currently integration of 'green chemistry' principles into nanotechnology is one of the key issues in nanoscience research. Utilization of nontoxic chemicals, environmentally benign solvents, and renewable materials are some of the key issues for a green synthesis strategy. In recent years, biomolecules are used in the synthesis of Au nanomaterials [8-12]. Synthesis of gold nanoparticles (Au NPs) using chitosan as both reducing and protecting agent was reported by Huang et al. [13]. Microorganisms are also used for the synthesis of Au NPs [14-16]. In this chapter, an environmentally benign method for preparation of Au NPs using aqueous solution of a hetero polysaccharide [17], isolated from katira gum acting both as reducing and stabilizing agent is reported.

Recently, the role of metal nanoparticles in the field of catalysis opens a new horizon. Au NPs serve as an effective catalyst in the reduction of various pollutants like 4-NP, the most common organic pollutant in industrial and agricultural waste water. 4-NP is toxic in nature and imparts odor to water and used as building blocks of many dyes, explosives, pesticides. It breaks down in water and surface soil. Therefore drinking water, eating foods grown in soil that contain 4-NP, can lead to critical health hazards to human beings. So much attention has been given to develop an efficient methodology for the conversion of 4-NP. Here a safe method for the conversion of 4-NP with Au NPs synthesized using a hetero polysaccharide has also been reported.

5.2. Present work

5.2.1. Synthesis of Au NPs

Katira gum was washed with methanol, dried, and made powder and then soxhletted using different solvents. The crude material was then dissolved in water, dialyzed, and centrifuged and the filtrate was precipitated in alcohol to get crude polysaccharide which

was further purified through Sepharose 6B column as reported by Ojha et al. [17]. The structure of the pure polysaccharide was confirmed by NMR studies [17] as

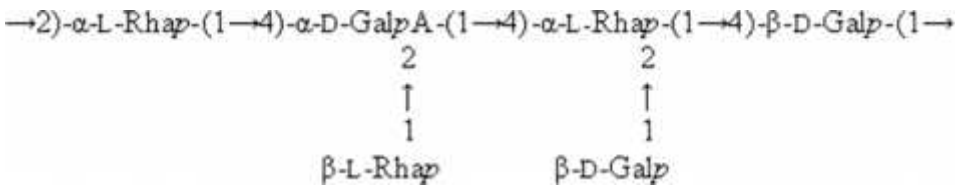

Andthis purified polysaccharide was used for the synthesis of Au NPs. For the synthesis of Au NPs, 2 mL aqueous solution of $HAuCl_4$ with a concentration of 10^{-3} M was added to 6 mL 0.2 % (w/v) aqueous polysaccharide solution. The mixture was then heated at 70 °C for 6 h with continuous stirring on a magnetic stirrer and UV-vis spectra of the reaction mixture were recorded at different time interval till the completion of the reaction.

5.2.2. Characterization of Au NPs

5.2.2.1. UV- vis spectroscopic analysis

A pale pink color was appeared after 10 min of the reaction and the color was gradually intensified as the reaction was continued with heating. A typical plasmon resonance band at 544 nm appeared after 1 h indicating formation of Au NPs. The time dependent UV-vis absorption spectra are shown in Figure 1. The intensity of the absorption band gradually increased and the maximum intensity of absorption was attained after 6 h of the reaction. This gradual increase in the absorption band is attributed to the fact that Au NPs concentration increases in the media as the reduction reaction proceeds. After 6 h, no significant change in intensity at 528 nm was observed which indicated almost complete reduction of Au^{+3}. The shifting of surface plasmon absorption maxima from 544 nm to a fixed value 528 nm at 6 h may be due to decrease in particles size [18].

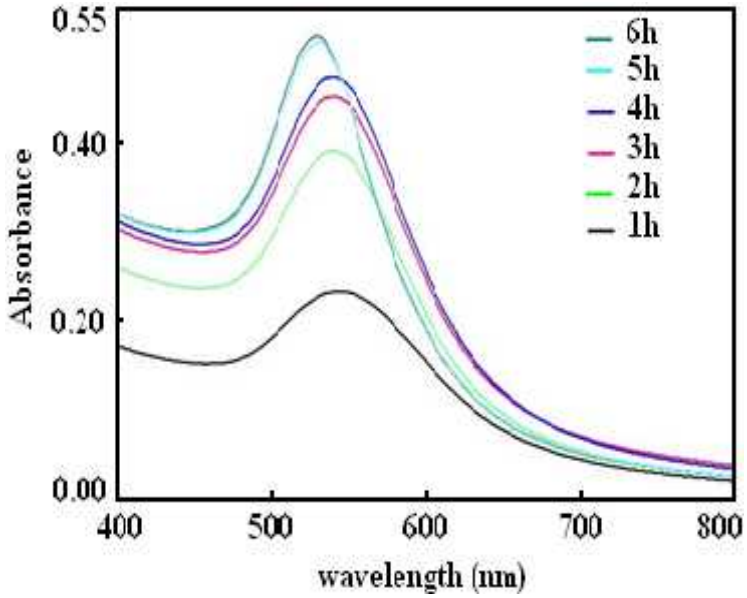

Figure 1. UV-vis spectra of Au NPs at different time intervals.

5.2.2.2. TEM and XRD analysis

The shape, morphology, and size distribution of the Au NPs were analyzed using high resolution transmission electron microscopy (HR-TEM). HR-TEM image [Figure 2] showed that the particles are mostly spherical with a few having rod and decahedral morphology. The average size of the particles is 6.9 nm as revealed from particle size distribution histogram [Figure 3]. The Selected area electron diffraction (SAED) pattern [Figure 4] showing rings ascribed to (111), (200), (220), (311), and (331) planes exhibited the face centered cubic (fcc) crystalline structure of gold. The crystalline nature of Au NPs was further confirmed by X-ray diffraction (XRD) analysis. A typical XRD pattern [Figure 5] exhibited peaks at 38.22º, 44.40º, 64.51º, and 77.49º that can be indexed to the (111), (200), (220), and (311) facets, respectively of fcc gold.

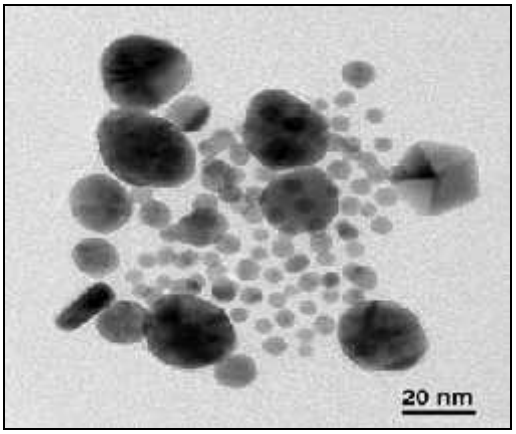

Figure 2. HR-TEM images of Au NPs-polysaccharide bioconjugates

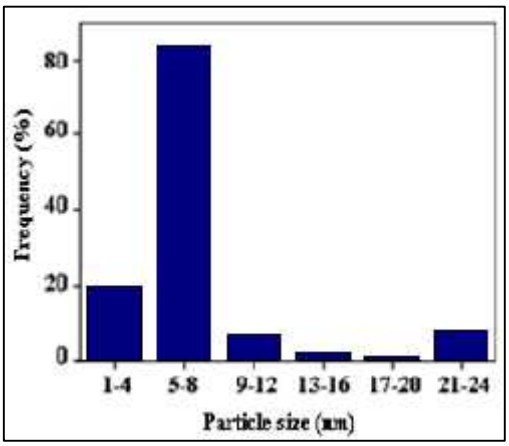

Figure 3. The particle size distribution histogram of Au NPs-polysaccharide bioconjugates

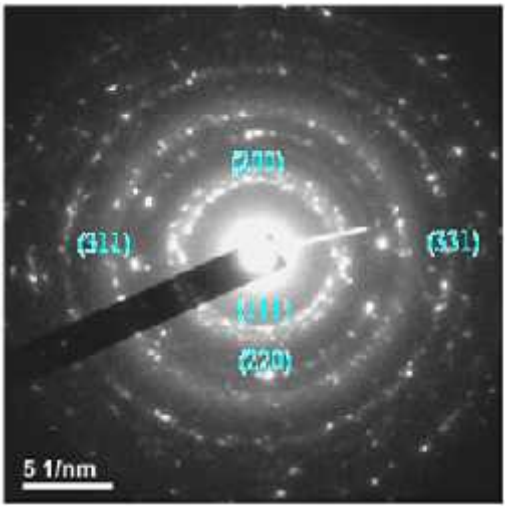

Figure 4. SAED patterns of Au NPs-polysaccharide bioconjugates

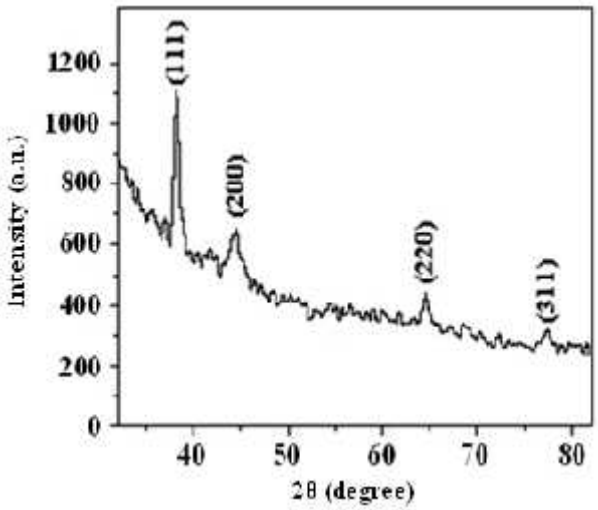

Figure 5. XRD patterns of dried Au NPs-polysaccharide bioconjugates

.

5.2.2.3. Fourier transform-infrared spectra (FT-IR) analysis

In order to investigate the interaction of Au NPs with the polysaccharide, FT-IR experiment of both the polysaccharide and Au NPs-polysacharide bioconjugates were carried out. In the FT-IR spectrum of polysaccharide [Figure 6a], two partially overlapped peaks at 1071 and 1043 cm^{-1} were assigned to C-OH stretching [19] along with a broad stretching peak at 3428 cm^{-1} for hydroxyl group and a weak band at 2935 cm^{-1} for aliphatic C-H stretching. In the FT-IR spectrum of Au NPs-polysaccharide bioconjugates [Figure 6b], two overlapped peak at 1071 and 1043 cm^{-1} merged to give a single peak at 1044 cm^{-1}, which is possibly due to the interaction of Au^{+3} with the oxygen of hydroxyl group (C-OH) from polysaccharide [20]. The peaks for hydroxyl group (3400 cm^{-1}),

aliphatic C-H (2924 cm^{-1}) and C-OH (1044 cm^{-1}) are also appeared in the spectrum of Au NPs-polysaccharide bioconjugates which are the characteristic peaks of polysaccharides. So, it can be believed that there is some interaction between the Au NPs and polysaccharide with the help of which the Au NPs attain stability.

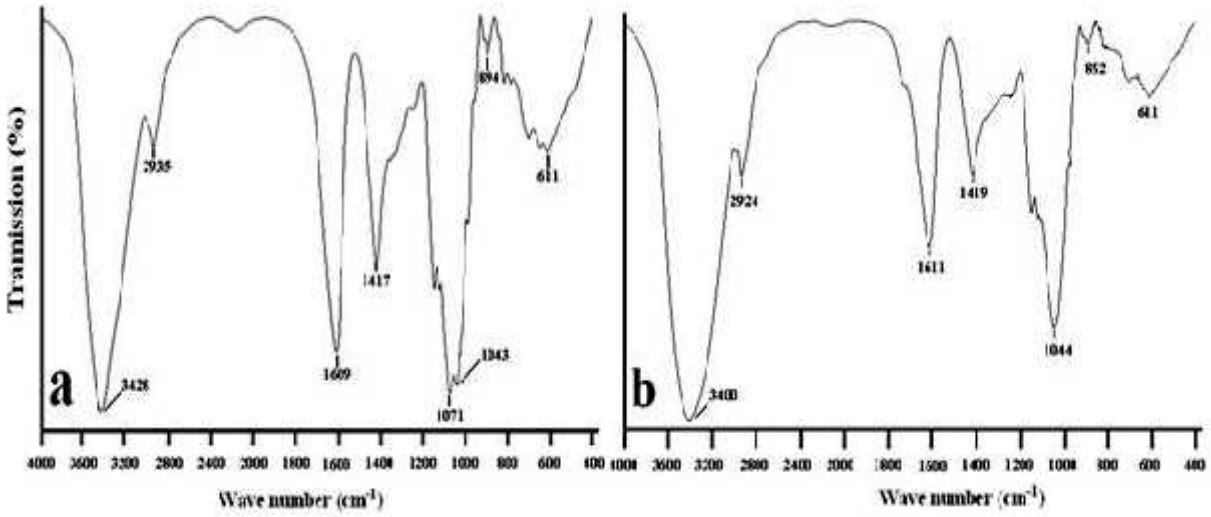

Figure 6. FT-IR spectra of (a) polysaccharide and (b) Au NPs-polysaccharide bioconjugates.

5.2.3. Catalytic properties of Au NPs for 4-nitrophenol reduction

To investigate the catalytic activity of Au NPs-polysaccharide bioconjugates, the reduction of 4-nitrophenol (4-NP) to 4-aminophenol (4-AP) by $NaBH_4$ in aqueous phase was chosen as a model reaction. The absorption peak of 4-NP was red shifted from 317 to 400 nm [Figure 7] immediately after the addition of $NaBH_4$ solution, which also associated with a color change of 4-NP solution from yellow to yellow green due to formation of 4-aminophenolate ion in alkaline condition. The absorption peak at 400 nm remained unaltered for a long duration in absence of Au NPs-polysaccharide bioconjugates. In contrast, with the addition of Au NPs-polysaccharide bioconjugates, the absorption peak height at 400 nm successively decreased with a concomitant appearance of two new absorption peaks around 230 and 300 nm with time, which was because of the generation of 4-AP. Evaluation of small bubbles of H_2 gas surrounding the catalyst particles helped in stirring the reaction mixture [21].

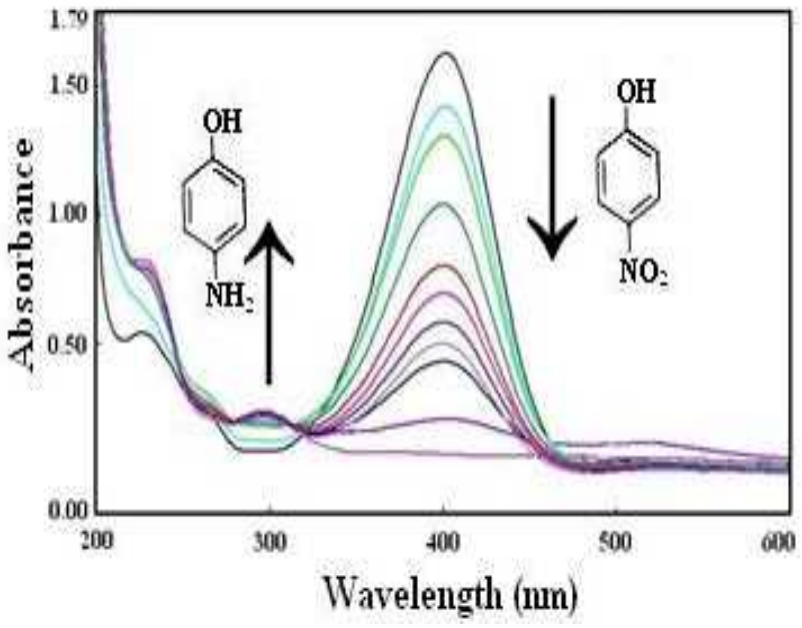

Figure 7. UV-vis spectra for the catalytic reduction of 4-nitrophenol by Au NPs-polysaccharide bioconjugates.

The blank experiment by adding only the hetero polysaccharide into the aqueous solution of 4-NP and $NaBH_4$ mixture, did not change the color or absorption peak of 4-nitrophenolate ions for more than 24 h, which clearly demonstrated that the reduction of 4-NP by $NaBH_4$ is solely activated by Au NPs-polysaccharide bioconjugates. In the UV-vis spectra two points are obvious where all the spectra intersect each other, indicating that no by-products are formed during the reaction [22]. The formation of 4-AP in the catalytic reaction was furthered confirmed by the ^1H NMR study in D_6-DMSO. In the spectrum, a doublet of doublet signal was appeared in the range of δ 6.48-6.6 which is due to aromatic protons ortho and para to amino group. The peak in the downfield region at δ 8.41 can be assigned as phenolic proton and peak at δ 4.39 can be assigned as aromatic amine protons. The ^1H NMR spectrum for the product is comparable to that of the authentic 4-AP. As the initial concentration of $NaBH_4$ largely greater than the initial concentration of 4-NP, it can be assumed that concentration of $NaBH_4$ remains constant with time during the reaction. Hence, the reaction rate is independent on the concentration of $NaBH_4$. So pseudo-first-order rate kinetics with respect to 4-NP concentration was used to evaluate the rate of the reaction. Figure 8 shows a good linear correlation of ln (A) versus time and reaction rate constant is determined to be 2.67×10^{-2} min^{-1}.

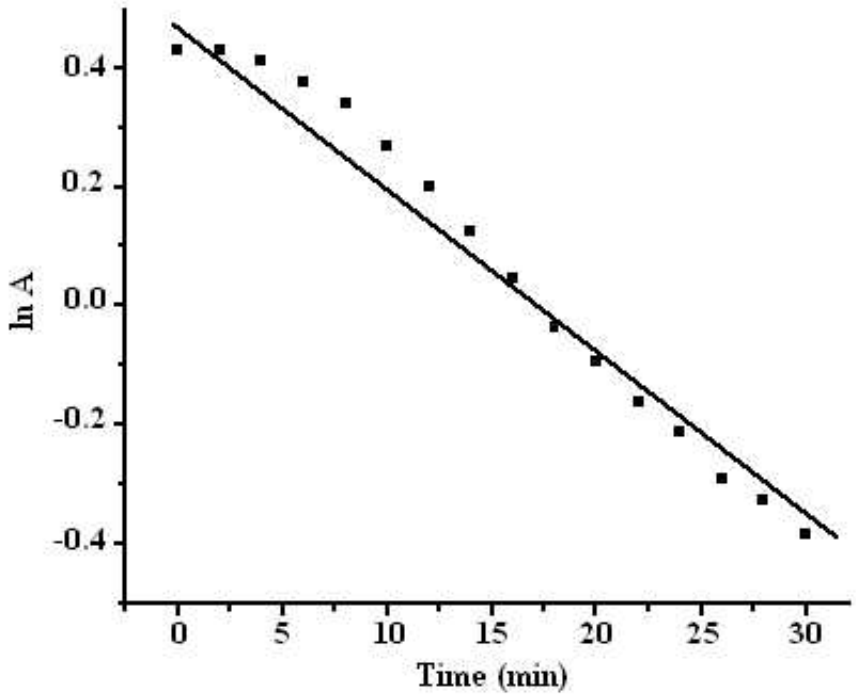

Figure 8. Plot of ln (A) versus time for the catalytic reduction of 4-nitrophenol by Au NPs- polysaccharide bioconjugates.

5.3. References

[1] Zhang, Z.; Wu, Y. *Langmuir*. **2010**, *26*, 9214-9223.

[2] Rivas, L.; Sanchez-Cortes, S.; Garcia-Ramos, J. V.; Morcillo, G. *Langmuir*. **2001**, *17*, 574-577.

[3] Plyuto, Y.; Berquier, J.; Jacquiod, C.; Ricolleau, C. *Chem. Commun.* **1999**, 1653-1654.

[4] Wang, T.; Zhang, D.; Xu, W.; Yang, J.; Han, R.; Zhu, D. *Langmuir*. **2002**, *18*, 1840-1848.

[5] Guari, Y.; Thieuleux, C.; Mehdi, A.; Reye, C.; Corriu, R. J. P.; Gomez-Gallardo, S.; Philippot, K.; Chaudret, B. *Chem. Mater.* **2003**, *15*, 2017-2024.

[6] Tan, Y.; Jiang, L.; Li, Y.; Zhu, D. *J. Phys. Chem. B.* **2002**, *106*, 3131-3138.

[7] Pastoriza-Santos, I.; Liz-Marzan, L. M. *Langmuir*. **1999**, *15*, 948-951.

[8] Mucic, R. C.; Storhoff, J. J.; Mirkin, C. A.; Letsinger, R. L. *J. Am. Chem. Soc*. **1998**, *120*, 12674- 12675.

[9] Esumi, K.; Takei, N.; Yoshimura, T. *Colloids Surf. B.* **2003**, *32*, 117-123.

[10] Philip, D.; Unni, C. *Physica E.* **2011**, *43*, 1318-1322.

[11] Philip, D. *Physica E.* **2010**, *42*, 1417-1424.

[12] Vijayakumar, R.; Devi, V.; Adavallan, K.; Saranya, D. *Physica E*. **2011**, *44*, 665-671.

[13] Huang, H.; Yang, X. *Biomacromolecules*. **2004**, *5*, 2340-2346.

[14] Bhambure, R.; Bule, M.; Shaligram, N.; Kamat, M.; Singhal, R. *Chem. Eng. Technol.* **2009**, *32*, 1036-1041.

[15] Ahmad, A.; Senapati, S.; Khan, M. I.; Kumar, R.; Ramani, R.; Srinivas, V.; Sastry, M. *Nanotechnology*. **2003**, *14*, 824-828.

[16] Singaravelu, G.; Arockiamary, J. S.; Kumar, V. G.; Govindaraju, K. *Colloids Surf. B.* **2007**, *57*, 97-101.

[17] Ojha, A. K.; Maiti, D.; Chandra, K.; Mondal, S.; Das, D.; Roy, S. K.; Ghosh, K.; Islam, S. S. *Carbohydr. Res.* **2008**, *343*, 1222-1231.

[18] Brause, R.; Moltgen, H.; Kleinermanns, K. *Appl. Phys. B.* **2002**, *75*, 711-716.

[19] Hromadkova, Z.; Ebringerova, A.; Sasinkova, V.; Sandula, J.; Hribalova, V.; Omelkova, J. *Carbohydr. Polym.* **2003**, *51*, 9-15.

[20] Bellamy, L. J. The Infra-red Spectra of Complex Molecules, third ed., Chapman and Hall, London. **1978**.

[21] Wei, D.; Ye, Y.; Jia, X.; Yuan, C.; Qian, W. *Carbohydr. Res.* **2010**, *345*, 74-81.

[22] Panigrahi, S.; Basu, S.; Praharaj, S.; Pande, S.; Jana, S.; Pal, A.; Ghosh, S. K.; Pal, T. *J. Chem. C.* **2007**, *111*, 4596-4605.

LIST OF PUBLICATIONS

1. Green synthesis of gold nanoparticles using gum polysaccharide of Cochlospermum religiosum (katira gum) and study of catalytic activity. **Saikat Maity**, Ipsita Kumar Sen, Syed Sirajul Islam. ***Physica E***, 2012, *45*, 130-134.
2. Structural study of an immunoenhancing polysaccharide isolated from an edible hybrid mushroom of *Pleurotus florida* and *Lentinula edodes*. **Saikat Maity**, Eshita Kar Mandal, Kousik Maity, Sanjoy K. Bhunia, Birendra Behera, Tapas K. Maiti, Pijush Mallick, Samir R. Sikdar, Syed S. Islam. ***Bioactive Carbohydrates and Dietary Fiber***, 2013, *1*, 72-80.
3. A heteropolysaccharide from an edible hybrid mushroom pfle 1p: structural and immunostimulating studies. **Saikat Maity**, Sanjoy K. Bhunia, Ipsita K. Sen, Eshita Kar Mandal, Kousik Maity, Birendra Behera, Tapas K. Maiti, Pijush Mallick, Samir R. Sikdar, Syed S. Islam. ***Carbohydrate Research***, 2013, *374*, 89-95.
4. Structural characterization of an immunoenhancing cytotoxic heteroglycan isolated from an edible mushroom *Calocybe indica* var. APK2. Eshita Kar Mandal, Kousik Maity, **Saikat Maity**, Sanjoy K. Gantait, Swatilekha Maiti, Tapas K. Maiti, Samir R. Sikdar, Syed S. Islam. ***Carbohydrate Research***, 2011, *346*, 2237-2243.
5. Chemical analysis and study of immunoenhancing and antioxidant property of a glucan isolated from an alkaline extract of a somatic hybrid mushroom of *Pleurotus florida* and *Calocybe indica* variety APK2. Kousik Maity, Eshita Kar (Mandal), **Saikat Maity**, Sanjoy K. Gantait, Debsankar Das, Swatilekha Maiti, Tapas K. Maiti, Samir R. Sikdar, Syed. S. Islam. ***International Journal of Biological Macromolecules***, 2011, *49*, 555-560.
6. Structural characterization and study of immunoenhancing and antioxidant property of a novel polysaccharide isolated from the aqueous extract of a somatic hybrid mushroom of *Pleurotus florida* and *Calocybe indica* variety APK2. Kousik Maity, Eshita Kar (Mandal), **Saikat Maity**, Sanjoy K. Gantait, Debsankar Das, Swatilekha Maiti, Tapas K. Maiti, Samir R. Sikdar, Syed S. Islam. ***International Journal of Biological Macromolecules***, 2011, *48*, 304-310.
7. Chemical analysis of an immunostimulating $(1\rightarrow4)$-, $(1\rightarrow6)$-branched glucan from an edible mushroom, *Calocybe indica*. Eshita Kar Mandal, Kousik Maity, **Saikat Maity**, Sanjoy K. Gantait, Birendra Behera, Tapas K. Maiti, Samir R. Sikdar, Syed S. Islam. ***Carbohydrate Research***, 2012, *347*, 172-177.

8. Structural studies of an immunostimulating gluco-arabinan from seeds of *Caesalpinia bonduc*. Eshita Kar Mandal, Soumitra Mandal, **Saikat Maity**, Birendra Behera, Tapas K. Maiti, Syed S. Islam. ***Carbohydrate Polymers***, 2013, *92*, 704-711.

9. An immunostimulating water insoluble β-glucan of an edible hybrid mushroom: Isolation and characterization. Kousik Maity, Surajit Samanta, Sunil K. Bhanja, **Saikat Maity**, Ipsita K. Sen, Swatilekha Maiti, Birendra Behera, Tapas K. Maiti, Samir R. Sikdar, Syed S. Islam. ***Fitoterapia***, 2013, *84*, 15-21.

APPENDIX

Paper-1: Green synthesis of gold nanoparticles using gum polysaccharide of Cochlospermum religiosum (katira gum) and study of catalytic activity. **Saikat Maity**, Ipsita Kumar Sen, Syed Sirajul Islam. ***Physica E***, 2012, *45*, 130-134.

Paper-2: Structural study of an immunoenhancing polysaccharide isolated from an edible hybrid mushroom of *Pleurotus florida* and *Lentinula edodes*. **Saikat Maity**, Eshita Kar Mandal, Kousik Maity, Sanjoy K. Bhunia, Birendra Behera, Tapas K. Maiti, Pijush Mallick, Samir R. Sikdar, Syed S. Islam. ***Bioactive Carbohydrates and Dietary Fiber***, 2013, *1*, 72-80.

Paper-3: A heteropolysaccharide from an edible hybrid mushroom pfle 1p: structural and immunostimulating studies. **Saikat Maity**, Sanjoy K. Bhunia, Ipsita K. Sen, Eshita Kar Mandal, Kousik Maity, Birendra Behera, Tapas K. Maiti, Pijush Mallick, Samir R. Sikdar, Syed S. Islam. ***Carbohydrate Research***, 2013, *374*, 89-95.

Physica E 45 (2012) 130–134

Contents lists available at SciVerse ScienceDirect

Physica E

journal homepage: www.elsevier.com/locate/physe

Green synthesis of gold nanoparticles using gum polysaccharide of *Cochlospermum religiosum* (katira gum) and study of catalytic activity

Saikat Maity, Ipsita Kumar Sen, Syed Sirajul Islam *

Department of Chemistry and Chemical Technology, Vidyasagar University, Midnapore 721102, West Bengal, India

HIGHLIGHTS

- Au NPs were synthesized using hetero-polysaccharide, extracted from katira gum.
- NPs were characterized by UV–vis, HR-TEM, XRD and FT-IR analysis.
- These NPs useful as heterogeneous catalyst in the reduction of 4-NP.

GRAPHICAL ABSTRACT

Gold nanoparticles were synthesized using a hetero-polysaccharide through green route. These gold nanoparticles function as an efficient heterogeneous catalyst in the reduction of 4-nitrophenol.

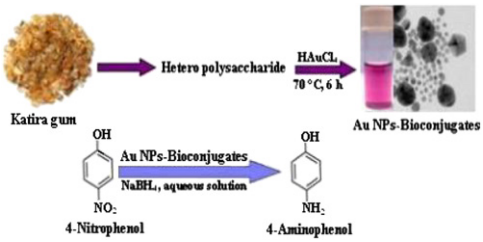

ARTICLE INFO

Article history:
Received 5 March 2012
Received in revised form
12 July 2012
Accepted 17 July 2012
Available online 10 August 2012

ABSTRACT

A green synthesis of gold nanoparticles (Au NPs) using aqueous solution of a hetero-polysaccharide, extracted from the gum of *Cochlospermum religiosum* (katira gum), has been demonstrated in this work. The hetero-polysaccharide plays the role of both reducing and stabilizing agent. The synthesized Au NPs were characterized by UV–vis spectroscopy, HR-TEM, XRD and FT-IR experiments. The surface plasmon resonance (SPR) band of UV–vis spectrum around 528 nm confirmed the formation of Au NPs. Transmission electron microscopic analysis showed an average size of Au NPs of 6.9 nm. The fcc crystalline nature of these particles was identified by XRD analysis and SAED pattern. These Au NPs also function as an efficient heterogeneous catalyst in the reduction of 4-nitrophenol (4-NP) to 4-aminophenol (4-AP). The reduction of 4-NP follows pseudo-first-order kinetics with rate constant 2.67×10^{-2} min^{-1}.

1. Introduction

Metal nanoparticles are important to researchers due to their unique properties and wide ranging application in a variety of areas including physics, chemistry, material science and biomedical science. Numerous methods for the synthesis of nanoparticles are reported, amongst them, most conventional is the reduction of metal salt solution by means of reducing agent like sodium borohydride, *N*,*N*-dimethyl formamide, trisodium citrate, or other organic compounds [1–7]. But the use of such reducing agents may be associated with environmental toxicity or biological hazards. Currently integration of 'green chemistry' principles into nanotechnology is one of the key issues in nanoscience research. Utilization of nontoxic chemicals, environmentally benign solvents and renewable materials are some of key issues for a green synthesis strategy. In recent years, biomolecules are used in the synthesis of Au nanomaterials [8–12]. Synthesis of gold nanoparticles using chitosan as both reducing and protecting agent was reported by Huang et al. [13]. Microorganisms are also used for the synthesis of gold nanoparticles [14–16]. In this work, an environmentally benign method for preparation of Au NPs using aqueous solution of a hetero-polysaccharide [17], isolated from katira gum acting both as reducing and stabilizing agent is reported.

* Corresponding author. Tel.: +91 3222 276558x437; fax: +91 3222 275329.
E-mail address: sirajul_1999@yahoo.com (S. Sirajul Islam).

1386-9477/$ - see front matter © 2012 Elsevier B.V. All rights reserved.
http://dx.doi.org/10.1016/j.physe.2012.07.020

Recently, the role of metal nanoparticles in the field of catalysis opens a new horizon. Au NPs serve as an effective catalyst in the reduction of various pollutants like 4-NP, the most common organic pollutant in industrial and agricultural waste water. The 4-NP is toxic in nature, strong skin irritant and imparts odor to water and used as building blocks of many dyes, explosives, pesticides. It breaks down in water and surface soil. Therefore drinking water, eating foods grown in soil that contain 4-NP, can lead to critical health hazards to human beings. So much attention has been given to develop an efficient methodology for the conversion of 4-NP. Here a safe method for the conversion of 4-NP with Au NPs synthesized using a hetero-polysaccharide has been reported. Hence, the synthesized Au NPs have several excellent properties including long-term dispersion stability at room temperature, effectiveness as a heterogeneous catalyst in the conversion of 4-NP.

2. Materials and methods

2.1. Materials

Chloroauric acid ($HAuCl_4$) was purchased from Sigma-Aldrich, 4-NP and sodium borohydride ($NaBH_4$) were procured from Merck Ltd. Hetero-polysaccharide from katira gum [17] was used both as reducing and stabilizing agent. Deionized double distilled water was used throughout the experiment.

2.2. Synthesis of Au NPs

Katira gum was washed with methanol, dried, and made powder and then soxhletted using different solvents. The crude material was then dissolved in water, dialyzed, centrifuged and the filtrate was precipitated in alcohol to get crude polysaccharide which was further purified through Sepharose-6B column as reported in our earlier paper [17]. The structure of the pure polysaccharide was confirmed by NMR studies [17] as

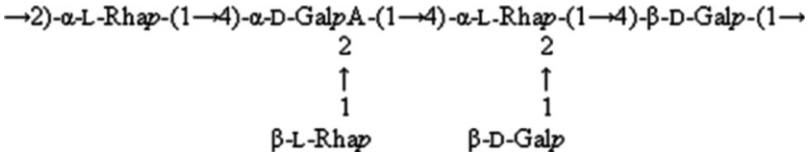

and used for the synthesis of Au NPs. For the synthesis of Au NPs, 2 mL aqueous solution of $HAuCl_4$ with a concentration of 10^{-3} M was added to 6 mL 0.2% (w/v) aqueous polysaccharide solution. The mixture was then heated at 70 °C, 6 h with continuous stirring on a magnetic stirrer and UV–vis spectra of the reaction mixture were recorded at different time interval till the completion of the reaction.

2.3. Characterization

The UV–vis absorption spectra were taken at room temperature on a Shimadzu UV-1601 spectrometer using a quartz cuvette with a 1 cm optical path. One milliliter of each solution was diluted with equal volume of water for taking spectra. Double distilled water was used as the blank. For transmission electron microscopy (TEM), a drop of reaction solution was placed on the carbon coated copper grid and dried under IR lamp. TEM images were taken by means of a JEOL–JEM-2100 HR-TEM operated at 200 kV. For XRD analysis, the reaction solution of Au NPs was drop-coated on a glass substrate and measurements were carried out with a Rigaku Miniflex II X-ray diffractometer, using Ni-filtered Cu Kα (λ=0.15406 nm) radiation. The diffraction intensities were recorded from 30° to 80° 2θ angle. The aqueous solution of the synthesized Au NPs was freeze-dried and the dried sample was used for FT-IR analysis. FT-IR analysis of the dried sample was performed in a FT-IR-8400 S (Shimadzu) instrument between 4000 and 400 cm^{-1} using KBr pellet technique.

2.4. Catalytic properties of Au NPs for 4-nitrophenol reduction

The reduction of 4-NP was studied as a model reaction to prove the catalytic activity of synthesized Au NPs. The catalytic reaction was performed in a standard quartz cuvette with a 1-cm path length. Double distilled water (2 mL) was mixed with 120 μL of 2 mM 4-NP solution followed by the addition of 1 mL of 15 mM freshly prepared $NaBH_4$ solution. Thereafter 3.5 mg of solid freeze dried Au NPs-polysaccharide bioconjugates were added to the above reaction mixture as heterogeneous catalyst. Immediately after the addition of Au NPs, the absorption spectra were recorded in 2 min interval in the range of 200–600 nm at room temperature.

3. Results and discussion

3.1. UV–vis spectroscopic analysis

A pale pink color was appeared after 10 min of the reaction and the color was gradually intensified as the reaction was continued with heating. A typical plasmon resonance band at 544 nm appeared after 1 h indicating formation of Au NPs. The time dependent UV–vis absorption spectra are shown in Fig. 1. The intensity of the absorption band gradually increased and the maximum intensity of absorption was attained after 6 h of the reaction. This gradual increase in the absorption band is attributed to the fact that Au NPs concentration increases in the media as the reduction reaction proceeds. After 6 h, no significant change in intensity at 528 nm was observed which indicated

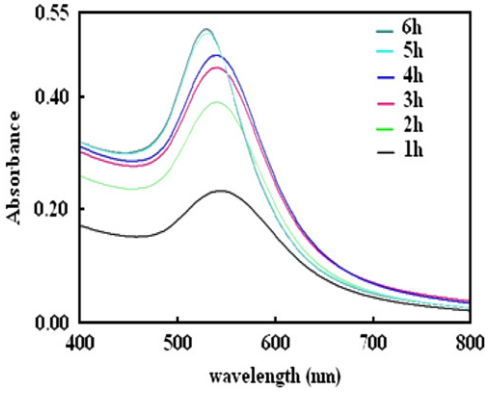

Fig. 1. UV–vis spectra of Au NPs at different time intervals.

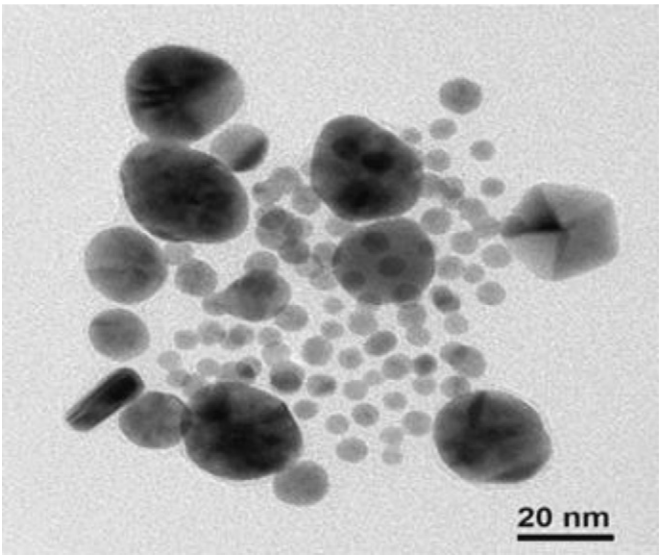

Fig. 2. HR-TEM images of hetero-polysaccharide synthesized Au NPs.

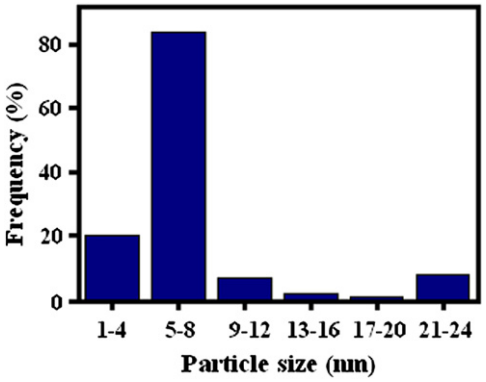

Fig. 3. The particle size distribution histogram of Au NPs.

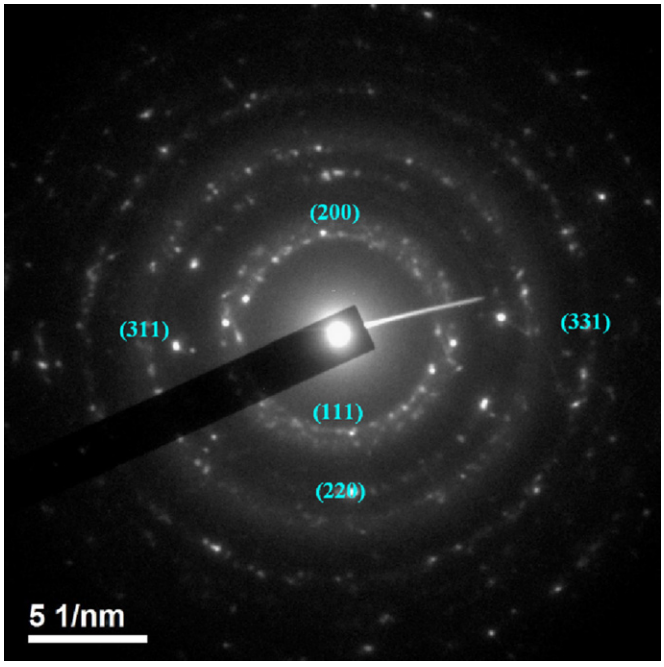

Fig. 4. Selected area electron diffraction (SAED) patterns of Au NPs.

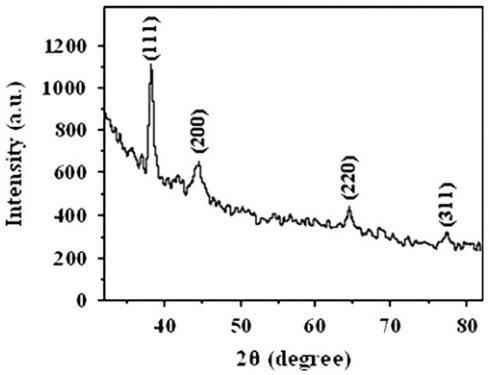

Fig. 5. XRD patterns of dried Au NPs-polysaccharide bioconjugates. All peaks could be indexed to fcc gold.

almost complete reduction of Au^{+3}. The shifting of surface plasmon absorption maxima from 544 nm to a fixed value 528 nm at 6 h may be due to decrease in particles size [18].

3.2. TEM and XRD analysis

The shape, morphology, and size distribution of the Au NPs were analyzed using high resolution transmission electron microscopy (HR-TEM). HR-TEM image (Fig. 2) showed that the particles are mostly spherical with a few having rod and decahedral morphology. The average size of the particles is 6.9 nm as revealed from particle size distribution histogram (Fig. 3). The SAED pattern (Fig. 4) showing rings ascribed to (1 1 1), (2 0 0), (2 2 0), (3 1 1) and (3 3 1) planes exhibited the face centered cubic (fcc) crystalline structure of gold. The crystalline nature of Au NPs was further confirmed by X-ray diffraction (XRD) analysis. A typical XRD pattern (Fig. 5) exhibited peaks at 38.22°, 44.40°, 64.51°, 77.49° that can be indexed to the (1 1 1), (2 0 0), (2 2 0), (3 1 1) facets respectively of fcc gold.

3.3. Fourier transform-infrared spectra (FT-IR) analysis

In order to investigate the interaction of Au NPs with the polysaccharide, FT-IR experiment of both the polysaccharide and Au NPs-polysaccharide bioconjugates were carried out. In the FT-IR spectrum (Fig. 6a) of polysaccharide, two partially overlapped peaks at 1071 and 1043 cm^{-1} were assigned to C–OH stretching [19] along with a broad stretching peak at 3428 cm^{-1} for hydroxyl group and a weak band at 2935 cm^{-1} for aliphatic C–H stretching. In the FT-IR spectrum of Au NPs-polysaccharide bioconjugates (Fig. 6b), two overlapped peak at 1071 and 1043 cm^{-1} merged to give a single peak at 1044 cm^{-1}, which is possibly due to the interaction of Au NPs with the oxygen of hydroxyl group (C–OH) from polysaccharide [20]. The peaks for hydroxyl group (3400 cm^{-1}), aliphatic C–H (2924 cm^{-1}) and C–OH (1044 cm^{-1}) are also appeared in the spectrum of Au NPs-polysaccharide bioconjugates which are the characteristic peaks of polysaccharides. So, it can be believed that there is some interaction between the Au NPs and polysaccharide with the help of which the Au NPs attain stability.

3.4. Catalytic properties of Au NPs for 4-nitrophenol reduction

To investigate the catalytic activity of Au NPs-polysaccharide bioconjugates, the reduction of 4-NP to 4-AP by $NaBH_4$ in aqueous phase was chosen as a model reaction. The absorption peak of 4-NP was red shifted from 317 to 400 nm (Fig. 7) immediately after the addition of $NaBH_4$ solution, which also associated with a color change of 4-NP solution from yellow to yellow green due to

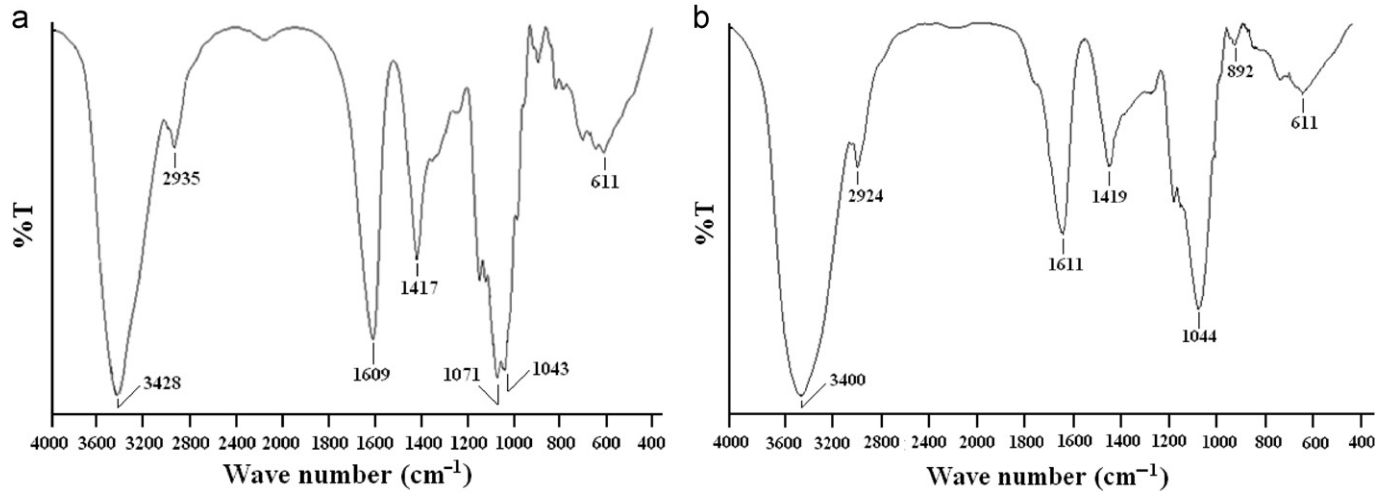

Fig. 6. FT-IR spectra of (a) polysaccharide and (b) Au NPs-polysaccharide bioconjugates.

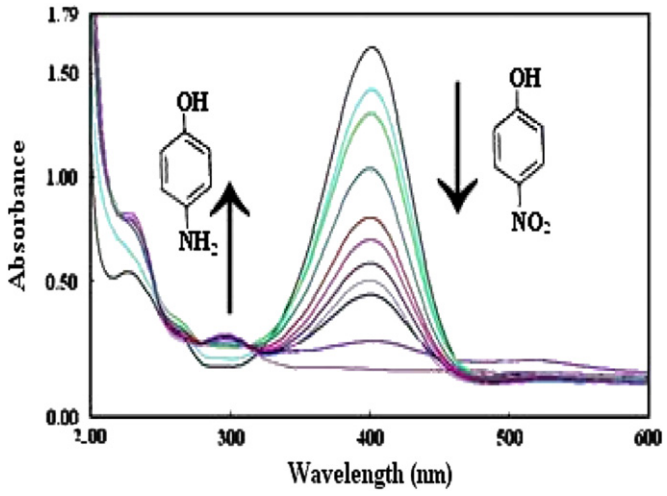

Fig. 7. UV–vis spectra for the catalytic reduction of 4-nitrophenol by Au NPs-polysaccharide bioconjugates.

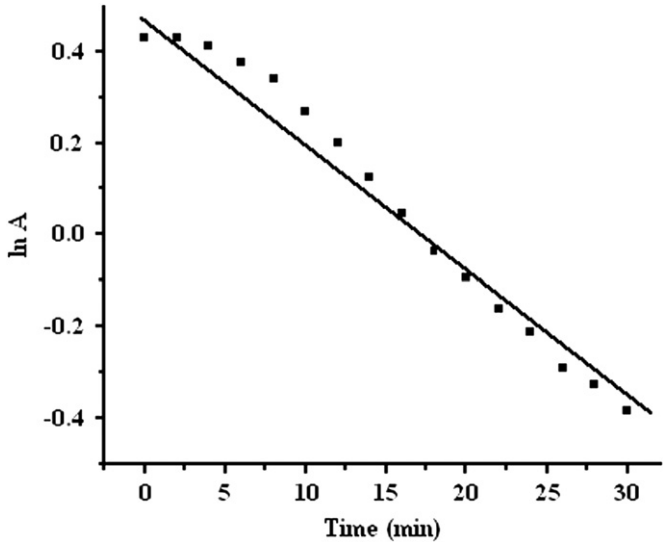

Fig. 8. Plot of ln (A) versus time for the catalytic reduction of 4-nitrophenol by Au NPs-polysaccharide bioconjugates.

formation of 4-aminophenolate ion in alkaline condition. The absorption peak at 400 nm remained unaltered for a long duration in absence of Au NPs-polysaccharide bioconjugates. In contrast, with the addition of Au NPs-polysaccharide bioconjugates, the absorption peak height at 400 nm successively decreased with a concomitant appearance of two new absorption peaks around 230 and 300 nm with time, which was because of the generation of 4-AP. Evaluation of small bubbles of H_2 gas surrounding the catalyst particles helped in stirring the reaction mixture [21]. The blank experiment by adding only the hetero-polysaccharide into the aqueous solution of 4-NP and $NaBH_4$ mixture, did not change the color or absorption peak of 4-nitrophenolate ions for more than 24 h, which clearly demonstrated that the reduction of 4-NP by $NaBH_4$ is solely activated by Au NPs-polysaccharide bioconjugates. In the UV–vis spectra two points are obvious where all the spectra intersect each other, indicating that no by-products are formed during the reaction [22]. The formation of 4-AP in the catalytic reaction was further confirmed by the ^{1}H NMR study in D_6-DMSO. In the spectrum, a doublet of doublet signal was appeared in the range of δ 6.48–6.6 which is due to aromatic protons ortho and para to amino group. The peak in the downfield region at δ 8.41 can be assigned as phenolic proton and peak at δ 4.39 can be assigned as aromatic amine protons. The ^{1}H NMR spectrum for the product is comparable to that of the authentic 4-AP. As the initial concentration of $NaBH_4$ largely greater than the initial concentration of 4-NP, it can be assumed that concentration of $NaBH_4$ remains constant with time during the reaction. Hence, the reaction rate is independent on the concentration of $NaBH_4$. So pseudo-first-order rate kinetics with respect to 4-NP concentration was used to evaluate the rate of the reaction. Fig. 8 shows a good linear correlation of ln (A) versus time and reaction rate constant is determined to be 2.67×10^{-2} min^{-1}.

4. Conclusions

A simple green approach towards the synthesis of Au NPs using a hetero-polysaccharide has been reported herein. The hetero-polysaccharide serves the role of selfreducing and stabilizing agent and thus the hazards associated with the use of extra stabilizing agent are avoided. These Au NPs are highly stable and do not show any sign of agglomeration even after storage of three months at room temperature. They also exhibit good catalytic activity for the reduction of 4-NP in aqueous phase. This catalytic

performance of the Au NPs may perhaps be used for the treatment of waste water.

Acknowledgments

The support rendered by the department of Physics and Technophysics, Vidyasagar University for the XRD analysis is acknowledged. S.M. (one of the authors) thanks the CSIR for offering junior research fellowship (CSIR-09/599(0039)/2010-EMR-I).

References

[1] Z. Zhang, Y. Wu, Langmuir 26 (2010) 9214.
[2] L. Rivas, S. Sanchez-Cortes, J.V. Garcia-Ramos, G. Morcillo, Langmuir 17 (2001) 574.
[3] Y. Plyuto, J. Berquier, C. Jacquiod, C. Ricolleau, Chemical Communications (1999) 1653.
[4] T. Wang, D. Zhang, W. Xu, J Yang, R. Han, D. Zhu, Langmuir 18 (2002) 1840.
[5] Y. Guari, C. Thieuleux, A. Mehdi, C. Reye, R.J.P. Corriu, S. Gomez-Gallardo, K. Philippot, B. Chaudret, Chemistry of Materials 15 (2003) 2017.
[6] Y. Tan, L. Jiang, Y. Li, D. Zhu, Journal of Physical Chemistry B 106 (2002) 3131.
[7] I Pastoriza-Santos, L.M Liz-Marzan, Langmuir 15 (1999) 948.
[8] R.C. Mucic, J.J. Storhoff, C.A. Mirkin, R.L. Letsinger, Journal of American Chemical Society 120 (1998) 12674.
[9] K. Esumi, N. Takei, T. Yoshimura, Colloids and surfaces B 32 (2003) 117.
[10] D. Philip, C. Unni, Physica E 43 (2011) 1318.
[11] D. Philip, Physica E 42 (2010) 1417.
[12] R. Vijayakumar, V. Devi, K. Adavallan, D. Saranya, Physica E 44 (2011) 665.
[13] H. Huang, X. Yang, Biomacromolecules 5 (2004) 2340.
[14] R. Bhambure, M. Bule, N. Shaligram, M. Kamat, R. Singhal, Chemical Engineering and Technology 32 (2009) 1036.
[15] A. Ahmad, S. Senapati, M.I. Khan, R. Kumar, R. Ramani, V. Srinivas, M. Sastry, Nanotechnology 14 (2003) 824.
[16] G. Singaravelu, J.S. Arockiamary, V.G. Kumar, K. Govindaraju, Colloids and Surfaces B 57 (2007) 97.
[17] A.K. Ojha, D. Maiti, K. Chandra, S. Mondal, D. Das, S.K. Roy, K. Ghosh, S.S. Islam, Carbohydrate Research 343 (2008) 1222.
[18] R. Brause, H. Moltgen, K. Kleinermanns, Applied Physics B 75 (2002) 711.
[19] Z. Hromadkova, A. Ebringerova, V. Sasinkova, J. Sandula, V. Hribalova, J. Omelkova, Carbohydrate Polymers 51 (2003) 9.
[20] L.J. Bellamy, The Infra-red Spectra of Complex Molecules, third ed., Chapman and Hall, London, 1978.
[21] D. Wei, Y. Ye, X. Jia, C. Yuan, W. Qian, Carbohydrate Research 345 (2010) 74.
[22] S. Panigrahi, S. Basu, S. Praharaj, S. Pande, S. Jana, A. Pal, S.K. Ghosh, T. Pal, Journal of Physical Chemistry C 111 (2007) 4596.

Bioactive Carbohydrates and Dietary Fibre 1 (2013) 72–80

Available online at www.sciencedirect.com

SciVerse ScienceDirect

www.elsevier.com/locate/bcdf

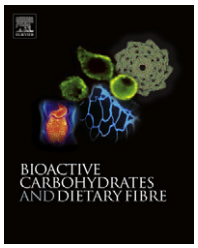

Structural study of an immunoenhancing polysaccharide isolated from an edible hybrid mushroom of *Pleurotus florida* and *Lentinula edodes*

Saikat Maity[a], *Eshita Kar Mandal*[a], *Kousik Maity*[a], *Sanjoy K. Bhunia*[a], *Birendra Behera*[b], *Tapas K. Maiti*[b], *Pijush Mallick*[c], *Samir R. Sikdar*[c], *Syed S. Islam*[a,*]

[a]*Department of Chemistry & Chemical Technology, Vidyasagar University, Midnapore, West Bengal 721102, India*
[b]*Department of Biotechnology, Indian Institute of Technology (IIT) Kharagpur, Kharagpur, West Bengal 721302, India*
[c]*Division of Plant Biology, Bose Institute, P-1/12, C.I.T. Scheme VII M, Kolkata, 700054 West Bengal, India*

ARTICLE INFO

Article history:
Received 23 August 2012
Received in revised form
21 January 2013
Accepted 23 January 2013

Keywords:
Hybrid mushroom
Polysaccharide
Structure
NMR analysis
Immunoenhancing activity

ABSTRACT

The water-soluble polysaccharide isolated from hot aqueous extract of the fruit bodies of somatic hybrid mushroom (*pfle 1q*) obtained through intergenic protoplast fusion between *Pleurotus florida* and *Lentinula edodes* consists of D-galactose and D-mannose in a molar ratio of nearly 2:1. The polysaccharide showed immunoenhancing activity by stimulating the macrophage, splenocyte, and thymocyte. Based on the results of acid hydrolysis, methylation analysis, periodate oxidation, and NMR experiments (^{1}H, ^{13}C, DEPT-135, DQF-COSY, TOCSY, NOESY, ROESY, HSQC and HMBC) the repeating unit of the purified polysaccharide was established as

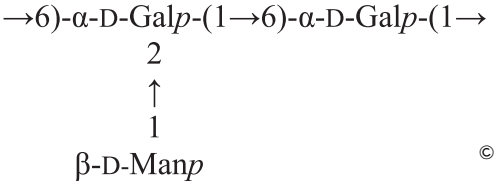

1. Introduction

Mushrooms have been consumed globally as tasty food and nutritional supplements. Mushroom polysaccharides have been recognized as the most potent antitumor and immunostimulating materials (Borchers, Stern, Hackman, Keen, & Gershwin, 1999; Nanba, Hamaguchi, & Kuroda, 1987; Mizuno et al., 1990). Various mushroom polysaccharides such as Lentinan derived from *Lentinula edodes*, Krestin (PSK) derived from *Coriolus versidor* have been recommended for use as anticancer drugs (Sasaki & Takasuka, 1976; Sakagami, Aoki, Simpson, & Tanuma, 1991). A variety of immunoenhancing polysaccharides from edible mushrooms (Bhunia et al., 2010) and edible hybrid mushrooms (Patra et al., 2011) were reported by our group. Four different immunostimulating polysaccharides isolated from *Pleurotues florida* were also reported by our group (Rout, Mondal, Chakraborty, Pramanik, & Islam, 2004, 2005;Rout, Mondal, Chakraborty, & Islam, 2006, 2008). Water insoluble (Sasaki & Takasuka, 1976) and soluble β-glucans (Yu et al., 2010) extracted from *L. edodes* were reported. Protoplast fusion between the strains of *P. florida* and *L. edodes* produced nine new hybrid strains adopting the procedures as applied earlier (Chakraborty & Sikdar, 2010), and among them six strains, i.e., *pfle 1o*, *pfle 1p*, *pfle 1q*, *pfle 1r*, *pfle 1s*, and *pfle 1v* produced fruit bodies. Recently a (1→6)(1→3)-β-D-glucan was isolated from fruit bodies of one of the hybrid strains *pfle 1r* (Maji et al., 2012). Aqueous extract of the fruit bodies of another hybrid strain, *pfle 1q*, yielded a

*Corresponding author. Tel.: +91 03222 276558x437; Mob.:+91 99326 29971; fax: +91 03222 275329.
E-mail address: sirajul_1999@yahoo.com (S.S. Islam).

2212-6198/$ - see front matter © 2013 Elsevier Ltd. All rights reserved.
http://dx.doi.org/10.1016/j.bcdf.2013.01.003

single polysaccharide through Sepharose 6B gel purification. The present polysaccharide is a mannogalactan consisting of a main chain of (1→6)-linked D-galactopyranosyl moieties with terminal D-mannopyranosyl linked at C-2 of the D-galactopyranosyl residues, which was not obtained from any of the parent mushrooms. Hence, the detailed structural characterization and the immunoenhancing properties of this polysaccharide were carried out and reported herein.

2. Materials and methods

2.1. Preparation of hybrid mushroom strain produced between P. florida and L. edodes

The hybrid mushroom strain *pfle 1q* was produced through polyethyleneglycol (30% PEG, MW-3350)-mediated somatic protoplast fusion between *P. florida* and *L. edodes*. Hybrid strains were selected based on the double selection method and afterwards maintained in Potato-Dextrose–Agar medium. Spawn of the hybrid strain was produced on paddy grain and mushroom was produced on paddy straw substrate.

2.2. Isolation, fractionation, and purification of the crude polysaccharide

The hybrid mushroom of *pfle 1q* was cultivated and collected from Falta experimental farm, Bose Institute. The fruit bodies (500 g) were washed thoroughly and then boiled for 8 h with distilled water. After filtration through linen cloth, the filtrate was centrifuged at 7670*g* (using a Heraeus Biofuge stratos centrifuge) for 45 min at 4 °C and the supernatant was collected and precipitated in ethanol (1:5, v/v). It was kept overnight at 4 °C and again centrifuged as above. The precipitated material was washed four times with ethanol and then freeze dried. The freeze dried material was dissolved in 40 mL of distilled water, and dialyzed through cellulose membrane (Sigma-Aldrich, retaining $M_w > 12{,}400$ Da) against distilled water for 48 h to remove low molecular weight carbohydrate materials. The aqueous solution was then collected from the dialysis tube and freeze-dried, to yield crude polysaccharide (315 mg).

The crude polysaccharide (25 mg) was passed through Sepharose 6B gel permeation column (90×2.1 cm^2) using water as an eluant with a flow rate of 0.4 mL/min. Ninety-five test tubes (2 mL each) were collected using Redifrac fraction collector and monitored spectrophotometrically at 490 nm with phenol–sulfuric acid reagent (York, Darvill, McNeil, Stevenson, & Albersheim ,1986) using a Shimadzu UV–vis spectrophotometer, model-1601. A single fraction (test tubes 34–47) was collected and freeze-dried, yielding 10 mg purified polysaccharide (PS). The purification process was carried out in several lots.

2.3. Monosaccharide analysis

PS (3.0 mg) was hydrolyzed with 2 M CF_3COOH (2 mL) in a round-bottom flask at 100 °C for 18 h in a water bath. The excess acid was completely removed by co-distillation with water. Then, the hydrolyzed product was reduced with $NaBH_4$ (9 mg), followed by acidification with dilute CH_3COOH, and then co-distilled with pure CH_3OH to remove excess boric acid. The reduced sugars (alditol) were acetylated with 1:1 pyridine–acetic anhydride in a boiling water bath for 1 h to give the alditol acetates, which were analyzed by GLC. Quantization was carried out from the peak area, using response factors from standard monosaccharides.

2.4. Methylation analysis

PS (4.0 mg) was methylated using the procedure described by Ciucanu and Kerek (1984). The methylated products were isolated by making partition between $CHCl_3$ and H_2O (5:2, v/v) for four times. The organic layer containing products was collected and dried. The methylated product was then hydrolyzed with 90% formic acid (1 mL) at 100 °C for 1 h and excess formic acid was evaporated by co-distillation with distilled water. The hydrolyzed product was then reduced with sodium borohydride and acetylated with pyridine–acetic anhydride (1:1). The alditol acetates of methylated sugars were analyzed by GLC–MS.

2.5. Periodate oxidation

PS (5 mg) was added to 2 mL 0.1 M sodium metaperiodate solution and the mixture was kept in the dark at 27 °C for 48 h. The excess periodate was destroyed by adding 1,2-ethanediol and the solution was dialyzed against distilled water for 2 h. The dialyzed material was reduced with $NaBH_4$ for 15 h and neutralized with acetic acid. The resulting material was dried by co-distillation with methanol. The periodate-oxidized material (Goldstein, Hay, Lewis, & Smith, 1965; Hay, Lewis, & Smith, 1965) was divided into two portions. One portion was hydrolyzed with 2 M CF_3COOH for 18 h and this hydrolyzed material was used for alditol acetates preparation as usual for GLC analysis. Another portion was methylated by the method of Ciucanu and Kerek (1984), followed by preparation of alditol acetates which were analyzed by GLC–MS.

2.6. Absolute configuration of monosaccharide

The absolute configuration of monosaccharide was determined by the method of Gerwig, Kamerling, and Vliegenthart (1978). PS (1.0 mg) was hydrolyzed with CF_3COOH, and then the acid was removed by co-distillation with water. 250 μL 0.625 M HCl solution treated with R− (+)-2-butanol was added to the hydrolyzed product and heated at 80 °C for 16 h. Then the reactants were evaporated and TMS-derivatives were prepared with N,O-bis (trimethylsilyl) trifluroacetamide (BSTFA). The products were analyzed by GLC using a capillary column SPB-1 (30 m × 0.26 mm) with a temperature program (3 °C/min) from 150 to 210 °C. The resulting 2,3,4,6-tetra-O-TMS-(+)-2-butylglycosides were identified by comparison with those prepared from the D and L enantiomers of different monosaccharides.

2.7. Optical rotation

Optical rotation was measured on a Jasco Polarimeter model P-1020 at 30.9 °C.

2.8. Determination of molecular weight

The average molecular weight of PS was determined by a gel permeation chromatography (Hara, Kiho, Tanaka, & Ukai, 1982). Standard dextrans T-200, T-70, and T-40 were passed through a Sepharose-6B column and then the elution volumes were plotted against the logarithms of their respective molecular weights. The elution volume of PS was then plotted on the same graph, and the average molecular weight of PS was determined.

2.9. GLC experiments

GLC experiment was performed on a gas–liquid chromatograph Hewlett-Packard model 5730 MSD, having a flame ionization detector and glass columns (1.8 m × 6 mm) packed with 3% ECNSS-M (A) on Gas Chrom Q (100–120 mesh) and 1% OV-225 (B) on Gas Chrom Q (100–120 mesh). All GLC analyses were performed at 170 °C.

2.10. GLC–MS experiments

The gas–liquid chromatography–mass spectrometric (GLC–MS) analysis was performed on a Shimadzu GLC–MS Model QP-2010 Plus automatic system, using ZB-5MS capillary column (30 m × 0.25 mm). The program was isothermal at 150 °C; hold time 5 min, with a temperature gradient of 2 °C/min up to a final temperature of 200 °C.

2.11. NMR studies

PS was dried over P_2O_5 in vacuum for several days and then exchanged with deuterium (Dueñas Chaso et al., 1997) followed by lyophilizing with D_2O (99.96% atom ^2H, Aldrich) for four times Then ^1H, ^{13}C, TOCSY, DQF-COSY, ROESY, NOESY, HSQC and HMBC NMR spectra were recorded on a Bruker Avance DPX-500 spectrometer at 30 °C. 0.25% and 1.2% (w/v) of PS solution in D_2O were used for ^1H and ^{13}C experiments respectively. The ^1H NMR spectrum was recorded by suppressing the HOD signal (fixed at δ 4.70 ppm) using the WEFT pulse sequence (Hård, Zadelhoff, Moonen, Kamerling, & Vliegenthart, 1992). The 2D-DQF-COSY experiment was carried out using standard Bruker software. The TOCSY experiment was recorded at a mixing time of 150 ms, and complete assignment required several TOCSY experiments having mixing times ranging from 60 to 300 ms. The NOESY and ROESY mixing delay were 200 ms. The ^{13}C NMR experiments of the PS were recorded using acetone as an internal standard, fixing the methyl carbon signal at 31.05 ppm. The delay time in the HMBC experiment was 80 ms.

2.12. Test for macrophage activity by nitric oxide assay

RAW 264.7 growing in Dulbecco's modified Eagle's medium (DMEM) was seeded in 96 well flat bottom tissue culture plates at a concentration of 5×10^5 cells/mL (180 μL). Cells were left overnight for attachment and then different concentrations of PS (12.5, 25, 50, 100 and 200 μg/mL) were added. After 48 h of treatment, culture supernatant of each well was collected and NO content was estimated using the Griess reagent (1:1 of 0.1% in 1-napthylethylenediamine in 5% phosphoric acid and 1% sulfanilamide in 5% phosphoric acid). Lipopolysaccharide (LPS), L6511 of *Salmonella enterica* serotype typhimurium (Sigma), was used as a positive control.

2.13. Splenocyte and thymocyte proliferation assay

A single cell suspension of spleen and thymus was prepared from normal mice under aseptic conditions by homogenization in Hank's balanced salt solution (HBSS). The suspension was centrifuged to obtain cell pellet. The contaminating red blood cells were removed by hemolytic Gey's solution. After washing two times with HBSS, the cells were resuspended in complete RPMI. Cell concentration was adjusted to 1×10^6 cells/mL and viability of splenocyte and thymocyte (as tested by trypan blue dye exclusion) was always over 90%. The cells (180 μL) were plated in 96 well flat bottom tissue culture plates and incubated with 20 μL of different concentrations (12.5, 25, 50 and 100 μg/mL) of PS. PBS (10 mM, phosphate buffer saline, pH-7.4) was taken as a negative control whereas lipopolysaccharide (LPS, 1 μg/mL, Sigma, USA, Catalog no. L-6511, source: *S. typhimurium*) served as positive controls. All cultures were set up for 72 h at 37 °C in a humidified atmosphere of 5% CO_2. Proliferation of splenocyte (% Splenocyte Proliferation Index or % SPI) and thymocyte (% Thymocyte Proliferation Index or % TPI) were determined by the MTT assay method (Ohno et al., 1993).

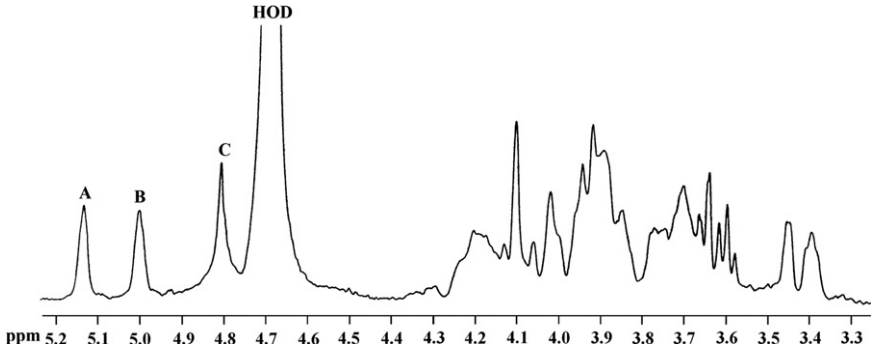

Fig. 1 – ^1H NMR spectrum (500 MHz, D_2O, 30 °C) of the PS isolated from hybrid mushroom (*Pfle 1q*) of *Pleorutus florida* and *Lentinula edodes*.

All the experiments were done twice with five replicates and the results were represented as mean ± standard deviation. *P* value was calculated using one tailed student t-test in Excel software. Difference in parameter between the treatment group and the control group was considered as statistically significant if $P<0.05$ (indicated with a "*" mark).

3. Results and discussion

3.1. *Isolation, purification and chemical analysis of the polysaccharide*

The total carbohydrate of the PS was estimated to 98% using the sulfuric acid–phenol method (York et al., 1986). In order to check the presence of protein, UV analysis was monitored at 280 nm but lack of absorbance at 280 nm in the UV spectrum indicated that the sample was free from protein The apparent average molecular weight (Hara et al., 1982) of the PS fraction was estimated as 1.55×10^5 Da, as determined from the calibration curve using dextrans of known molecular weight. The PS showed a specific rotation of $[\infty]_D^{30.9}$+50.08 (*c* 0.09, water). The GLC analysis of the alditol acetates of the hydrolyzed product of PS confirmed the presence of mannose and galactose in a molar ratio of nearly 1:2. The absolute configuration of the monosaccharides was determined as D. The GLC–MS analysis of partially methylated alditol acetates revealed the presence of 1,5-di-O-acetyl-2,3,4,6-tetra-O-methyl-D-mannitol, 1,5,6-tri-O-acetyl-2,3,4-tri-O-methyl-D-galactitol, 1,2,5,6-tetra-O-acetyl-3,4-di-O-methyl-D-galactitol in a molar ratio of nearly 1:1:1. Thus, PS was assumed to consist of terminal D-mannopyranosyl, (1→6)-linked D-galactopyranosyl, and (1→2,6)-linked D-galactopyranosyl moieties respectively. These linkages were further confirmed by the periodate oxidation experiment. The GLC–MS analysis of the alditol acetates of periodate oxidized–reduced (Goldstein et al., 1965; Hay et al., 1965), methylated PS showed total disappearance of sugar residues. These results indicated that all the sugar residues were consumed during oxidation. Thus, the mode of linkages present in the PS was confirmed.

3.2. *NMR and structural analysis of polysaccharide*

The ^{1}H NMR spectrum (Fig. 1) of PS showed the presence of three signals in the anomeric region at δ 5.14, 5.00 and 4.81 ppm in a ratio of nearly 1:1:1. They were designated **A**, **B**, and **C** according to their decreasing proton chemical shifts. Three signals in the anomeric region of ^{13}C spectrum (Fig. 2) at δ 101.6, 98.3, and 97.8 ppm correlated to the residues **C**, **A**, and **B** respectively from the HSQC spectrum (Fig. 3). The rest of the ^{1}H and ^{13}C signals (Table 1) were assigned from

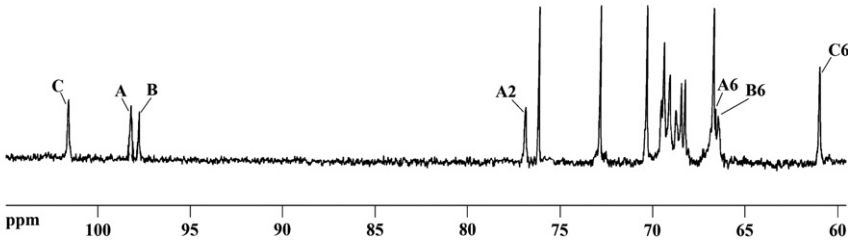

Fig. 2 – ^{13}C NMR spectrum (125 MHz, D_2O, 30 °C) of the PS isolated from hybrid mushroom (*Pfle 1q*) of *Pleorutus florida* and *Lentinula edodes*.

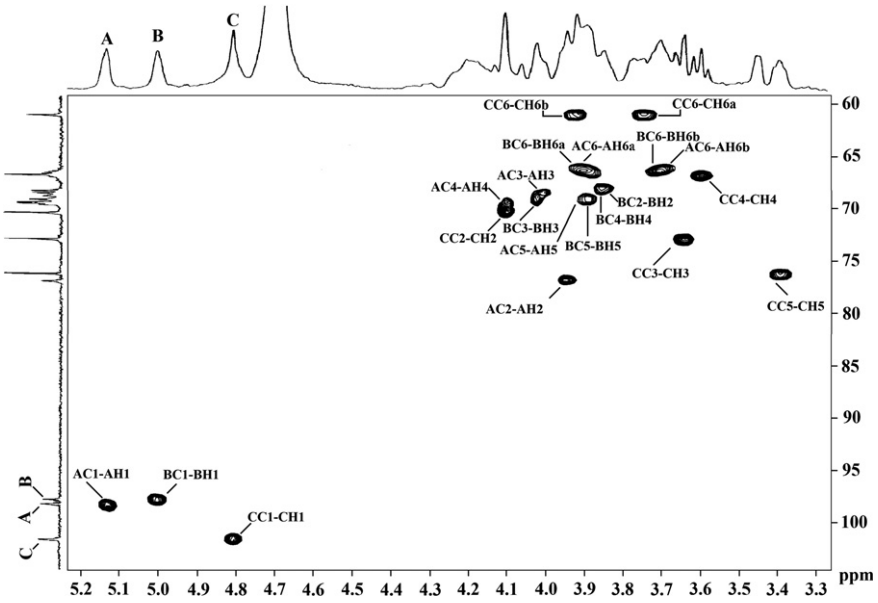

Fig. 3 – HSQC spectrum (D_2O, 30 °C) of the PS isolated from hybrid mushroom (*Pfle 1q*) of *Pleorutus florida* and *Lentinula edodes*.

Table 1 – The ^{1}H and ^{13}C NMR chemical shifts for the PS isolated from *Pfle 1q*[a,b] in D_2O at 30°C

Glycosyl residue	H-1/C-1	H-2/C-2	H-3/C-3	H-4/C-4	H-5/C-5	H-6a, H-6b/C-6
→2,6)-α-D-Galp-(1→	5.14	3.95	4.01	4.12	3.90	3.70[c], 3.90[d]
A	98.3	76.9	68.5	69.5	69.1	66.6
→6)-α-D-Galp-(1→	5.00	3.85	4.02	3.86	3.89	3.71[c], 3.91[d]
B	97.8	68.3	68.8	68.3	69.1	66.5
β-D-Manp-(1→	4.81	4.11	3.64	3.60	3.39	3.74[c], 3.92[d]
C	101.6	70.4	72.9	66.7	76.2	61.0

[a] Values of the ^{1}H chemical shifts were recorded with respect to the HOD signal fixed at δ 4.70 at 30 °C.
[b] Values of the ^{13}C chemical shifts were recorded with reference to acetone as the internal standard and fixed at δ 31.05 at 30 °C.
[c] Interchangeable.
[d] Interchangeable.

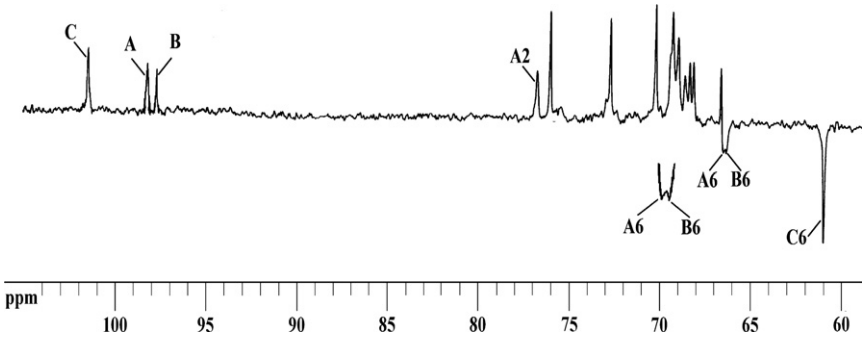

Fig. 4 – DEPT-135 spectrum (D_2O, 30 °C) of the PS isolated from hybrid mushroom (*Pfle 1q*) of *Pleorutus florida* and *Lentinula edodes*.

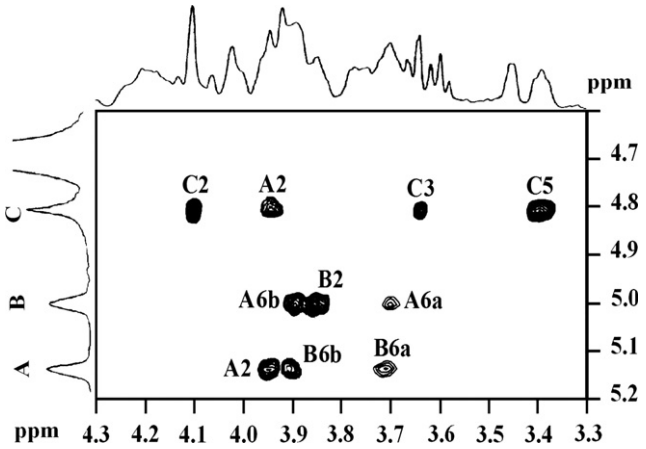

Fig. 5 – Part of the ROESY spectrum of the PS isolated from hybrid mushroom (*Pfle 1q*) of *Pleorutus florida* and *Lentinula edodes*.

Table 2 – ROESY data for the PS isolated from hybrid mushroom *Pfle 1q*.

Glycosyl residue	Anomeric proton	ROE contact protons	
	δ	δ	Residue, atom
→2,6)-α-D-Galp-(1→	5.14	3.95	**A** H-2
A		3.71	**B** H-6a
		3.91	**B** H-6b
→6)-α-D-Galp-(1→	5.00	3.85	**B** H-2
B		3.70	**A** H-6a
		3.90	**A** H-6b
β-D-Manp-(1→	4.81	4.11	**C** H-2
C		3.64	**C** H-3
		3.39	**C** H-5
		3.95	**A** H-2

DQF-COSY, TOCSY, and HSQC experiments. The proton coupling constants were measured from DQF-COSY experiment.

Among these three residues, residues **A** and **B** had coupling constant values of $J_{H\text{-}2,\ H\text{-}3}$ ~9 Hz and $J_{H\text{-}3,\ H\text{-}4}$ ~3.5 Hz and thus, they were confirmed as D-galactopyranosyl residues. The anomeric proton (δ 5.14 ppm for **A** and δ 5.00 ppm for **B**) and anomeric carbon chemical shifts (δ 98.3 ppm for **A** and δ 97.8 ppm for **B**) as well as the coupling constant values ($J_{H\text{-}1,H\text{-}2}$ ~3.1 Hz and $J_{C\text{-}1,H\text{-}1}$ ~171 Hz) confirmed that these residues were present in α-configuration. In case of residue **A**, all the proton and carbon chemical shifts except C-2 and C-6 were nearly matched with the standard values of methyl glucosides (Agarwal, 1992; Rinaudo & Vincendon, 1982). The downfield shifts of C-2 (δ 76.9 ppm) and C-6 (δ 66.6 ppm) with respect to standard values indicated that it was linked at C-2 and C-6. The linkage at C-6 was also supported by DEPT-135 spectrum (Fig. 4). Thus, **A** was confirmed as (1→2,6)-linked α-D-galactopyranosyl residue. For residue **B**, the downfield shift of C-6 (δ 66.5 ppm) with respect to standard values of methyl glucosides confirmed that residue **B** contained C-6 linkage. The linkage at C-6 was

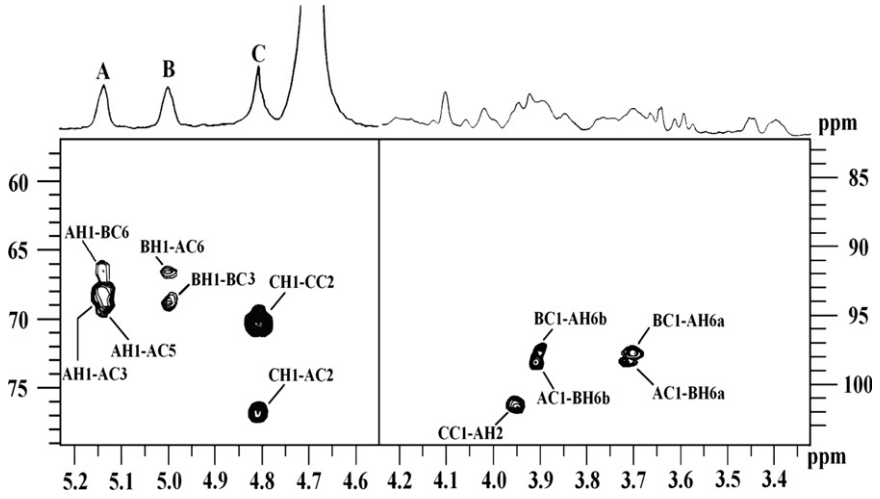

Fig. 6 – Part of the HMBC spectrum of the PS isolated from hybrid mushroom (*Pfle 1q*) of *Pleorutus florida* and *Lentinula edodes*. The delay time in the HMBC experiment was 80 ms.

Table 3 – The significant $^{3}J_{H,C}$ connectivities observed in an HMBC spectrum for the anomeric protons/carbons of the sugar residues of the PS isolated from hybrid mushroom *Pfle 1q*.

Residue	Sugar linkage	H-1/C-1	Observed connectivities		
		δ_H/δ_C	δ_H/δ_C	Residue	Atom
A	→2,6)-α-D-Gal*p*-(1→	5.14	68.5	**A**	C-3
		98.3	69.1	**A**	C-5
			66.5	**B**	C-6
			3.71	**B**	H-6a
			3.91	**B**	H-6b
B	→6)-α-D-Gal*p*-(1→	5.00	68.8	**B**	C-3
		97.8	66.6	**A**	C-6
			3.70	**A**	H-6a
			3.90	**A**	H-6b
C	β-D-Man*p*-(1→	4.81	70.4	**C**	C-2
		101.6	76.9	**A**	C-2
			3.95	**A**	H-2

further supported by DEPT-135 spectrum (Fig. 4). Therefore, **B** was confirmed as (1→6)-linked α-D-galactopyranosyl residue. The large coupling constant values ($J_{H\text{-}3,\ H\text{-}4}$ ~7.5 Hz and $J_{H\text{-}4,\ H\text{-}5}$ ~10 Hz) of residue **C** confirmed its mannopyranosyl configuration. The anomeric proton (δ 4.81 ppm) and anomeric carbon chemical shifts (δ 101.6 ppm) as well as the low coupling constant values ($J_{H\text{-}1,H\text{-}2}$ ~0, $J_{C\text{-}1,H\text{-}1}$ ~161) confirmed that residue **C** was present in β-configuration. All the proton and carbon chemical shifts of residue **C** corresponded nearly to the standard values of methyl glycosides of β-D-mannose. Thus, **C** was confirmed as terminal β-D-mannopyranosyl residue.

The different linkages that connected these three residues were determined from ROESY (Fig. 5; Table 2) as well as NOESY (not shown) spectrum. In ROESY spectrum, the inter-residual connectivities were observed between **A**H-1/**B**H-6a and **B**H-6b, **B**H-1/**A**H-6a and **A**H-6b, and **C**H-1/**A**H-2 along with other intra-residual contacts. Thus, from ROESY spectrum the following linkages were established.

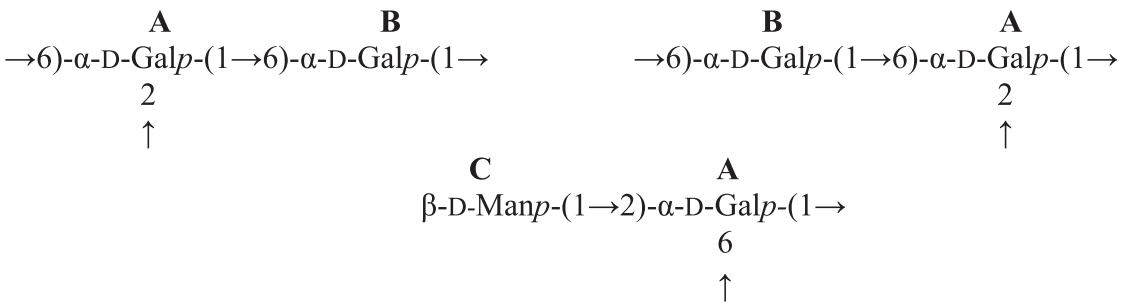

These connectivities were further confirmed from the HMBC experiment (Fig. 6; Table 3). In HMBC spectrum the inter-residual cross-peaks were observed between AH-1/BC-6, AC-1/BH-6a and BH-6b, BH-1/AC-6, BC-1/AH-6a and AH-6b, CH-1/AC-2, and CC-1/AH-2. Thus, the HMBC and ROESY connectivities clearly supported the presence of the following repeating unit in the PS:

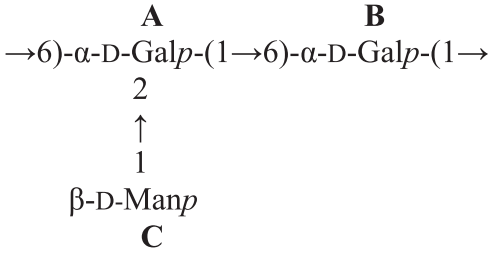

3.3. Assay for macrophage activity by NO

Mushroom polysaccharides function as immunostimulator by activating the macrophages (Wasser, 2002). Macrophages are white blood cells which play key roles in immune system defense. They usually engulf and destroy bacteria and viruses. Hence, macrophage activation induced by the PS was tested *in vitro*. On treatment with different concentrations of this PS it was observed that 25–34% of NO production increased up to 25 μg/mL. This was further increased by 87–114% at 50 and 100 μg/mL respectively, but decreased at 200 μg/mL (Fig. 7a). Hence, an enhanced production of NO i.e., the effective dose of this PS was observed at 100 μg/mL with optimum production of 12.8 μM NO/5 × 10^5 macrophages.

3.4. Splenocyte and thymocyte proliferation assay

Proliferation of splenocyte and thymocyte is an indicator of immunostimulation (Ohno et al., 1993). The splenocyte and thymocyte activation tests were carried out in mouse cell culture medium with the PS by the MTT [3-(4,5-dimethylthiazol-2-yl)-2,5-diphenyltetrazolium bromide] method (Ohno et al., 1993). The PS was tested to stimulate splenocytes and thymocytes and the results are shown in Fig. 7b and c respectively. The asterisks on the columns indicated the statistically significant differences compared to phosphate buffer saline (PBS) control. The splenocyte and thymocyte proliferation indices as compared to PBS control if closer to 100 or below indicate low stimulatory effect on immune system. Both the splenocyte and thymocyte proliferation indices were found maximum at 50 μg/mL, above and below which it decreases. Hence, it can be concluded that 50 μg/mL is the optimum concentration of the PS for splenocyte and thymocyte proliferation.

Mushroom polysaccharides have been recognized as biological response modifiers (BRMs). Biological response modifiers (BRMs) are the compounds which are capable of interacting with the immune system to upregulate or downregulate the host immune response. BRMs affect different cell types involving hematopoietic stem cells, innate (nonspecific) and adaptive (specific) immune systems, and cytokine networks and signaling pathways and the activities also depend on their mechanism of action or the site of activity (Tzianabos, 2000).

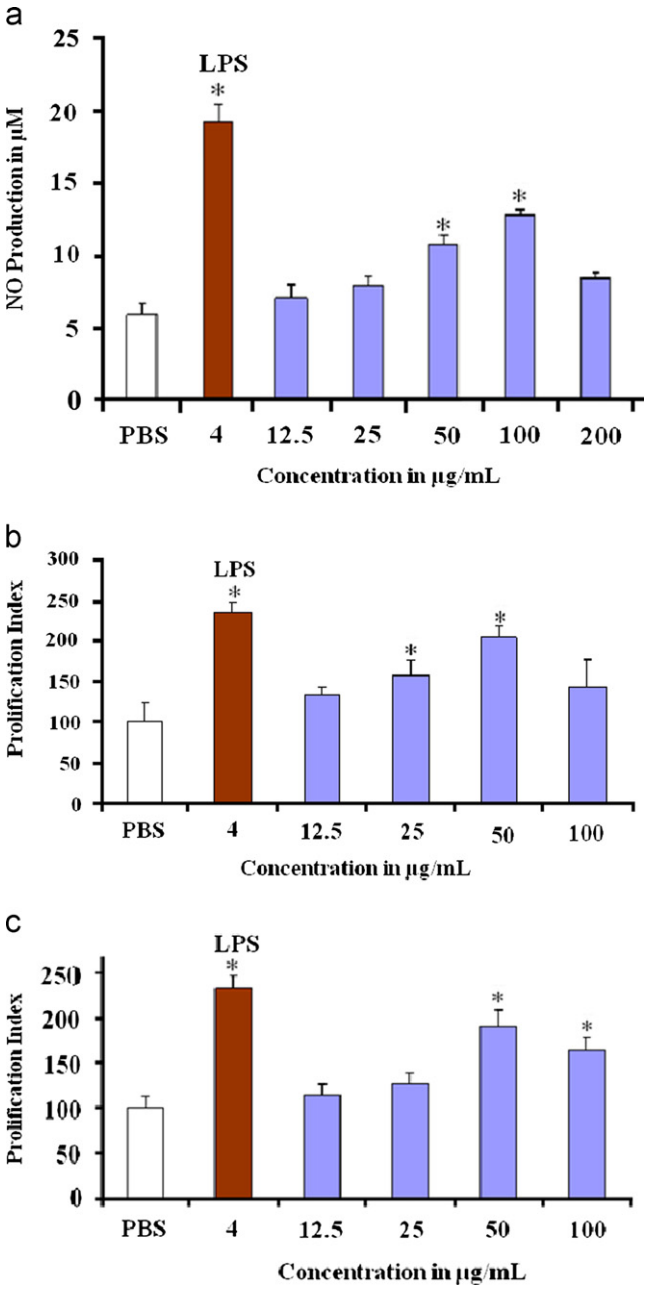

Fig. 7 – (a) *In vitro* activation of macrophage stimulated with different concentrations of the PS isolated from hybrid mushroom (*Pfle* 1*q*) of *Pleorutus florida* and *Lentinula edodes* in terms of NO production. Effect of different concentrations of the PS isolated from hybrid mushroom (*Pfle* 1*q*) of *Pleorutus florida* and *Lentinula edodes* on splenocyte (b) and thymocyte (c) proliferation ('*' means data is significant compared to the PBS control with $P < 0.05$).

The studies like NO production by macrophages, splenocyte and thymocyte proliferations are preliminary steps to explore whether the PS has any immunomodulating property or not. However, further studies are needed in order to identify the specific cells or cytokine pathway through which the PS exerts its action. It is expected that the PS showing immunomodulating properties *in vitro* may exhibit similar effect *in vivo* and help in combating microbial infection including tuberculosis, tumor cell eradication and autoimmune diseases.

4. Conclusions

A water soluble polysaccharide (PS) was isolated from aqueous extract of the fruit bodies of hybrid mushroom strain *pfle 1q* obtained through intergenic protoplast fusion between *P. florida* and *L. edodes*. The purified polysaccharide obtained through Sepharose gel-filtration contained a main chain of (1→6)-linked D-galactopyranosyl moieties with terminal D-mannopyranosyl linked to C-2 of some of the D-galactopyranosyl residues. This polysaccharide showed significant macrophage, thymocyte and splenocyte activations. On the basis of chemical analysis and NMR studies the structure of the repeating unit of the PS was established as

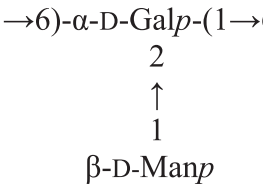

Acknowledgments

The authors are grateful to Professor S. Roy, Director, IICB, Kolkata, for providing instrumental facilities. Mr. Barun Majumdar of Bose Institute, Kolkata, is acknowledged for preparing NMR spectra. S.M. (one of the authors) thanks the CSIR for offering senior research fellowship (CSIR-09/599(0039)/2010-EMR-I).

REFERENCES

Agrawal, P. K. (1992). NMR spectroscopy in the structural elucidation of oligosaccharides and glycosides. *Phytochemistry*, *31*, 3307–3330.

Bhunia, S. K., Dey, B., Maity, K. K., Patra, S., Mandal, S. Maiti, S. Structural characterization of an immunoenhancing heteroglycan isolated from an aqueous extract of an edible mushroom, *Lentinus squarrosulus* (Mont.) Singer. *Carbohydrate Research*, *345*, 2542–2549.

Borchers, A. T., Stern, J. S., Hackman, R. M., Keen, C. L., & Gershwin, M. E. (1999). Mushrooms, tumors, and immunity. *Proceedings of the Society for Experimental Biology and Medicine*, *221*, 281–293.

Chakraborty, U., & Sikdar, S. R. (2010). Intergeneric protoplast fusion between *Calocybe indica* (milky mushroom) and *Pleurotus florida* aids in the qualitative and quantitative improvement of sporophore of the milky mushroom. *World Journal of Microbiology and Biotechnology*, *26*, 213–225.

Ciucanu, I., & Kerek, F. (1984). A simple and rapid method for the permethylation of carbohydrates. *Carbohydrate Research*, *131*, 209–217.

Dueñas Chaso, M. T., Rodriguez-Carvajal, M. A., Mateo, P. T., Franko-Rodriguez, G., Espartero, J. L. Iribas, A. I. Structural analysis of the exopolysaccharide produced by *Pediococcus damnosus*. *Carbohydrate Research*, *303*, 453–458.

Gerwig, G. J., Kamerling, J. P., & Vliegenthart, J. F.G. (1978). Determination of the D and L configuration of neutral monosaccharides by high-resolution capillary g.l.c. *Carbohydrate Research*, *62*, 349–357.

Goldstein, I. J., Hay, G. W., Lewis, B. A., & Smith, F. (1965). Controlled degradation of polysaccharides by periodate oxidation, reduction and hydrolysis. *Methods in Carbohydrate Chemisrty*, *5*, 361–370.

Hara, C., Kiho, T., Tanaka, Y., & Ukai, S. (1982). Anti-inflammatory activity and conformational behavior of a branched (I–+3)-/Y-D-glucan from an alkaline extract of *Dictyophora indusiata* FISCH. *Carbohydrate Research*, *110*, 77–87.

Hård, K., Zadelhoff, G. V., Moonen, P., Kamerling, J. P., & Vliegenthart, J. F.G. (1992). The Asn-linked carbohydrate chains of human Tamm-Horsfall glycoprotein of one male Novel sulfated and novel N-acetylgalactosamine-containing N-linked carbohydrate chains. *European Journal of Biochemistry*, *209*, 895–915.

Hay, G. W., Lewis, B. A., & Smith, F. (1965). Periodate oxidation of polysaccharides: General procedure. *Methods in Carbohydrate Chemistry*, *75*, 357–361.

Maji, P. K., Sen, I. K., Behera, B., Maiti, T. K., Mallick, P. Sikdar, S. R. Structural characterization and study of immunoenhancing properties of a glucan from hybrid mushroom of *Pleurotus florida* and *Lentinula edodes*. *Carbohydrate Research*, *358*, 110–115.

Mizuno, T., Inagaki, R., Kanao, T., Hagiwara, T., Nakamura, T. Ito, H. Antitumor activity and some properties of water-insoluble hetero-glycans from "Himematsutake," the fruiting body of *Agaricus blazei* Murill. *Agricultural and Biological Chemistry*, *54*, 2897–2905.

Nanba, H., Hamaguchi, A., & Kuroda, H. (1987). The chemical structure of an antitumor polysaccharide in fruit bodies of *Grifola frondosa* (Maitake). *Chemical and Pharmaceutical Bulletin*, *35*, 1162–1168.

Ohno, N., Saito, K., Nemoto, J., Kaneko, S., Adachi, Y. Nishijima, M. Immunopharmacological characterization of a highly branched fungal (1→3)-β-D-glucan, OL-2, isolated from Omphalia lapidescens. *Biological and Pharmaceutical Bulletin*, *16*, 414–419.

Patra, S., Maity, K. K., Bhunia, S. K., Dey, B., Mandal, S. Maity, T. K. Structural characterization and study of immunoenhancing properties of heteroglycan isolated from a somatic hybrid mushroom (*PfloVv1aFB*) of *Pleurotus florida* and *Volvariella volvacea*. *Carbohydrate Research*, *346*, 1967–1972.

Rinaudo, M., & Vincendon, M. (1982). ^{13}C NMR structural investigation of scleroglucan. *Carbohydrate Polymers*, *2*, 135–144.

Rout, D., Mondal, S., Chakraborty, I., & Islam, S. S. (2006). The structure of a polysaccharide from Fraction-II of an edible mushroom, *Pleurotus florida*. *Carbohydrate Research*, *341*, 995–1002.

Rout, D., Mondal, S., Chakraborty, I., & Islam, S. S. (2008). The structure and conformation of a water-insoluble (1→3)-,(1→6)-β-D-glucan from the fruiting bodies of *Pleurotus florida*. *Carbohydrate Research*, *343*, 982–987.

Rout, D., Mondal, S., Chakraborty, I., Pramanik, M., & Islam, S. S. (2005). Chemical analysis of a new (1→3)-, (1→6)-branched glucan from an edible mushroom, *Pleurotus florida*. *Carbohydrate Research*, *340*, 2533–2539.

Rout, D., Mondal, S., Chakraborty, I., Pramanik, M., & Islam, S. S. (2004). Structural characterisation of an immunomodulating polysaccharide isolated from aqueous extract of *Pleurotus florida* fruit-bodies. *Medicinal Chemistry Research*, *13*, 509–517.

Sakagami, H., Aoki, T., Simpson, A., & Tanuma, S. I. (1991). Induction of immunopotentiation activity by a protein-bound polysaccharide, PSK. (Review). *Anticancer Research*, *11*, 993–999.

Sasaki, T., & Takasuka, N. (1976). Further study of the structure of lentinan, an anti-tumor polysaccharide from *Lentinus edodes*. *Carbohydrate Research*, *47*, 99–104.

Tzianabos, A. O. (2000). Polysaccharide immunomodulators as therapeutic agents: Structural aspects and biologic function. *Clinical Microbiology Reviews*, *13*, 523–533.

Yu, Z., Ming, G., Kaiping, W., Zhixiang, C., Liquan, D. Jingyu, L. Structure, chain conformation and antitumor activity of a novel polysaccharide from *Lentinus edodes*. *Fitoterapia*, *81*, 1163–1170.

York, W. S., Darvill, A. G., McNeil, M., Stevenson, T. T., & Albersheim, P. (1986). Isolation and characterization of plant cell walls and cell wall components. *Methods in Enzymology*, *118*, 3–40.

Wasser, S. P. (2002). Medicinal mushrooms as a source of antitumor and immunomodulating polysaccharides. *Applied Microbiology and Biotechnology*, *60*, 258–274.

Carbohydrate Research 374 (2013) 89–95

Contents lists available at SciVerse ScienceDirect

Carbohydrate Research

journal homepage: www.elsevier.com/locate/carres

A heteropolysaccharide from an edible hybrid mushroom *pfle 1p*: structural and immunostimulating studies

Saikat Maity [a], Sanjoy K. Bhunia [a], Ipsita K. Sen [a], Eshita Kar Mandal [a], Kousik Maity [a], Birendra Behera [b], Tapas K. Maiti [b], Pijush Mallick [c], Samir R. Sikdar [c], Syed S. Islam [a,*]

[a] Department of Chemistry & Chemical Technology, Vidyasagar University, Midnapore 721102, West Bengal, India
[b] Department of Biotechnology, Indian Institute of Technology (IIT) Kharagpur, Kharagpur 721302, West Bengal, India
[c] Division of Plant Biology, Bose Institute, P-1/12, C.I.T. Scheme VII M, Kolkata 700054, West Bengal, India

ARTICLE INFO

Article history:
Received 21 February 2013
Received in revised form 3 April 2013
Accepted 7 April 2013
Available online 13 April 2013

Keywords:
Hybrid mushroom
Heteropolysaccharide
NMR experiments
Immunostimulating activity

ABSTRACT

A water-soluble heteropolysaccharide (PS-I) having molecular weight ~2.1 × 10^5 Da was isolated from hot aqueous extract of the fruit bodies of hybrid mushroom *pfle 1p*. The hybrid mushroom *pfle 1p* was obtained through intergenic protoplast fusion between *Pleurotus florida* and *Lentinula edodes*. The heteropolysaccharide contained D-glucose, D-galactose, and D-mannose in a molar ratio of nearly 4:2:1. The structural investigation of PS-I has been carried out using sugar and methylation analyses as well as 1D/2D NMR experiments (^{1}H, ^{13}C, DEPT-135, DQF-COSY, TOCSY, NOESY, ROESY, HSQC, and HMBC). Based on the results of these experiments, the repeating unit of the PS-I was established as:

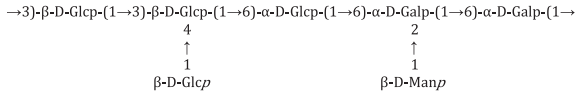

PS-I showed in vitro macrophage activation by NO production and also stimulated splenocytes and thymocytes.

1. Introduction

Mushrooms are enriched with various bioactive molecules. Among them, β-glucans have been extensively studied and considered as the most potent antitumor and immunostimulating materials.[1–3] Lentinan, a (1→3)-, (1→6)-β-glucan isolated from *Lentinula edodes* is well known for its high antitumor activity.[4,5] Different types of glucans from *Pleurotus florida* also exhibit significant immunostimulating properties.[6,7] In addition to the antitumor β-glucans, researchers have focused on heteroglycan which also has significant biological activities.[2,3] The structure of different heteroglycans may contain backbones of (1→6)- and (1→3)- or both (1→6)-(1→3)-linked α-galactose, α-glucose, or β-glucose with mainly fucose, mannose, or glucose as nonreducing residues.[8–11] Recently, Dey et al. and Patra et al. have isolated different immunostimulating heteroglycans from edible mushroom and hybrid mushroom.[12,13] Protoplast fusion between the strains of *Pleurotus florida* and *Lentinula edodes* produced nine new hybrid strains adopting the procedure as applied earlier[14] out of which six strains, that is, *pfle 1o*, *pfle 1p*, *pfle 1q*, *pfle 1r*, *pfle 1s*, and *pfle 1v* produced fruit bodies. Recently, a (1→3)-, (1→6)-β-D-glucan, and a heteroglycan have been isolated from one such hybrid strain *pfle 1r*.[15,16] Two water soluble polysaccharides (PS-I and PS-II) were isolated from the fruit bodies of *pfle 1p*. PS-I was found to consist of D-glucose, D-galactose, and D-mannose in a molar ratio of nearly

Abbreviations: Da, Dalton; *pfle 1p*, hybrid mushroom obtained through the protoplast fusion between *Pleurotus florida* and *Lentinula edodes*; ETOH, ethyl alcohol; Gal, galactose; Glc, glucose; GLC, gas liquid chromatography; GLC–MS, gas liquid chromatography-mass spectrometry; HBSS, Hank's balanced salt solution; HMBC, heteronuclear multiple bond correlation spectroscopy; HSQC, heteronuclear single quantum coherence spectroscopy; Man, mannose; Me, methyl; NO, nitric oxide; NOESY, nuclear overhauser effect spectroscopy; PBS, phosphate buffered saline; ROESY, rotating frame overhauser effect spectroscopy; TMS, tri methyl silyl; TOCSY, total correlation spectroscopy.

* Corresponding author. Tel.: +91 03222 276558x437, mobile: +91 9932629971; fax: +91 03222 275329.
E-mail address: sirajul_1999@yahoo.com (S.S. Islam).

0008-6215/$ - see front matter © 2013 Elsevier Ltd. All rights reserved.
http://dx.doi.org/10.1016/j.carres.2013.04.007

4:2:1 and PS-II consisted of mannose, 3-*O*-Me-galactose, and galactose in a ratio of nearly 1:1:1. In the present work, the detailed structural investigation and study of immunostimulating properties of PS-I were carried out and reported herein.

2. Results and discussion

2.1. Isolation, purification and chemical analysis of PS-I

The fresh mushroom fruit bodies were washed thoroughly and then boiled with distilled water for 10 h followed by filtration, centrifugation, and precipitation in ethyl alcohol (EtOH), and freeze drying to yield 290 mg of crude polysaccharide. Purification of this water soluble crude polysaccharide (25 mg) through Sepharose 6B column yielded two fractions. Fraction I (test tubes, 15–23) and fraction II (test tubes, 29–35) were collected and freeze dried, yielding purified polysaccharide of 11 mg PS-I and 8 mg PS-II, respectively. The PS-I showed specific rotation $[\alpha]_D^{29.2}$ +32.6 (*c* 0.886, water). The average molecular weight of PS-I was estimated as $\sim 2.1 \times 10^5$ Da from a calibration curve prepared with standard dextrans. GLC analysis of alditol acetates of hydrolyzed product of PS-I confirmed the presence of glucose, galactose, and mannose almost in a ratio of 4:2:1. The absolute configuration of the sugar residues was determined as D. The GLC–MS analysis of partially methylated alditol acetates of PS-I revealed the presence of seven peaks. The peaks were assigned as 2,3,4,6-Me_4-Glc, 2,3,4,6-Me_4-Man, 2,3,4-Me_3-Gal, 2,3,4-Me_3-Glc, 2,4,6-Me_3-Glc, 2,6-Me_2-Glc, and 3,4-Me_2-Gal in a ratio of nearly 1:1:1:1:1:1:1. Thus, PS-I was assumed to consist of terminal D-glucopyranosyl, and D-mannopyranosyl, (1→6)-linked D-galactopyranosyl, (1→6)-linked D-glucopyranosyl, (1→3)-linked D-glucopyranosyl, (1→3,4)-linked D-glucopyranosyl, and (1→2,6)-linked D-galactopyranosyl moieties, respectively. These linkages were further confirmed by periodate oxidation experiment. The GLC–MS analysis of the alditol acetates of periodate oxidized-reduced and methylated PS-I showed the presence of 2,6-Me_2-Glc and 2,4,6-Me_3-Glc in a molar ratio of nearly 1:1. These results clearly indicated that the all other moieties except (1→3,4)-linked D-glucopyranosyl and (1→3)-linked D-glucopyranosyl were consumed during oxidation. Thus, the mode of linkages present in the PS-I was confirmed.

2.2. NMR and structural analysis of PS-I

The ^{1}H NMR spectrum (Fig. 1) showed seven peaks in the anomeric region. The peaks were observed at δ 5.35, 5.12, 4.98, 4.78, 4.75, 4.51, and 4.49 in a ratio of nearly 1:1:1:1:1:1:1. They were designated as **A**, **B**, **C**, **D**, **E**, **F**, and **G** according to their decreasing proton chemical shifts. Seven peaks in the anomeric region of ^{13}C spectrum (Fig. 2a) at δ 97.8, 98.2, 99.7 101.7, 102.4, 102.5, 102.8 correlated to the residues **C**, **B**, **A**, **D**, **E**, F, and **G**, respectively, from the HSQC spectrum (Fig. 3 and Table 1). All the ^{1}H and ^{13}C signals were assigned using DQF-COSY, TOCSY, HSQC experiments. The proton coupling constants were measured from DQF-COSY experiment. Among these seven residues, residues **A**, **E**, **F**, and **G** have large coupling constant values of $J_{H\text{-}2,H\text{-}3}$, and $J_{H\text{-}3,H\text{-}4}$ (~10 Hz) and thus they are confirmed as D-glucopyranosyl residues. Again, among these D-glucopyranosyl residues, residue **A** is the only α anomer ($J_{H\text{-}1,H\text{-}2}$ ~3.0 Hz and $J_{H\text{-}1,C\text{-}1}$ ~170 Hz) and the rest are β anomers ($J_{H\text{-}1,H\text{-}2}$ ~8.5 Hz and $J_{H\text{-}1,C\text{-}1}$ ~161 Hz). Similarly, from the coupling constant values, **B** and **C** are established as α-linked ($J_{H\text{-}1,H\text{-}2}$ ~3.1 and $J_{C\text{-}1,H\text{-}1}$ ~171 Hz) D-galactopyranosyl ($J_{H\text{-}2,H\text{-}3}$ ~9 Hz and $J_{H\text{-}3,H\text{-}4}$ ~3.5 Hz) moieties and **D** is determined as β-linked ($J_{H\text{-}1,H\text{-}2}$ ~0, $J_{C\text{-}1,H\text{-}1}$ ~161) mannopyranosyl ($J_{H\text{-}3,H\text{-}4}$ ~7.5 Hz and $J_{H\text{-}4,H\text{-}5}$ ~10 Hz) moiety.

In the case of residues **A** and **C**, all the proton and carbon chemical shifts except C-6 were matched nearly with the standard values of methyl glycosides.[17,18] A downfield shift of C-6 (66.9 ppm for **A** and 66.6 ppm for **C**) was observed. These observations confirmed that both the residues **A** and **C** contained C-6 linkages. Therefore, **A** was determined as (1→6)-linked α-D-glucopyranosyl residue and **C** as (1→6)-linked α-D-galactopyranosyl residue. Furthermore, the DEPT-135 spectrum (Fig. 2b) confirmed the C-6 linkages in both of these residues. On the other hand, the downfield shifts of C-2 (77 ppm) and C-6 (66.4 ppm) of residue **B** with respect to standard values indicated that it was linked at C-2 and C-6. The linkage at C-6 of residue **B** was also supported by DEPT-135 spectrum. Thus, **B** was confirmed as (1→2,6)-linked α-D-galactopyranosyl residue. All the proton and carbon chemical shifts for residues **D** and **G** corresponded nearly to the standard values of methyl glycosides of mannose and glucose, respectively. Thus, **D** was confirmed as terminal β-D-mannopyranosyl residue and **G** as terminal β-D-glucopyranosyl residue. The downfield shift of C-3 (84 ppm) of residue **E** in comparison to the standard values indicated that it was linked at C-3 position. Hence, **E** was established as the (1→3)-linked β-D-glucopyranosyl residue. In case of residue **F**, downfield shifts at C-3 and C-4 were observed indicating that it was linked at C-3 and C-4. Thus, **F** was confirmed as (1→3,4)-linked β-D-glucopyranosyl residue. Since, residue **F** was present in the rigid part of the molecule, its C-3 (83.1 ppm) appeared at the more upfield region in comparison to the C-3 (84 ppm) of **E**.

The different linkages that connected these seven residues were determined from NOESY (Fig. 4 and Table 2) as well as ROESY spectrum (not shown). In NOESY spectrum, the inter-residual connectivities were observed between **A**H-1/**B**H-6a; **A**H-1/**B**H-6b; **B**H-1/**C**H-6a; **B**H-1/**C**H-6b; **C**H-1/**E**H-3; **D**H-1/**B**H-2; **E**H-1/**F**H-3; **F**H-1/**A**H-6a; **F**H-1/**A**H-6b; **G**H-1/**F**H-4 along with other intra-residual contacts. Finally, these connectivities were confirmed from HMBC spectrum (Fig. 5a and b). In this spectrum the inter-residual cross-peaks (Table 3) were observed between **A**H-1/**B**C-6; **A**C-1/**B**H-6a and **B**H-6b; **B**H-1/**C**C-6; **B**C-1/**C**H-6a and **C**H-6b; **C**H-1/**E**C-3; **C**C-1/

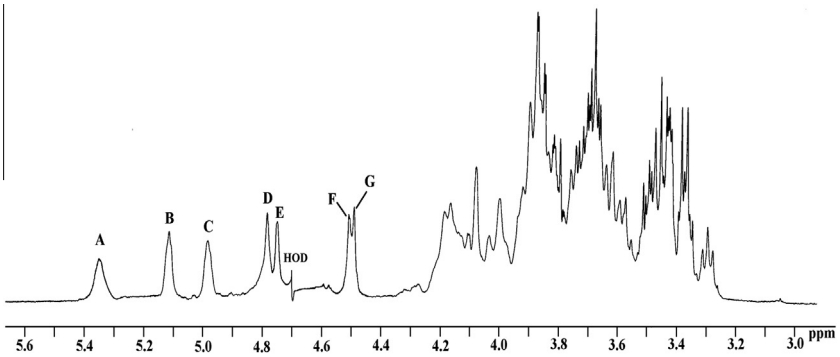

Figure 1. ^{1}H NMR spectrum (500 MHz, D_2O, 30 °C) of PS-I, isolated from hydrid mushroom *pfle 1p*.

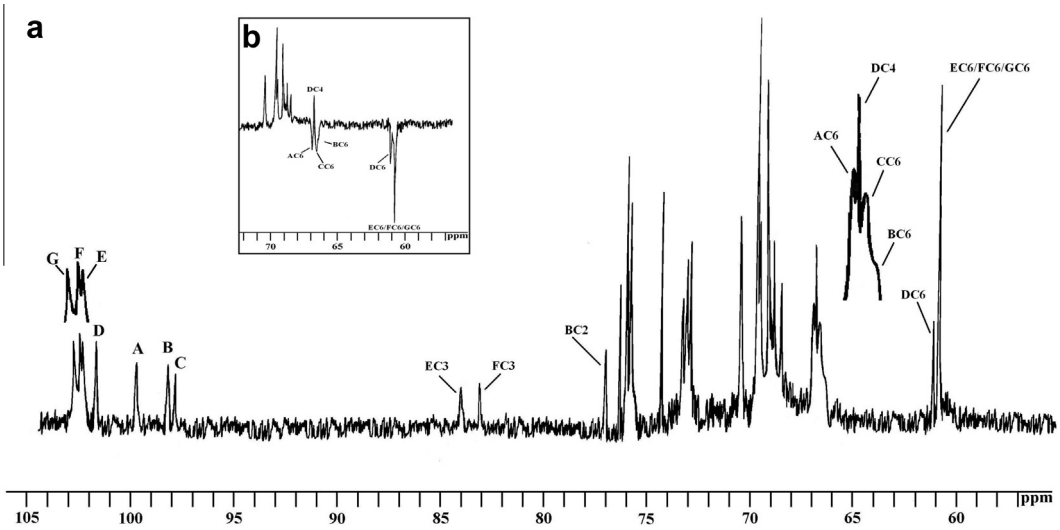

Figure 2. (a) ^{13}C NMR spectrum (125 MHz, D_2O, 30 °C) (b) with insert of the part of DEPT-135 spectrum (D_2O, 30 °C) of the PS-I, isolated from hydrid mushroom *pfle 1p*.

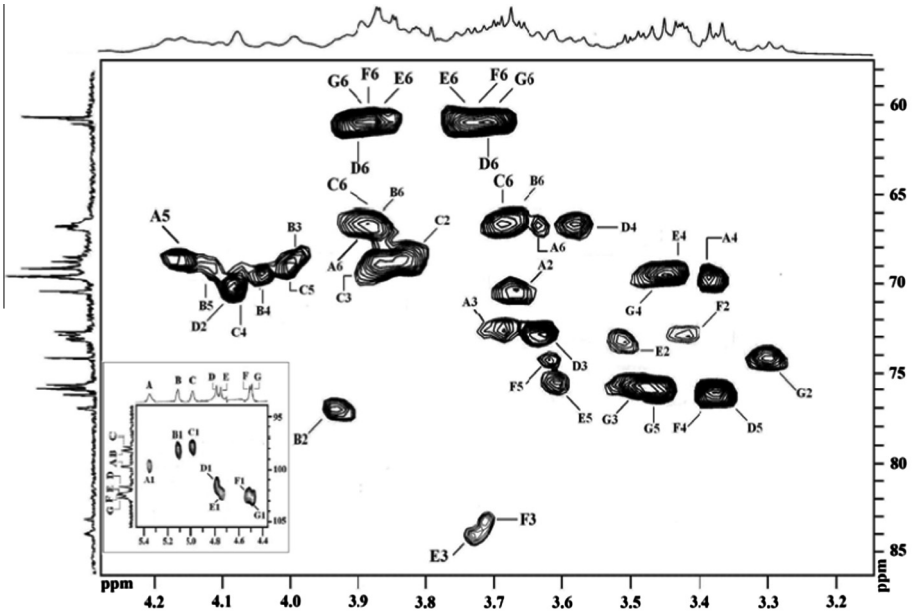

Figure 3. HSQC spectrum of PS-I, isolated from hydrid mushroom *pfle 1p*.

Table 1
The ^1H and ^{13}C NMR chemical shifts for the PS-I isolated from *pfle 1p*[a,b] in D_2O at 30 °C

Glycosyl residue	H-1/C-1	H-2/C-2	H-3/C-3	H-4/C-4	H-5/C-5	H-6a, H-6b/C-6
→6)-α-D-Glc*p*-(1→	5.35	3.67	3.69	3.38	4.16	3.88,[c] 3.64[d]
A	99.7	70.4	72.8	69.6	68.8	66.9
→2,6)-α-D-Gal*p*-(1→	5.12	3.94	3.99	4.04	4.11	3.87,[c] 3.66[d]
B	98.2	77.0	68.5	69.6	69.1	66.4
→6)-α-D-Gal*p*-(1→	4.98	3.83	3.87	4.08	4.01	3.88,[c] 3.68[d]
C	97.8	68.8	69.1	70.4	69.1	66.6
β-D-Man*p*-(1→	4.78	4.09	3.63	3.58	3.37	3.90 ,[c] 3.71 [d]
D	101.7	70.4	73.0	66.8	76.3	61.1
→3)-β-D-Glc*p*-(1→	4.75	3.51	3.73	3.43	3.61	3.86,[c] 3.73[d]
E	102.4	73.2	84.0	69.5	75.8	60.8
→3,4)-β-D-Glc*p*-(1→	4.51	3.42	3.71	3.38	3.62	3.88,[c] 3.72[d]
F	102.5	73.0	83.1	76.3	74.2	60.8
β-D-Glcp-(1→	4.49	3.30	3.49	3.45	3.47	3.89,[c] 3.70[d]
G	102.8	74.2	76.0	69.6	76.0	60.8

[a] Values of the ^1H chemical shifts were recorded with respect to the HOD signal set at δ 4.70 ppm at 30 °C.
[b] Values of the ^{13}C chemical shifts were recorded with reference to acetone as the internal standard and set at δ 31.05 ppm at 30 °C.
[c,d] Interchangeable.

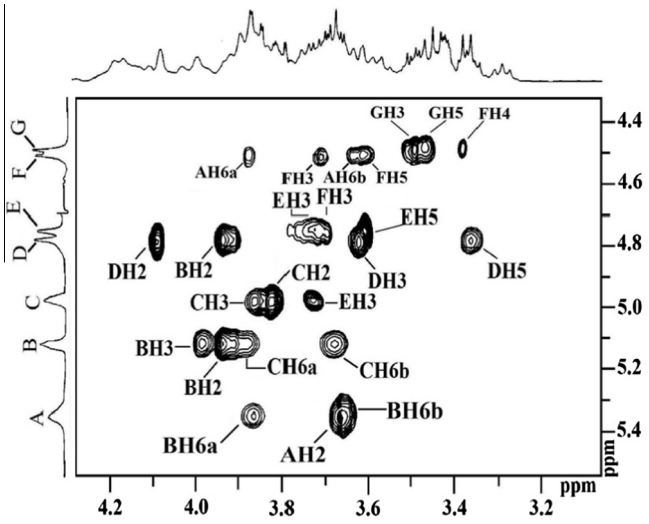

Figure 4. Part of NOESY spectrum of PS-I, isolated from hydrid mushroom *pfle 1p*. The NOESY mixing time was 300 ms.

Table 2
NOESY data for the PS-I isolated from hybrid mushroom *pfle 1p*

Glycosyl residue	Anomeric proton	NOE contact protons	
	δ	δ	Residue, atom
→6)-α-D-Glc*p*-(1→**A**	5.35	3.67	**A**H-2
		3.87	**B**H-6a
		3.66	**B**H-6b
→2,6)-α-D-Gal*p*-(1→**B**	5.12	3.94	**B**H-2
		3.99	**B**H-3
		3.88	**C**H-6a
		3.68	**C**H-6b
→6)-α-D-Gal*p*-(1→**C**	4.98	3.83	**C**H-2
		3.87	**C**H-3
		3.73	**E**H-3
β-D-Man*p*-(1→**D**	4.78	4.09	**D**H-2
		3.63	**D**H-3
		3.37	**D**H-5
		3.94	**B**H-2
→3)-β-D-Glc*p*-(1→**E**	4.75	3.73	**E**H-3
		3.61	**E**H-5
		3.71	**F**H-3
→3,4)-β-D-Glc*p*-(1→**F**	4.51	3.71	**F**H-3
		3.62	**F**H-5
		3.88	**A**H-6a
		3.64	**A**H-6b
β-D-Glcp-(1→**G**	4.49	3.49	**G**H-3
		3.47	**G**H-5
		3.38	**F**H-4

EH-3; **D**H-1/**B**C-2; **D**C-1/**B**H-2; **E**H-1/**F**C-3; **E**C-1/**F**H-3; **F**H-1/**A**C-6; **F**C-1/**A**H-6a and **A**H-6b; **G**H-1/**F**C-4; and **G**C-1/**F**H-4. Thus, the probable structural motif present in PS-I was established as:

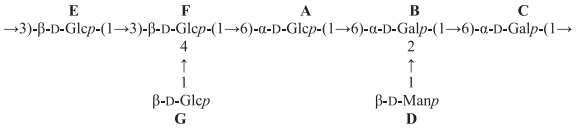

2.3. Assay for macrophage activity by NO

To test immunomodulatory effects of PS-I, murine macrophages were incubated with PS-I in a humidified atmosphere of 5% CO_2 at 37 °C for 48 h and the production of nitric oxide (NO) was measured using Griess reagent (1:1 of 0.1% in 1-napthylethylenediamine in 5% phosphoric acid and 1% sulfanilamide in 5% phosphoric acid). On treatment with different concentrations of the PS-I, it was observed that NO production increased with increase in concentration up to 50 μg/mL with optimum production of 19.27 μM NO per 5×10^5 macrophages at 50 μg/mL which subsequently decreased with increase in concentration (Fig. 6a). Hence, the effective dose of the PS-I for macrophage activation was 50 μg/mL.

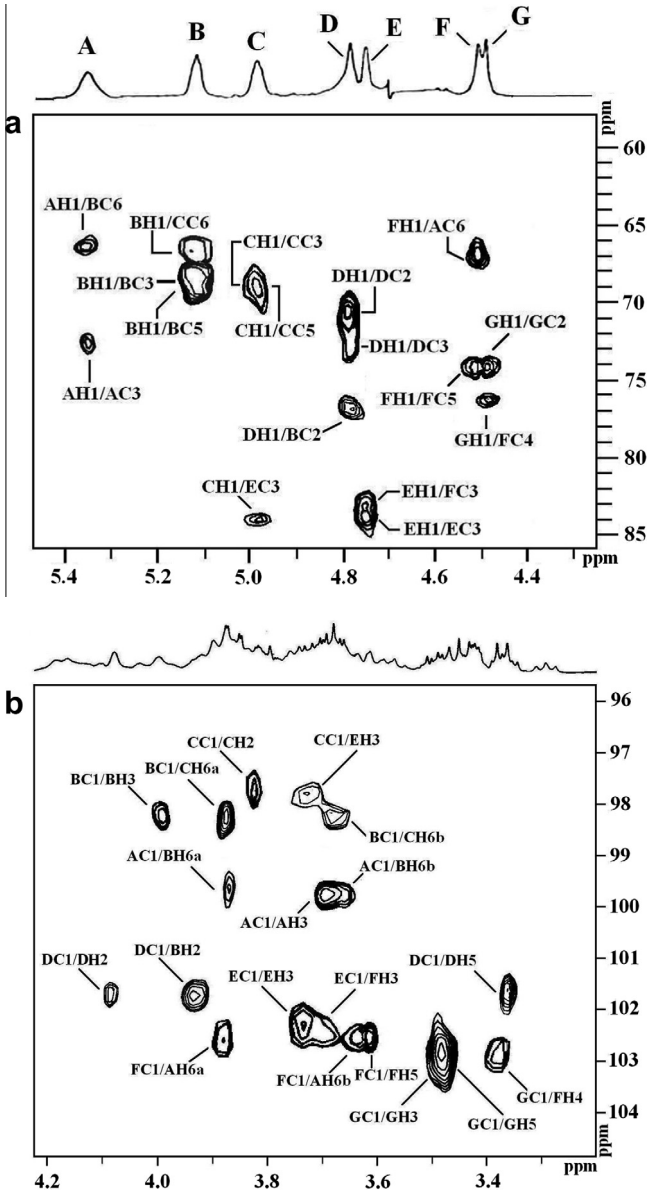

Figure 5. (a) The part of HMBC spectrum for anomeric protons, and (b) the part of HMBC spectrum for anomeric carbons of PS-I, isolated from hydrid mushroom *pfle 1p*.

2.4. Splenocytes and thymocytes proliferation assay

Spenocytes are the cells present in the spleen that include T cells, B cells, dendritic cells, etc that stimulate the immune response in living organism whereas thymocytes are hematopoietic cells present in the thymus and the primary function of which is the generation of T cells. Proliferation of splenocytes and thymocytes is an indicator of immunostimulation.[19] Spenocytes and

Table 3
The significant $^{3}J_{H,C}$ connectivities observed in an HMBC spectrum for the anomeric protons/carbons of the sugar residues of the PS-I isolated from hybrid mushroom *pfle 1p*

Residue	Sugar linkage	H-1/C-1	Observed connectivities		
		δ_H/δ_C	δ_H/δ_C	Residue	Atom
A	→6)-α-D-Glc*p*-(1→	5.35	72.8	**A**	C-3
			66.4	**B**	C-6
		99.7	3.69	**A**	H-3
			3.87	**B**	H-6a
			3.66	**B**	H-6b
B	→2,6)-α-D-Gal*p*-(1→	5.12	68.5	**B**	C-3
			69.1	**B**	C-5
			66.6	**C**	C-6
		98.2	3.99	**B**	H-3
			3.88	**C**	H-6a
			3.68	**C**	H-6b
C	→6)-α-D-Gal*p*-(1→	4.98	69.1	**C**	C-3
			69.1	**C**	C-5
			84.0	**E**	C-3
		97.8	3.83	**C**	H-2
			3.73	**E**	H-3
D	β-D-Man*p*-(1→	4.78	70.4	**D**	C-2
			73.0	**D**	C-3
			77.0	**B**	C-2
		101.7	4.09	**D**	H-2
			3.37	**D**	H-5
			3.94	**B**	H-2
E	→3)-β-D-Glc*p*-(1→	4.75	84.0	**E**	C-3
			83.1	**F**	C-3
		102.4	3.73	**E**	H-3
			3.71	**F**	H-3
F	→3,4)-β-D-Glc*p*-(1→	4.51	74.2	**F**	C-5
			66.9	**A**	C-6
		102.5	3.62	**F**	H-5
			3.88	**A**	H-6a
			3.64	**A**	H-6b
G	β-D-Glcp-(1→	4.49	74.2	**G**	C-2
			76.3	**F**	C-4
		102.8	3.49	**G**	H-3
			3.47	**G**	H-5
			3.38	**F**	H-4

thymocytes proliferation in the presence of PS-I was used to evaluate cell stimulatory effects on the immune cell activation. The PS-I was tested to stimulate splenocytes and thymocytes and the results are shown in Figure 6b and c, respectively. All the experiments were done twice with seven replicates and the results were represented as mean ± standard deviation using two tailed statistical analysis. The splenocytes and thymocytes proliferation indices as compared to PBS control if closer to 100 or below indicate low stimulatory effect on immune system. Difference in parameter between the treatment group and the control group was considered as statistically significant if $P < 0.05$ (indicated with a '*' mark). Both the splenocytes and thymocytes proliferation indices were found maximum at 50 μg/mL, above and below which it decreases. Hence, it can be concluded that 50 μg/mL is the optimum concentration of the PS-I for splenocytes and thymocytes proliferation.

3. Materials and methods

3.1. Preparation of hybrid mushroom strain *pfle 1p*

The hybrid mushroom strain *pfle 1p* was produced through polyethyleneglycol (30% PEG, MW-3350)-mediated somatic protoplast fusion between *Pleurotus florida* and *Lentinula edodes*. Hybrid strains were selected based on double selection method and afterward maintained in Potato–Dextrose–Agar medium. Spawn of the hybrid strain was produced on paddy grain and mushroom was produced on paddy straw substrate.

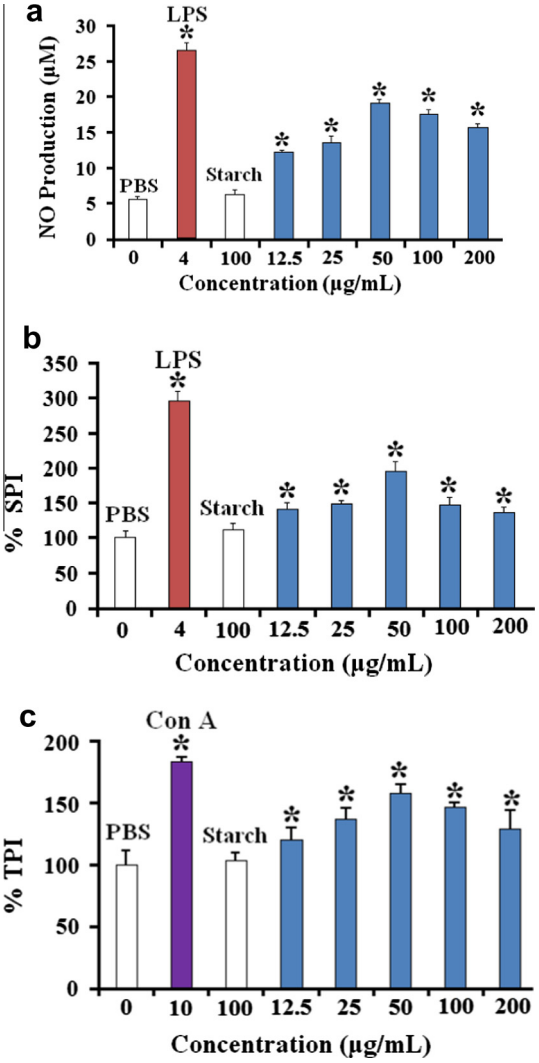

Figure 6. (a) In vitro activation of macrophage stimulated with different concentrations of PS-I in terms of NO production. Effect of different concentrations of PS-I on (b) splenocyte and (c) thymocyte proliferation. ('*' means data are significant compared to the PBS control).

3.2. Isolation, fractionation, and purification of the crude polysaccharide

The hybrid mushroom of *pfle 1p* was cultivated and collected from the Falta experimental farm, Bose Institute. The fruit bodies (300 g) were washed thoroughly with distilled water and then boiled for 10 h with distilled water. Next the boiled mushroom extract was cooled and filtrated through a linen cloth. The filtrate was collected and centrifuged at 7670×*g* (using a Heraeus Biofuge stratos centrifuge) for 45 min at 4 °C. The supernatant was collected and precipitated in ethanol. It was kept overnight at 4 °C and again centrifuged. The precipitated material was washed four times with ethanol and then dissolved in a minimum volume of distilled water and dialyzed through cellulose membrane (Sigma–Aldrich, retaining M_w > 12,400 Da) against distilled water for 48 h to remove low molecular weight carbohydrate molecules. The aqueous solution was then collected from the dialysis tube and freeze-dried yielding 290 mg crude polysaccharide.

The crude polysaccharide (25 mg) was passed through Sepharose 6B gel permeation column (90 × 2.1 cm) using water as eluant with a flow rate of 0.4 mL/min. Ninety five test tubes (2 mL each) were collected using Redifrac fraction collector and monitored

spectrophotometrically at 490 nm with phenol-sulfuric acid reagent[20] using a Shimadzu UV–vis spectrophotometer, model-1601. Two fractions of purified polysaccharide named PS-I and PS-II were obtained. The purification process was carried out in several lots.

3.3. Monosaccharide analysis

PS-I (3.0 mg) was hydrolyzed with 2 M trifluoro acetic acid (CF_3COOH, 2 mL) in a round-bottomed flask at 100 °C for 18 h in a water bath. The excess acid was completely removed by co-distillation with water. The hydrolyzed product was reduced with sodium borohydride ($NaBH_4$, 9 mg), followed by acidification with dilute acetic acid (CH_3COOH), and then co-distilled with pure methanol (CH_3OH) to remove excess boric acid. The reduced sugars were acetylated with 1:1 pyridine/acetic anhydride in a boiling water bath for 1 h to prepare the alditol acetates, which were analyzed by GLC. Quantization was carried out from the peak area, using response factors from standard monosaccharides.

3.4. Methylation analysis

PS-I (4.0 mg) was methylated using the procedure described by Ciucanu and Kerek.[21] The methylated products were isolated by making a partition between chloroform ($CHCl_3$) and water (5:2, v/v) four times. The organic layer containing products was collected and dried. The methylated product was then hydrolyzed with 90% formic acid (1 mL) at 100 °C for 1 h and excess formic acid was evaporated by co-distillation with distilled water. The hydrolyzed product was then reduced with sodium borohydride and acetylated with pyridine-acetic anhydride (1:1). The alditol acetates of methylated sugars were analyzed by GLC–MS.

3.5. Periodate oxidation

PS-I (5 mg) was added to 2 mL 0.1 M sodium metaperiodate solution and the mixture was kept in the dark for 48 h at room temperature. The excess periodate was destroyed by adding 1,2-ethanediol, and the solution was dialyzed against distilled water for 2 h. The dialyzed material was reduced with sodium borohydride ($NaBH_4$) for 15 h and neutralized with acetic acid. The resulting material was dried by co-distillation with methanol. The periodate-oxidized material[22,23] was divided into two portions. One portion was hydrolyzed with 2 M trifluro aceic acid for 18 h, and this hydrolyzed material was used for alditol acetates preparation as usual for GLC analysis. Another portion was methylated by the method of Ciucanu and Kerek,[21] followed by the preparation of alditol acetates which were analyzed by GLC–MS.

3.6. Absolute configuration of monosaccharide

The absolute configuration of monosaccharide was determined by the method of Gerwig et al.[24] PS-I (1.0 mg) was hydrolyzed with CF_3COOH, and then the acid was removed by co-distillation with water. 250 μL 0.625 M HCl solution treated with *R*-(+)-2-butanol was added and heated at 80 °C for 16 h. The reactants were evaporated and trimethylsilyl (TMS) derivatives were prepared with *N*,*O*-bis (trimethylsilyl) trifluroacetamide (BSTFA). The products were analyzed by GLC using a capillary column SPB-1 (30 m × 0.26 mm) with a temperature program (3 °C min^{-1}) from 150 to 210 °C. The resulting (+)-2-butyl-2,3,4,6-tetra-*O*-TMS-glycosides were identified by comparison with those prepared from the D and L enantiomers of different monosaccharides.

3.7. Optical rotation

Optical rotation was measured on a Jasco Polarimeter model P-1020 at 29.2 °C.

3.8. Determination of molecular weight

The average molecular weight of PS-I was determined by gel permeation chromatography.[25] Standard dextrans T-200, T-70, and T-40 were passed through a Sepharose-6B column and then the elution volumes were plotted against the logarithms of their respective molecular weights. The elution volume of PS-I was plotted on the same graph, and the average molecular weight of PS-I was determined.

3.9. GLC experiments

GLC experiment was performed on a Hewlett–Packard model 5730 MSD, having a flame ionization detector and glass columns (1.8 m × 6 mm) packed with 3% ECNSS-M (A) on Gas Chrom Q (100–120 mesh) and 1% OV-225 (B) on Gas Chrom Q (100–120 mesh). All GLC analyses were performed at 170 °C.

3.10. GLC–MS experiments

The Gas–liquid chromatography–mass spectrometric (GLC–MS) analysis was performed on a Shimadzu GLC–MS Model QP-2010 Plus automatic system, using ZB-5MS capillary column (30 m × 0.25 mm). The program was isothermal at 150 °C; hold time 5 min, with a temperature gradient of 2 °C min^{-1} up to a final temperature of 200 °C.

3.11. NMR studies

PS-I was dried over P_2O_5 in vacuum for several days and then exchanged with deuterium[26] followed by lyophilizing with D_2O (99.96% atom ^2H, Aldrich) for four times. Then ^1H, ^{13}C, TOCSY, DQF-COSY, ROESY, NOESY, HSQC and HMBC NMR spectra were recorded on a Bruker Avance DPX-500 spectrometer in D_2O at 30 °C. The ^1H NMR spectrum was recorded by suppressing the HOD signal (set at δ 4.70 ppm) using the WEFT pulse sequence.[27] The 2D-DQF-COSY experiment was carried out using standard Bruker software. The TOCSY experiment was recorded at a mixing time of 150 ms, and complete assignment required several TOCSY experiments requiring several mixing times ranging from 60 to 300 ms. The NOESY and ROESY mixing delay was 200 ms. The ^{13}C NMR experiments were carried out using acetone as internal standard, setting the methyl carbon signal at δ 31.05 ppm. The delay time in the HMBC experiment was 80 ms. All the chemical shifts were reported in ppm.

3.12. Study of immunostimulating activities of PS-I

3.12.1. Test for macrophage activity by nitric oxide assay

RAW 264.7, a murine macrophage cell line growing in Dulbecco's modified Eagle's medium (DMEM) was seeded in 96 well flat bottomed tissue culture plate at a concentration of 5×10^5 cells/mL (180 μL).[28] Cells were left overnight for attachment and then incubated with different concentration of PS-I (12.5, 25, 50, 100, and 200 μg/mL) in a humidified atmosphere of 5% CO_2 at 37 °C for 48 h. After 48 h of treatment, culture supernatant of each well was collected and NO content was estimated using Griess reagent (1:1 of 0.1% in 1-napthylethylenediamine in 5% phosphoric acid and 1% sulfanilamide in 5% phosphoric acid).[29] Lipopolysaccharide (LPS, L6511 of *Salmonella enterica* serotype

typhimurium, Sigma, 4 μg/mL) was used as positive control and soluble starch (Merck, India, 100 μg/mL) as negative control.

3.12.2. Splenocytes and thymocytes proliferation assay

A single cell suspension of spleen and thymus was prepared from normal mice under aseptic conditions by homogenization in Hank's balanced salt solution (HBSS).[30] The suspension was centrifuged to obtain a cell pellet. The contaminating red blood cells were removed by hemolytic Gey's solution. After washing two times with HBSS, the cells were resuspended in complete Rose well Park Memorial Institute (RPMI) 1640 medium (Source-GIBCO, USA, Cat. No. 31800-022). Cell concentration was adjusted to 1×10^6 cells/mL and the viability of splenocytes and thymocytes (as tested by trypan blue dye exclusion) was always over 90%. The cells (180 μL) were plated in 96 well flat bottomed tissue culture plates (1.8×10^5 cells/well) and incubated with 20 μL of various concentrations of PS-I (12.5, 25, 50, 100, and 200 μg/mL). PBS (10 mM, phosphate buffered saline, pH 7.4) was taken as carrier control and soluble starch (Merck, India, 100 μg/mL) as negative control. Lipopolysaccharide (LPS, L6511 of *Salmonella enterica* serotype typhimurium, Sigma, 4 μg/mL) served as positive control for splenocytes and Concavalin A (Himedia, 10 μg/mL) for thymocytes. All cultures were set up at 37 °C for 72 h in a humidified atmosphere of 5% CO_2. Proliferation of splenocytes (% Splenocyte Proliferation Index or % SPI) and thymocytes (% Thymocyte Proliferation Index or % TPI) were determined by MTT 3-(4,5-dimethylthiazol-2-yl)-2,5-diphenyltetrazolium bromide assay method.[31,32] All the experiments were done twice with seven replicates. The results were represented as mean ± standard deviation and compared against the PBS control.[29,30]

Acknowledgments

The authors are grateful to Professor S. Roy, Director, IICB, Kolkata, for providing instrumental facilities. Mr. Barun Majumdar of Bose Institute, Kolkata, is acknowledged for preparing NMR spectra. S.M. (one of the authors) thanks the CSIR for offering a senior research fellowship (CSIR-09/599(0039)/2010-EMR-I).

Supplementary data

Supplementary data associated with this article can be found, in the online version, at http://dx.doi.org/10.1016/j.carres.2013.04.007.

References

1. Mizuno, T.; Inagaki, R.; Kanao, T.; Hagiwara, T.; Nakamura, T.; Ito, H., et al *Agric. Biol. Chem.* **1990**, *54*, 2897–2905.
2. Wasser, S. P. *Appl. Microbiol. Biotechnol.* **2002**, *60*, 258–274.
3. Zhang, M.; Cui, S. W.; Cheung, P. C. K.; Wang, Q. *Trends Food Sci. Technol.* **2007**, *18*, 4–19.
4. Sasaki, T.; Takasuka, N. *Carbohydr. Res.* **1976**, *47*, 99–104.
5. Chihara, G.; Hamuro, J.; Maeda, Y. Y.; Arai, Y.; Fukuoka, F. *Cancer Res.* **1970**, *30*, 2776–2781.
6. Rout, D.; Mondal, S.; Chakraborty, I.; Pramanik, M.; Islam, S. S. *Med. Chem. Res.* **2004**, *13*, 509–517.
7. Rout, D.; Mondal, S.; Chakraborty, I.; Pramanik, M.; Islam, S. S. *Carbohydr. Res.* **2005**, *340*, 2533–2539.
8. Bhunia, S. K.; Dey, B.; Maity, K. K.; Patra, S.; Mandal, S.; Maiti, S., et al *Carbohydr. Res.* **2010**, *345*, 2542–2549.
9. Nandi, A. K.; Samanta, S.; Sen, I. K.; Devi, K. S. P.; Maiti, T. K.; Acharya, K.; Isalm, S. S. *Carbohydr. Polym.* doi: http://dx.doi.org/10.1016/j.carbpol.2013.02.019.
10. Maity, K.; Kar Mandal, E.; Maity, S.; Gantait, S. K.; Das, D.; Maiti, S.; Maiti, T. K.; Sikdar, S. R.; Islam, S. S. *Int. J. Biol. Macromol.* **2011**, *48*, 304–310.
11. Bao, X.; Wang, X.; Dong, Q.; Fanj, J.; Li, X. *Phytochemistry* **2002**, *59*, 175–181.
12. Dey, B.; Bhunia, S. K.; Maity, K. K.; Patra, S.; Mandal, S.; Behera, B., et al *Int. J. Biol. Macromol.* **2013**, *52*, 312–318.
13. Patra, S.; Maity, K. K.; Bhunia, S. K.; Dey, B.; Mandal, S.; Maity, T. K., et al *Carbohydr. Res.* **2011**, *346*, 1967–1972.
14. Chakraborty, U.; Sikdar, S. R. *World J. Microbiol. Biotechnol.* **2010**, *26*, 213–225.
15. Maji, P. K.; Sen, I. K.; Behera, B.; Maiti, T. K.; Mallick, P.; Sikdar, S. R., et al *Carbohydr. Res.* **2012**, *358*, 110–115.
16. Maji, P. K.; Sen, I. K.; Devi, K. S. P.; Maiti, T. K.; Mallick, P.; Sikdar, S. R., et al *Carbohydr. Res.* **2013**, *368*, 22–28.
17. Agrawal, P. K. *Phytochemistry* **1992**, *31*, 3307–3330.
18. Rinaudo, M.; Vincendon, M. *Carbohydr. Polym.* **1982**, *2*, 135–144.
19. Ohno, N.; Saito, K.; Nemoto, J.; Kaneko, S.; Adachi, Y.; Nishijima, M., et al *Biol. Pharm. Bull.* **1993**, *16*, 414–419.
20. York, W. S.; Darvill, A. G.; McNeil, M.; Stevenson, T. T.; Albersheim, P. *Methods Enzymol.* **1986**, *118*, 3–40.
21. Ciucanu, I.; Kerek, F. *Carbohydr. Res.* **1984**, *131*, 209–217.
22. Hay, G. W.; Lewis, B. A.; Smith, F. *Methods Carbohydr. Chem.* **1965**, *5*, 357–361.
23. Goldstein, I. J.; Hay, G. W.; Lewis, B. A.; Smith, F. *Methods Carbohydr. Chem.* **1965**, *5*, 361–370.
24. Gerwig, G. J.; Kamerling, J. P.; Vliegenthart, J. F. G. *Carbohydr. Res.* **1978**, *62*, 349–357.
25. Hara, C.; Kiho, T.; Tanaka, Y.; Ukai, S. *Carbohydr. Res.* **1982**, *110*, 77–87.
26. Dueñas Chaso, M. T.; Rodriguez-Carvajal, M. A.; Mateo, P. T.; Franko-Rodriguez, G.; Espartero, J. L.; Iribas, A. I.; Gil-Serrano, A. M. *Carbohydr. Res.* **1997**, *303*, 453–458.
27. Hård, K.; Zadelhoff, G. V.; Moonen, P.; Kamerling, J. P.; Vliegenthart, J. F. G. *Eur. J. Biochem.* **1992**, *209*, 895–915.
28. Mallick, S. K.; Maiti, S.; Bhutia, S. K.; Maiti, T. K. *Cell Biol. Int.* **2011**, *35*, 617–621.
29. Green, L. C.; Wagner, D. A.; Glogowski, J.; Skipper, P. L.; Wishnok, J. S.; Tannenbaum, S. R. *Anal. Biochem.* **1982**, *126*, 131–138.
30. Maiti, S.; Bhutia, S.; Mallick, S. K.; Kumar, A.; Khadgi, N.; Maiti, T. K. *Environ. Toxicol. Pharmacol.* **2008**, *26*, 187–191.
31. Mosmann, T. *J. Immunol. Methods* **1983**, *65*, 55–63.
32. Sarangi, I.; Ghosh, D.; Bhutia, S. K.; Mallick, S. K.; Maiti, T. K. *Int. Immunopharmacol.* **2006**, *6*, 1287–1297.